Max-Planck-Institut
für Meteorologie

MAX-PLANCK-GESELLSCHAFT

Climatic effects of large volcanic eruptions

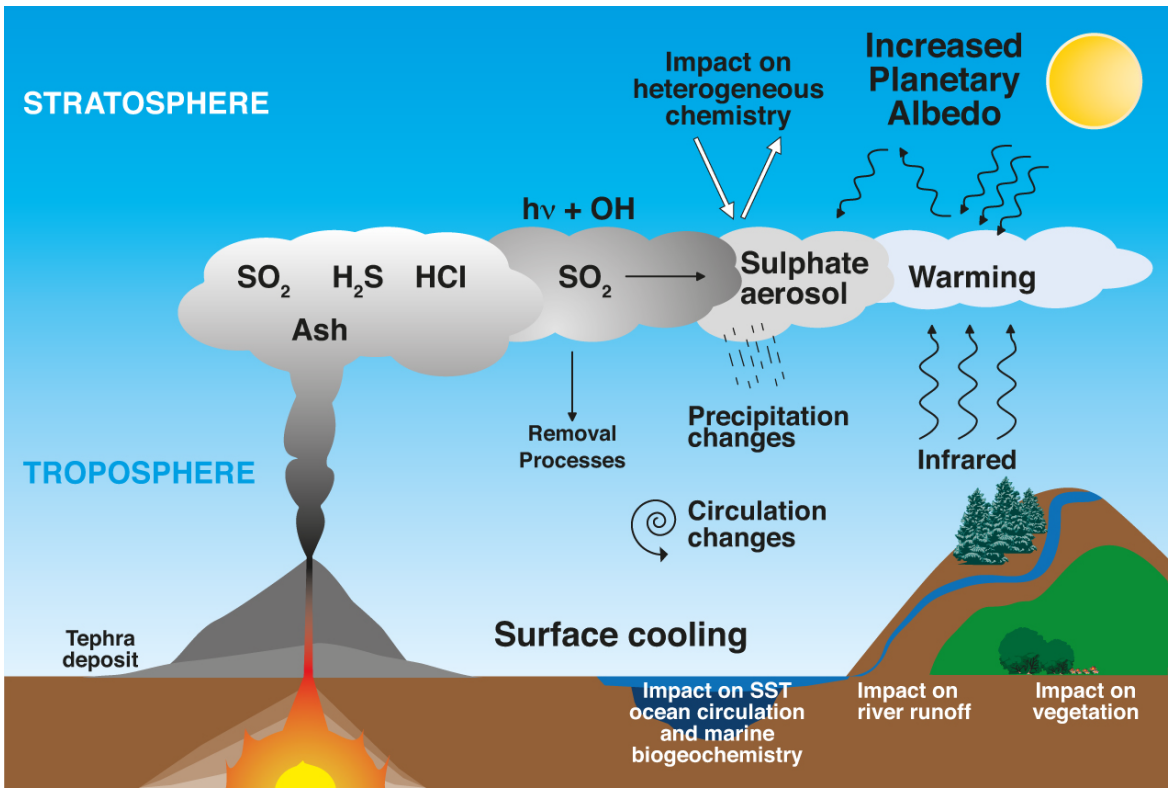

Claudia Timmreck

Hamburg 2018

Berichte zur Erdsystemforschung
Reports on Earth System Science

204
2018

Hinweis

Die Berichte zur Erdsystemforschung werden vom Max-Planck-Institut für Meteorologie in Hamburg in unregelmäßiger Abfolge herausgegeben.

Sie enthalten wissenschaftliche und technische Beiträge, inklusive Dissertationen.

Die Beiträge geben nicht notwendigerweise die Auffassung des Instituts wieder.

Die "Berichte zur Erdsystemforschung" führen die vorherigen Reihen "Reports" und "Examensarbeiten" weiter.

Notice

The Reports on Earth System Science are published by the Max Planck Institute for Meteorology in Hamburg. They appear in irregular intervals.

They contain scientific and technical contributions, including Ph. D. theses.

The Reports do not necessarily reflect the opinion of the Institute.

The "Reports on Earth System Science" continue the former "Reports" and "Examensarbeiten" of the Max Planck Institute.

Anschrift / Address

Max-Planck-Institut für Meteorologie
Bundesstrasse 53
20146 Hamburg
Deutschland

Tel./Phone: +49 (0)40 4 11 73 - 0
Fax: +49 (0)40 4 11 73 - 298

name.surname@mpimet.mpg.de
www.mpimet.mpg.de

Layout

Bettina Diallo and Norbert P. Noreiks
Communication

Copyright

Climatic effects of large volcanic eruptions

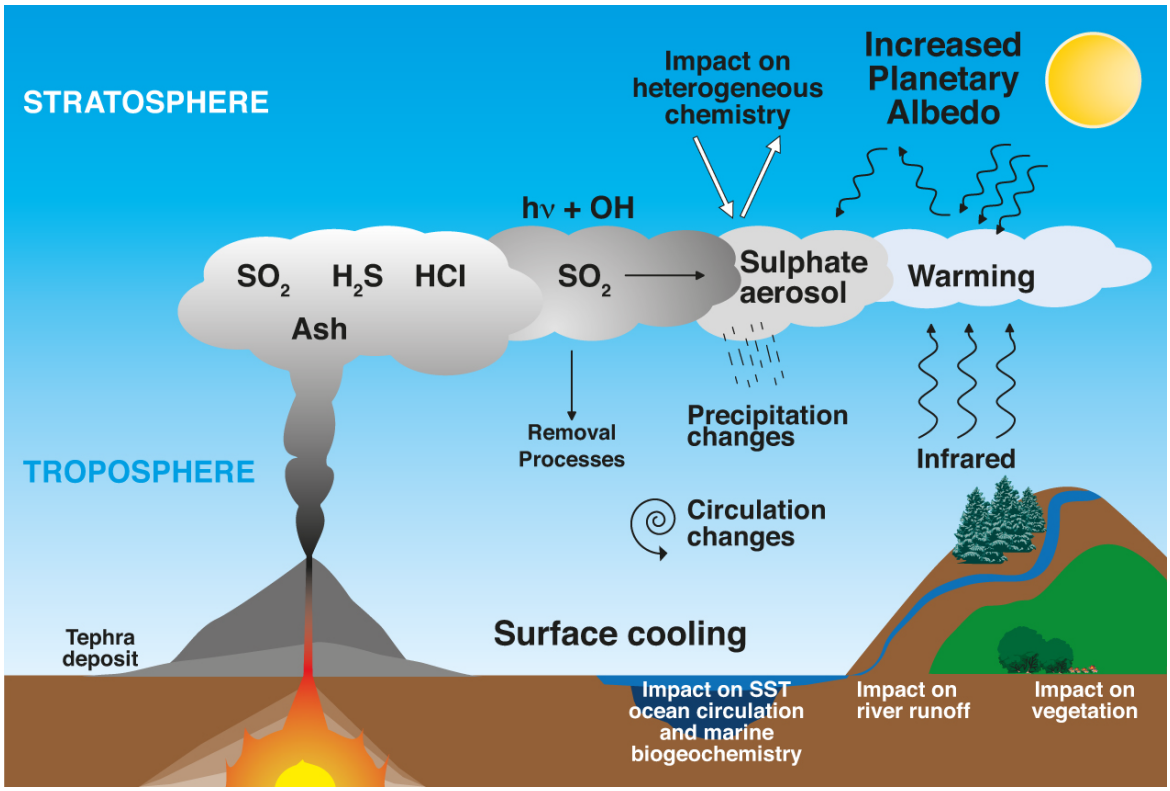

als Habilitationsschrift angenommen
vom Fachbereich Geowissenschaften der Universität Hamburg

Claudia Timmreck

Hamburg 2018

Claudia Timmreck

Max-Planck-Institut für Meteorologie
Bundesstrasse 53
20146 Hamburg

Tag der Habilitation: 29.01.2018

Als Habilitationsschrift angenommen vom Fachbereich Geowissenschaften
der Universität Hamburg im Juli 2017

Berichte zur Erdsystemforschung / Max-Planck-Institut für Meteorologie 204
Reports on Earth System Science / Max Planck Institute for Meteorology 2018

ISSN 1614-1199

In memory of

- Annette Barthelt, Marco Buchalla, Hans-Wilhelm Halbeisen and Daniel Reinschmidt, marine biologists from the University of Kiel, who were killed by a bomb attack on 18th March 1987 in Djibouti shortly before a METEOR scientific cruise towards the Indian Ocean.

- David A. Johnston an American volcanologist and principal scientist on the USGS monitoring team. He was the first to report the 1980 eruption of Mount St. Helens in Washington, transmitting "Vancouver! Vancouver! This is it!" before he was swept away by a lateral blast.

- and all other young scientists who never had the chance to have a scientific career

List of Contents

1. Introduction

Large explosive volcanic eruptions are a major driving factor of natural climate variability over the past centuries (Crowley, 2000; Hegerl et al., 2007a; *Jungclaus et al., 2010*[1]) by injecting large amounts of particulate matter (ash) and gases into the stratosphere (*Textor et al., 2004).* It is common to define the size of large volcanic eruptions by the volume or mass of magma released (Self, 2006). The volcanic climate effect results primarily from their stratospheric emission of sulfur-containing gases, mainly sulfur dioxide (SO_2) and hydrogen sulfide (H_2S). Due to its large particle size and density, volcanic ash falls rapidly out of the atmosphere and has therefore only a regional climate influence for a short time period i.e. a couple of weeks (*Niemeier et al., 2009*; Robock and Mass 1982). Volcanic emissions of water vapor (H_2O) and carbon dioxide (CO_2) are negligible in comparison to their atmospheric concentration (Gerlach, 1991). Initially the released water vapor might however locally affect the aerosols' composition and optical properties. Volcanic released halogen compounds (hydrogen chloride (HCl), other chlorine (Cl) and bromine (Br) substances) could be a critical parameter for the fate of the stratospheric ozone layer (*Textor et al., 2004*; Kutterolf et al., 2013). The volcanic halogen emission into the stratosphere is, however, highly uncertain, depending on the type of magma as well as on chemical and microphysical processes in the volcanic plume (Tabazadeh and Turco, 1993; Textor et al., 2003).

The climate-relevant large volcanic eruptions, which are mainly discussed here, are therefore those with a stratospheric SO_2 emission of several Tg (≥5Tg SO_2) and an eruption magnitude M[2] equal to or larger than 4. Table 1 gives an overview table of the large volcanic eruptions which are discussed here. Within an e-folding time of about one month, SO_2 and H_2S are converted to sulfuric acid vapor (H_2SO_4 (g)). H_2SO_4 (g) is then converted into stratospheric aerosols by microphysical processes, thereby increasing the stratospheric background aerosol layer or Junge layer[3]. In the stratosphere, a persistent sulfate aerosol layer mainly of supercooled hydrated H_2SO_4 particles with a sulfuric acid mass fraction in the range of 50-80% exists, which extends from the tropopause up to 30~km altitude. Height and maximum of the layer are seasonally and latitudinally dependent (e.g. Yue et al., 1984).

[1] All publications in which I am involved as author or co-author are indicated in Italic.
[2] The eruption magnitude M is defined as M = log(m)−7, where m is erupted magma mass in [kg] (Mason et al., 2004).
[3] The stratospheric background layer is often named Junge layer after its discoverer Christian Junge (Junge et al., 1961).

Volcano	Location	Time	M	VEI	SO_2	Peak AOD 0.55 µm
Yellowstone*, USA Huckleberry Ridge Tuff[$] Mesa Falls Tuff Lava Creek Tuff,	44 °N, 110 °W	2133k ± 2k yr BP 1270k yr BP 639k ± 2k yr BP	8.3[a] 7.8[a] 8.4[a]	8[b] 7[b] 8[b]	400 Tg[c]	0.4[d]
Younger Toba Tuff (YTT), Sumatra, Indonesia	2 °N, 98 °O	74k ± 2k yr BP	8.8[a]	8[b,e]	[f] 6600 Tg[f1] 1140-2200 Tg[f2], 70 Tg[f3]	0.4[d]
Samalas, Lombok, Indonesia	8 °S, 116 °E	July 1257	7[a]	7[e]	118.84 Tg[g]	0.64[h] 0.56[i]
Kuwae, Vanatu	16 °S, 168 °E	1458[#]	6.8[a]	6[e]	65.96 Tg[g]	0.39[i] 0.30[h]
Lakagígar (Laki), Iceland	64 °N, 18 °W	1783-1784	4.4[a]	4[e]	122 Tg[i]	0.25[i] 0.06[h]
1809 (Tropics)	Unknown	1809	≥ 6[a]	≥6[e,k]	38.52 Tg[g]	0.28[h] 0.25[i]
Tambora, Sumbawa Indonesia	8 °S, 116 °E	April 1815	7.3[l],7[m] 6.9[n]	7[b]	57.6 Tg[g], 60 Tg[o]	0.42[h] 0.35[i]
Cosigüina, Nicaragua	12 °N, 87 °W	January 1835	5.8[a]	5[e]	18.96 Tg[g]	0.2[h] 0.13[i]
Krakatau, Indonesia	6 °S, 105 °E	August 1883	6.5[a]	6[b]	18.68 Tg[g]	0.19[h] 0.12[i]
Novarupta (Katmai), USA	58 °N, 155 °W	June 1912	6.5[l]	6[b,e]	10.67 Tg[g]	0.07[h]
Agung, Bali, Indonesia	8 °S, 116 °E	March 1963	5[p]	4+[p]	7.66 Tg[g], 6.5 Tg[p], 2.5 Tg[q]	0.06[h]
El Chichón, Mexico	17 °N, 93 °W	April 1982	5.1[a]	5[e]	7 Tg[r]	0.11[h] 0.054[s]
Mt. Pinatubo, Luzon, Philippines	15 °N, 120 °E	June 1991	6.1[a]	6[e]	18-19 Tg[t], 17 Tg[u], 10-14 Tg[v]	0.16[h] 0.098[s]

Table 1: Overview of very large volcanic eruptions, which are discussed in this thesis in terms of eruption magnitude M, Volcanic Explosivity Index (VEI, Newhall and Self (1982)), SO_2 emission and peak aerosol optical depth (AOD). (*) 3 extremely large caldera forming Yellowstone eruptions are known (Smith and Siegl, 2000); ($) some divide the Huckleberry Ridge Tuff eruption into three phases (Ellis et al., 2012); (#) according to new ice core records (Sigl, et al., 2014; 2015); earlier studies e.g. Gao et al. (2006) date this eruption to 1453, Crowley and Untermann (2013) to 1456. (a) LaMEVE (Large Magnitude Explosive Volcanic Eruptions) database (Crosweller et al., 2012) and references therein, (b) Decker et al. (1990); (c) according to the petrological method, which gives a lower bound estimate (Self and Blake, 2008); (d) MPI-SV simulations based on an initial emission of 1700 Tg SO_2 (*Timmreck et al., 2010; Zanchettin et al., 2014*); (e) Smithsonian Institution http://www.volcano.si.edu/, (f) compilation from Oppenheimer (2002), estimates from (f1) mineral chemistry (Rose and Chesner, 1990), (f2) ice core sulfate deposition (Zielinski et al., 1996), (f3) experimental petrology (Scaillet et al., 1998); (g) Toohey and Sigl (2016), (h) Crowley and Unterman (2013); (i) EVA estimates with 2k sulfur emission data set (Toohey and Sigl, 2016); (j) Thordarson and Self, 2003; (k) Guevara-Murua et al. (2014); (l) Pyle (2000); (m) Kandlbauer et al. (2014); (n) Self et al. (2004); (o) Raible et al. (2016); (p) Fontijin et al. (2015) and references therein, (q) estimate from the petrological method, which gives a lower estimate (Self and King, 1996); (r) Bluth et al. (1997); (s) Chemistry-Climate Model Initiative (CCMI)data set (Arfeuille et al., 2013; Eyring et al., 2013); (t) Guo et al. (2004); (u) Read et al. (1993); (v) Recent modelling studies indicate smaller values (Dhomse et al., 2014; Sheng et al., 2015; Mills et al., 2016).

The global climate system is affected by stratospheric aerosol in manifold ways. The aerosol particles change directly the radiative balance of the atmosphere by scattering solar radiation back to space, thereby increasing the planetary albedo.The stratospheric aerosol load leads to more absorption of longwave (LW) radiation in the lower stratosphere, which heats up the aerosol layer and enhances downwelling LW radiation and reduces outgoing LW radiation (OLR). The climatic effects of stratospheric aerosol are especially evident if the aerosol concentration is enhanced after large volcanic eruptions (Figure 1).

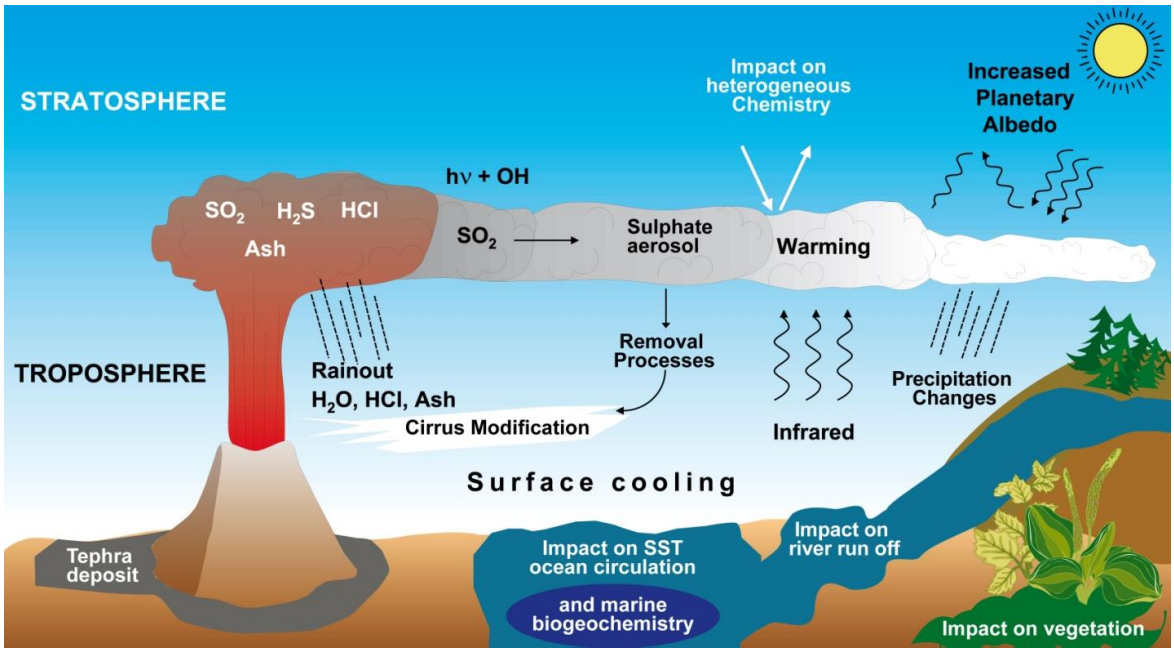

Figure 1: Schematic overview of the climate effects after a very large volcanic eruption, from *Timmreck (2012)*, originally modified from McCormick et al. (1995).

After the June 1991 Mt. Pinatubo eruption, which is the best-observed eruption so far, a global maximum cooling of about 0.4 K (Dutton and Christy, 1992; Thompson et al., 2009) and a stratospheric temperature increase of 2-3 K (Labitzke and McCormick, 1992) was detected, leading to a decrease in tropopause height (Santer et al., 2003). Furthermore, a stratospheric ozone decrease (Chipperfield et al., 2007; Randel et al., 1995) and significant changes of the hydrological cycle were observed, such as a reduction in tropical precipitation (Gu et al., 2007), river runoff (Trenberth and Dai, 2007), and sea level height (Church et al., 2005) as well as a drying of the troposphere (Soden et al., 2002). In 2000, two influential overview articles about volcanic eruptions and climate were published. Zielinski (2000) discussed the application of paleo records to understand the volcanic climate effects, while Robock (2000) focused on observational and modeling studies of the 1991 Mt. Pinatubo and 1982 El Chichón eruptions. Robock presented thereby the first detailed summary of the climate effect of volcanic eruptions in particular their atmospheric impacts on radiation, chemistry and dynamics. Ten years later,

Cole-Dai (2010) outlined the most significant accomplishments regarding the role of volcanism in climate in the last decade particularly related to the interpretation of ice core volcanic records. Significant improvements have been achieved due to long ice core records with unprecedented temporal accuracy and precision, and by the potential to identify climate-impacting stratospheric eruptions in the records (Cole-Dai, 2010).

In 2012, I summarized the "state of art" in the simulation of the climate effects of volcanic eruptions (*Timmreck, 2012*). Large volcanic eruptions are an ideal test case for the evaluation of comprehensive climate models and Earth system models (ESMs) as they strongly affect all components of the Earth system (Figure 1). In the last ten years, a number of model studies appeared which considered not only the volcanic impact on atmospheric composition and dynamics but also the impact on ocean dynamics and heat content (e.g. Stenchikov et al., 2009; *Zanchettin et al., 2012a; 2013b,* Ding et al., 2014), terrestrial and marine biogeochemistry (e.g. Robock et al., 2009, *Brovkin et al., 2010; Segschneider et al., 2013*), and the cryosphere (e.g. Miller et al., 2012; Berdahl and Robock, 2013; *Zanchettin et al., 2014*).

My contribution to this field over the last two decades was to develop global aerosol models and to adapt and to apply Earth system models guided by the overall arching question:

What are the impacts large volcanic eruptions have on the Earth system?

The purpose of this thesis is to give an overview of my work in the frame of general development and achievements in the scientific understanding of large volcanic eruptions. In chapter 2, I focus on the fundamental processes of the life cycle of stratospheric aerosol, in particular the formation and temporal development of the volcanic aerosol, by discussing simulations of microphysical processes in both simple box models as well as in global models and simulations of the global dispersal of the volcanic cloud. Chapter 3 covers the radiative forcing of volcanic aerosols. Chapter 4 deals with the surface temperature response and the manifold impacts large volcanic eruptions have on the different components of the Earth system. This encompasses most of the work carried out in the Max Planck Institute for Meteorology (MP-M) Super Volcano" (SV)[4] project, which I led. The thesis concludes with a summary of my main research achievements and a discussion of avenues for future research in chapter 5.

[4] From 2006 to 2011, MPI-M established the SV project as one of its crosscutting science projects. The major goal of this MPI-SV integrated project was the investigation of the climate effects of volcanic super eruptions, employing the full coupled MPI ESM.

2. Life cycle of volcanic aerosols

2.1 Life cycle of volcanic aerosol

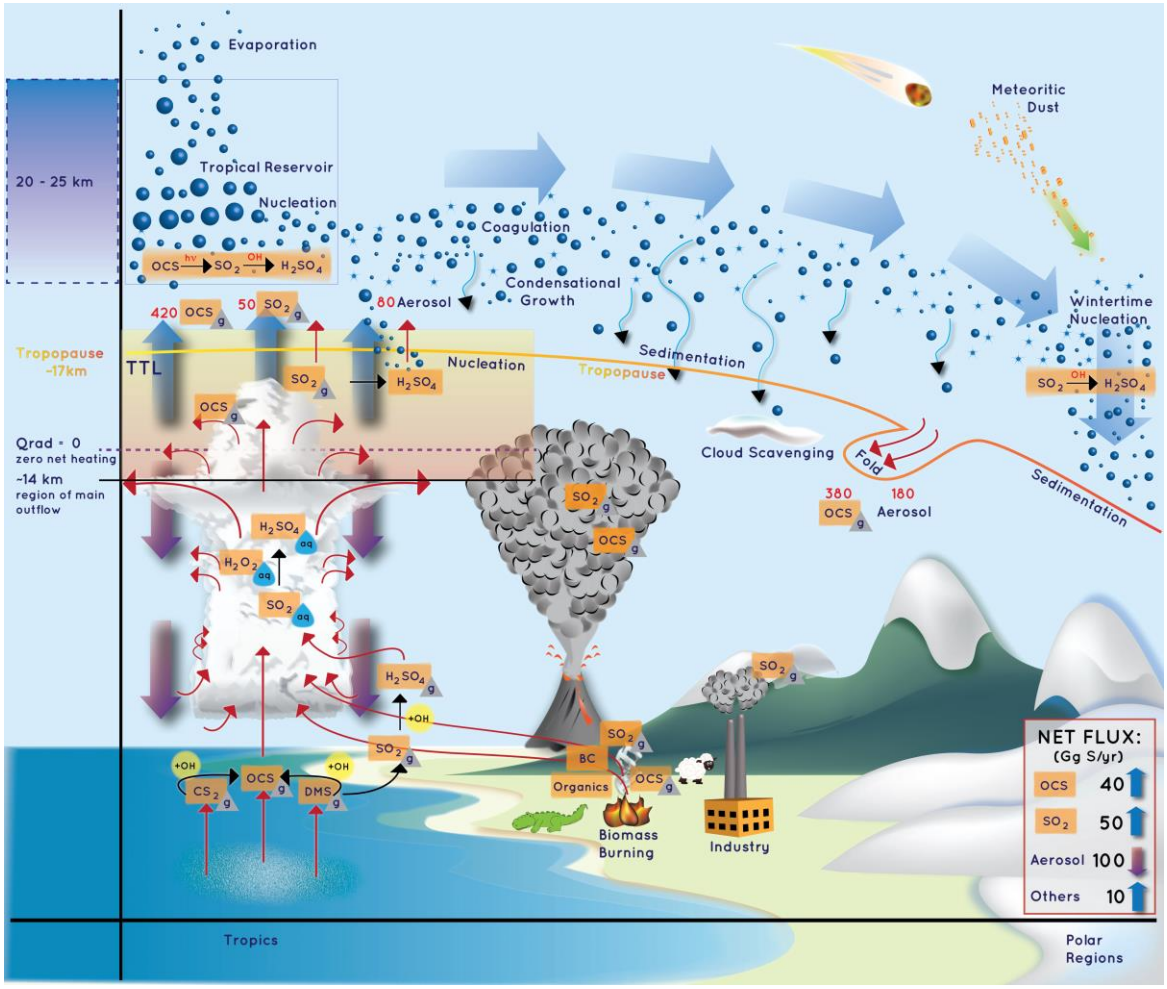

Figure 2: Schematic diagram of the stratospheric life cycle from *Kremser et al. (2016)*. The large blue arrows indicate the large-scale circulation; the red arrows indicate transport processes and the black arrows show chemical conversions between compounds. Different chemical species are marked as either gas phase (grey triangle) or aqueous phase (blue drop). The blue thin arrows represent sedimentation of aerosol from the stratosphere to the troposphere. The red numbers represent the flux of carbonyl sulfide (OCS) and sulfur dioxide (SO_2) as well as the flux of aerosol in Gg S/yr based on model simulations from Sheng et al. (2015). The approximate net flux of sulfur containing compounds across the tropopause is shown in the grey box (Sheng et al., 2015), where the 10 Gg S/yr contribution from "others" can be mostly attributed to dimethyl sulfide (DMS) and hydrogen sulfide (H_2S). Other chemical compounds shown in this figure are carbon disulfide (CS_2), sulfuric acid (H_2SO_4), and black carbon (BC).

The life cycle of stratospheric aerosol in general and volcanic aerosol in specific encompasses emission, transport and microphysical and removal processes (Figure 2). In an unperturbed atmosphere, aerosol precursor gases and particles enter the stratosphere through the tropical tropopause layer, while in the case of a large volcanic eruption the sulfur gases are directly injected into the stratosphere, where they are altered via microphysical processes. New sulfate particles are formed by binary homogenous nucleation, where H_2SO_4 (g) and water vapor condense simultaneously to form a liquid droplet (Kulmala et al., 2000). Due to H_2SO_4 (g)

condensation on preexisting particles and coagulation processes, the aerosol size distribution is shifted to larger radii (Hamill et al., 1997; *Timmreck, 1997*). The stratospheric aerosol particles are transported within the Brewer-Dobson circulation (BDC) and finally are removed through cross tropopause transport in the extra-tropics and through gravitational sedimentation. A detailed description of the stratospheric aerosol life cycle is given in Hamill et al. (1997), in the Stratosphere-troposphere Processes And their Role in Climate (SPARC) ASAP report (SPARC, 2006) here referred as *ASAP2006*[5] and in *Kremser et al. (2016)*.

The evolution and growth of volcanic aerosols is a large source of uncertainty in the simulation of volcanic climatic effects. The large amount of volcanic H_2SO_4 (g) significantly increases the stratospheric aerosol background concentration over a couple of years. A high atmospheric sulfate aerosol particle concentration leads therefore to higher collision rates, larger particle sizes and a faster removal, which results in a shorter lifetime of the volcanic aerosols (Pinto et al., 1989; *Timmreck et al., 2010*). Microphysical processes have therefore the potential to limit the volcanic impact on climate which was successfully demonstrated by *Timmreck et al. (2010; 2012)* for the extremely large Toba eruption, see section 4.7.

Chemical and microphysical processes are different for each individual volcanic eruption as they are strongly and nonlinearly dependent on the eruption parameters (emission strength, height of injection). Model studies (Bekki et al., 1996; Robock et al., 2009) indicate, that for high SO_2 emissions (100 times Mt. Pinatubo or even larger) the available hydroxyl radical (OH) concentration limits the oxidation process. This will delay the conversion process to H_2SO_4 (g) with the result of a reduced but longer-lasting peak of H_2SO_4 (g) concentration and a possible prolongation of the atmospheric lifetime of the volcanic cloud. However, the increased water vapor flux through the tropopause after large volcanic eruptions (Robock et al., 2009) might alter the OH concentration and therefore buffer the aforementioned chemical effect.

2.2 Treatment of aerosol microphysical processes in global models

Microphysical processes controlling the formation and temporal development of the volcanic aerosol size distribution are relative well understood. Their treatment in global climate models is however still a computational challenge *(Timmreck, 2012*). The size distribution and chemical composition of the volcanic aerosol are therefore parameterized in most global models with

[5] I am co-author of chapter 6 (Modeling of Stratospheric Aerosols) of the ASAP2006 report.

increased simplification for longer time periods considered and larger model dimensions. Therefore, the volcanic aerosol size distribution and the associated radiative forcing are usually prescribed in multi-decadal climate model studies. For large model intercomparison studies i.e. the Coupled Model Intercomparison Project 5 (CMIP5) (Taylor et al., 2012) or chemistry climate model (CCM) validation studies (Eyring et al., 2010; 2013), the volcanic size parameters have been mostly derived from satellite observations when available or from global aerosol model results. Common approaches to simulate the stratospheric aerosol distribution in global aerosols models interactively are the mass only (bulk) approach and size segregated approaches. In the mass approach only the aerosol mass is calculated interactively while for the calculation of size dependent microphysical processes and radiative calculations a typical size distribution is assumed (e.g. *Timmreck et al., 1999a; 1999b; 2003; Oman et al., 2005*). Two size segregated approaches are widely used, the modal approach (e.g. *Niemeier et al., 2009; Toohey et al., 2011;* Brühl et al., 2012; Mills et al., 2016), where the aerosol size distribution is prescribed preferentially with one or more log-normal size distributions, and the sectional approach (*Timmreck, 2001*; Weisenstein et al., 2007; Kokkola et al., 2008; English et al., 2011; *Hommel et al., 2011,* Sheng et al., 2015), where the aerosol size distribution is divided into size sections.

Timmreck (1997) was among the first who developed a global 3d stratospheric aerosol model, with interactive aerosol microphysics. This Stratospheric Aerosol Model, *SAM*[6], and its updated release *SAM2* (Hommel, 2008[7], *Hommel et al., 2011*), is a sectional bin model with 44 size bins covering a radius range from $3 \cdot 10^{-4}$ µm to 6.2 µm. *SAM* calculates the formation of stratospheric sulfuric acid aerosol via binary homogeneous nucleation of H_2SO_4 (g)/H_2O (g), its temporal development via condensation (evaporation) of H_2SO_4 (g) and H_2O (g) and coagulation, and its removal by sedimentation. Aerosol properties are estimated dependent on temperature, pressure and the atmospheric H_2SO_4 (g) and H_2O (g) concentration. Box model simulations with *SAM* show that the model's ability to reproduce important stratospheric aerosol characteristics, like the observed decrease of the aerosol mixing ratio and the strong increase of the aerosol size ratio above 50 hPa *(Timmreck and Graf, 2000).* The simulated temporal development of the aerosol spectrum for a Mt. Pinatubo case study is in the observational range of remote sensing and in-situ measurements (Russel et al., 1996) with maximum values of the effective radius (r_{eff})

[6] Italic style is used to distinguish the aerosol model *SAM (2)* from the Southern Annular model Index SAM.

[7] Phd thesis Uni. Hamburg supervised by me.

of 0.48 µm six to twelve months after the eruption (Figure 3). Due to the large amount of small, freshly nucleated particles, the simulated r_{eff} first decreases shortly after the eruption before it starts to increase.

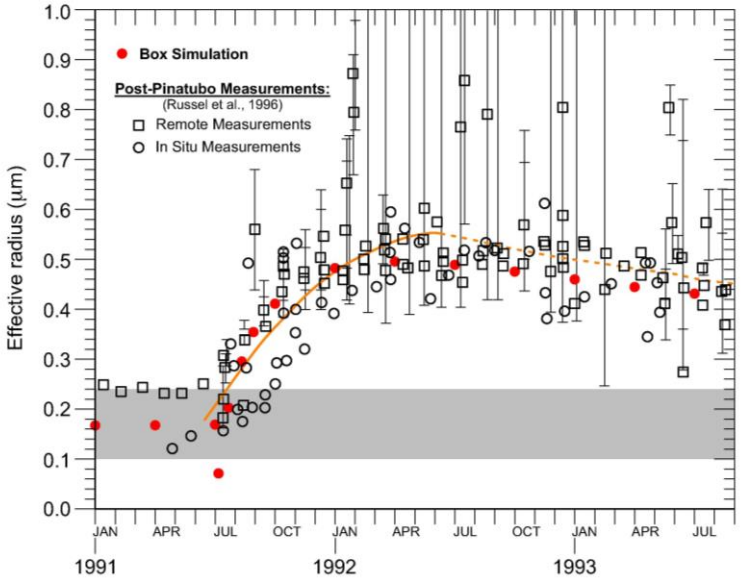

Figure 3: Comparison of observed effective radii after the Mt. Pinatubo eruption (Russell et al., 1996) with box results for an initial SO_2 concentration of $1 \cdot 10^{11}$ cm^{-3}. The solid and dashed lines are fits of the variety measurements (Russell et al., 1996). The shaded area indicates the range of the effective radius under background conditions. Figure from *Timmreck and Graf (2000).*

For the application in the general circulation model (GCM) ECHAM4 (Roeckner et al., 1996), the microphysical model *SAM* was combined with a tropospheric sulfur cycle (Feichter et al., 1996) to obtain the first three-dimensional multiyear simulation of stratospheric background aerosol (*Timmreck, 2001*). It shows that the stratospheric aerosol distribution is mainly determined by the aerosol flux from the troposphere. Simulated values of aerosol mass density and effective radius at Northern Hemisphere (NH) midlatitudes also agree quite well with observed background values of the Stratospheric Data Intercomparison (Kent et al., 1995) for the corresponding latitude and altitudes (Table 2). The large spread of the measurements shows not only the level of observational uncertainty but also the interannual variability of the stratospheric background aerosol. A detailed comparison of MAECHAM5-SAM2 results with SAGE II retrieved integrated aerosol quantities related to the size of particles shows a better agreement for higher moments of the aerosol size distribution than for lower ones (*Hommel et al., 2011*). Lower moments as the effective radius are significantly smaller in the model in large areas of the stratosphere. This is due to limitations of remote sensing instruments at the bottom end of the aerosol spectrum and a priori constraints in the retrieval methods, which do not take into account the formation and growth of new particles. This confirms key findings from the

ASAP2006, where it is stated that during volcanically quiescent periods, models and observations disagree significantly mainly due to the fraction of the surface area density produced by models residing in particles too small to be measured, especially near nucleation regions.

		Mass Density		**Effective Radius**	
Time	**Location/ Altitude**	**Observation ($\mu g\ m^{-3}$)**	**Model results ($\mu g\ m^{-3}$)**	**Observation (μm)**	**Model results (μm)**
1989	41°N, 18 - 22km	0.10 OPC[a] 0.19SAGEII[b]	0.07-0.12	0.26 OPC[a] 0.13 SAGEII[b]	0.14-0.18
Dec 1988	37°N, 19 km	0.06 PCS[c] 0.25 SAGE II[b]	0.11	0.25 PCS[c] 0.14 SAGE II[b]	0.16
Spring 1991	41°N ,17 - 21 km	0.02-0.06OPC[d] 0.19 SAGE II[b]	0.08-0.12	0.11-0.13 OPC[d] 0.14 SAGE II[b]	0.16-0.19

Table 2: Comparison of simulated aerosol mass density and effective radius at NH midlatitudes with observed background values of the Stratospheric Data Intercomparison (Kent et al., 1995) for the corresponding latitude and altitudes [a](Hofmann, 1990), [b]SAGEII (Kent et al., 1995),[c]PCS (Wilson et al., 1993), [d]OPC (Deshler et al., 1993). Table after *Timmreck (2001)*.

New particle formation through homogeneous nucleation occurs in the cold tropical lowermost stratosphere and upper troposphere and in polar spring at high latitudes (*Timmreck, 200*1). The calculation of the nucleation rate includes larges uncertainties (several orders of magnitude) and is computationally expensive. *Vehkamäki et al. (2002; 2013)* developed therefore a parameterization for the binary homogeneous nucleation rate of H_2SO_4 (g)/H_2O for global models applicable to all altitudes from the boundary layer to the stratosphere. The parameterization reduces the computing time by a factor 1/500 compared to non-parameterized nucleation rate calculations and reproduces the nucleation rate given by the classical theory well within order of magnitude for nucleation rates in the range of 10^{-7}-10^{10}/(cm^3s) and temperatures between 190 -305 K.

In order to test the reliability of different aerosol microphysics modules, box model intercomparison were carried out with varying SO_2 concentrations from background conditions to values consistent with stratospheric injections by large volcanic eruptions (*Kokkola et al., 2009*). The comparison was done between three modules implemented in the climate model ECHAM5: the modal aerosol microphysics module M7 (Vignati et al., 2004, Stier et al., 2005), which has been adapted to stratospheric purposes (*Niemeier et al., 2009*), and two sectional aerosol microphysics modules, SALSA (Kokkola et al., 2008), and *SAM2 (*Hommel, 2008*; Hommel et al., 2011)*. The detailed aerosol microphysical model MAIA (Lovejoy et al. 2004; Kazil et al., 2007) was used as a reference model. Under background conditions, all microphysics modules

similarly described the shape of the stratospheric aerosol size distribution, but the inter-model spread started to deviate with increasing initial SO_2 concentrations. In particular for the volcanic case, the set ups of the aerosol modules needed to be adapted in order to capture the evolution of the aerosol size distribution, and to perform well in global climate simulations. In a 2D model intercomparison study, Weisenstein et al. (2007) tested the impact of the applied aerosol model configuration on the simulated aerosol size distribution for three versions of a modal and a sectional aerosol model. They found that the representation of the size distribution could have an important impact on the simulated aerosol decay rates in the aftermath of the Mt. Pinatubo eruption.

A first global aerosol model intercomparison study has been carried out in the frame of *ASAP2006*. The intercomparison shows that global model results and satellite observations of stratospheric aerosol extinction agree reasonably well under background conditions for visible wavelengths but less satisfactorily for the infrared. The global aerosol models could however not reproduce the observed sharp vertical gradient in extinction between 17-20 km in the tropics which might be related to the relatively coarse vertical model resolution of at least several 100 meters in the stratosphere or to an incorrect simulation of transport processes (*ASAP2006*). For the volcanic case study the model results show no clear picture. Over- or under predicting SAGEII extinction measurements depends on the applied model and the assumed initial vertical emission height (*ASAP2006*). Since 2006 the number of global aerosol models has increased steadily. While *ASAP2006* analysed only 5 global two and three-dimensional stratospheric aerosol models, nowadays more than 15 global three-dimensional models available (*Kremser et al., 2016*). Several of these models also include the full interaction between aerosol, chemistry and radiation and a few e.g. CESM (WACCM) (Mills et al., 2016) also ocean dynamics. The large increase in global aerosol models together with the significant increase in satellite and in-situ observations over the last decade (*Kremser et al., 2016*) sets therefore the fundament for new model intercomparison and model validation studies. Such studies will be imperative to constrain the post-volcanic aerosol size distribution and radiative forcing (*Timmreck, 2012*). In chapter 5.2 ongoing efforts in this field will be illustrated.

2.3 Transport processes

The stratospheric aerosol layer is controlled by the transport of sulfur-containing species, mainly carbonyl sulfide (OCS), SO_2 and sulfate aerosol particles from the troposphere across the tropical tropopause to the stratosphere (e.g. *ASAP2006*; *Timmreck, 2001*; Brühl et al., 2012; *Kremser et al., 2016*) and by direct injection from large volcanic eruptions. Potential other transport

pathways of sulfur into the lower stratosphere outside the deep tropics have been identified, for example in the MAECHAM5-SAM2 studies (*Hommel et al., 2011*) from modeled aerosol mixing ratios. *Hommel et al*. (2011) indicate that convective updraft in the Asian Monsoon region significantly contributes to both stratospheric aerosol load and size. This result has been confirmed by satellite observations of the June 2011 Nabro volcanic eruption (Bourassa et al., 2012) and by observations of biomass burning plumes *(*Randel et al., 2010). Large volcanic eruptions, in particular the June 1991 eruption of Mt. Pinatubo with its large amount of observational data, provide a unique opportunity to study stratospheric transport processes. Satellite records of the spatial spread of the volcanic aerosol after tropical eruptions indicate that an upper and a lower transport regime exist in the stratosphere (Trepte and Hitchman, 1992; Trepte et al., 1993). The lower transport regime is characterized by fast meridional poleward transport. The upper transport regime is connected with a stratospheric tropical reservoir between 20 °S and 20 °N, caused by a subtropical transport barrier along isentropic surfaces, is especially stable during the easterly phase of the quasi-biennial oscillation (QBO). The dispersal of the Mt. Pinatubo cloud is therefore also an ideal test bed for the atmospheric tracer transport in global circulation models. Global models such as ECHAM4(-CHEM) (*Timmreck et al., 1999a;b; 2003*) and MAECHAM5-HAM (*Niemeier et al., 2009; Toohey et al., 2011*) are in general able to represent the formation of two observed distinct maxima in the zonal mean aerosol optical depth (AOD) after the Mt. Pinatubo eruption, even though atmospheric dynamics were not forced to represent the actual dynamics of the years 1991–1993 (Figure 4). These model as well as other global models (Oman et al., 2006a; English et al., 2013) fail however to reproduce the long persistence of the tropical aerosol reservoir (Figure 4). In the satellite data the tropical maximum can still be observed in April 1992, while in the simulation the maximum is shifted to high latitudes much earlier. *Timmreck et al. (2003)* could show that the inclusion of stratospheric chemistry and the interactive treatment of stratospheric ozone improve the model simulations slightly, because the volcanic aerosol cloud persists one month longer in the tropics. One reason for the fast decay of the tropical maximum seems to be the missing QBO in all these simulations, which has an important influence on the transport of aerosols from the tropical stratospheric reservoir to midlatitudes (Choi et al., 1998).

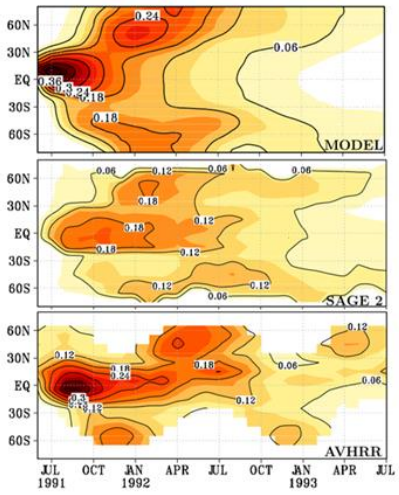

Figure 4: Aerosol optical depth at 0.55 µm, model results (top), SAGE II data (middle) (Thomason et al., 1997), and AVHRR data (bottom) (Long and Stowe, 1994). Figure from *Niemeier et al. (2009).*

Further insights into the model's capability to simulate the correct transport pattern after the Mt. Pinatubo eruption can be achieved by comparing the simulated aerosol surface area density with in balloon-borne measurements from Laramie, Wyoming (41 °N) (Deshler et al., 1992; 1993). Taking into account that in general it is difficult to compare in situ measurements under specific synoptic conditions with climate model simulations, the measurements are reproduced quite well especially at 22 km and 18 km (Figure 5) (*Timmreck et al., 2003*). However, in the two uppermost layers the model simulation overestimates the observations by a factor of 2–3 (Figure 5a). *Timmreck et al*. (2003) found a possible explanation by comparing observed vertical profiles of surface area density with model results for the corresponding grid box (Figure 5b). The model is not able to reproduce the observed layered small structures and the sharp decrease in the vertical profiles above 25 km. This might be related to the fact that the vertical resolution in the MAECHAM4 model in the stratosphere is ~2 km, twice as large as in the observations (1 km). Furthermore, numerical vertical diffusion leads to artificial vertical transport in the simulations and to a smoothing of the vertical profile. The observed vertically thin stable aerosol layers are known to occur not only for stratospheric volcanic aerosols but also for other natural systems. These processes, leading to stratification and layering, are not resolved in the current model versions (*Timmreck et al., 200*3).

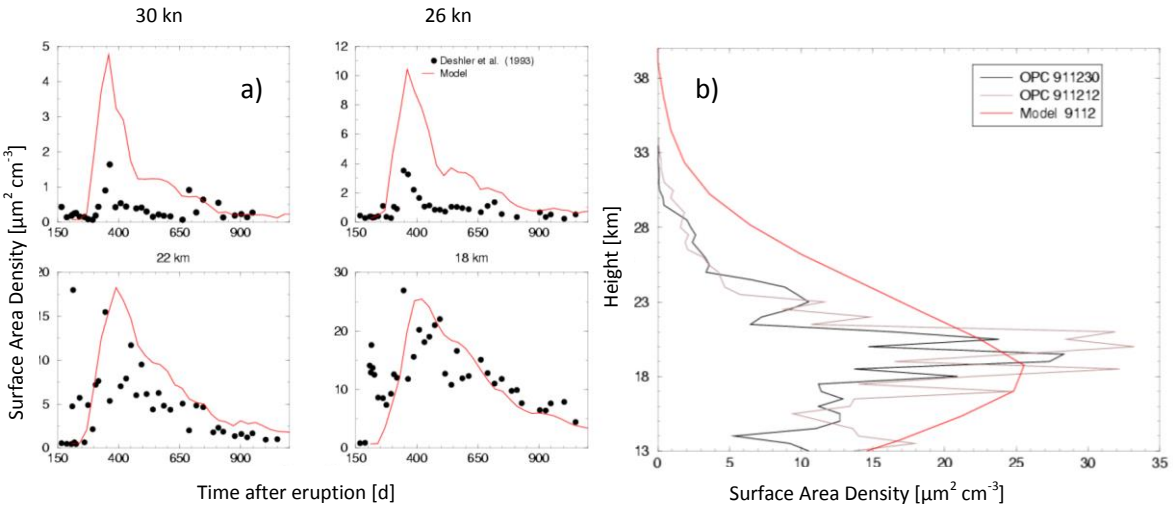

Figure 5: (a) Temporal development of the aerosol surface area density ($\mu m^2\ cm^{-3}$) at 41°N. The black dots indicate the measurements (Deshler et al., 1993) and the red line denotes the simulated monthly mean values for the corresponding grid. (b) Comparison of the observed aerosol surface area density ($\mu m^2\ cm^{-3}$) at 41°N (Deshler et al., 1993) in 2 specific days in December 1991 with simulated monthly mean values for the corresponding grid point. The black and brown lines denote the measurements and the red line the model results. Figure from *Timmreck et al., (2003).*

The volcanic aerosol cloud is not only transported by the prevailing wind fields like a passive tracer but it could also change the local circulation itself by the absorption of near infrared and infrared radiation. Aerosol induced heating is especially important in the first post-eruption months when the aerosol cloud is quite dense. Simulation of the global transport of the Mt. Pinatubo cloud with an offline transport model (Young et al., 1994) and a mechanistic model (Fairlie, 1995) showed that the dynamic response to local aerosol heating has an important influence on the initial dispersal of the volcanic cloud. Performing non-interactive and interactive Mt. Pinatubo simulations with a fully coupled GCM with prognostic volcanic aerosol, *Timmreck et al. (1999b*) indicated that an interactive coupling of the aerosol with the radiation scheme is necessary to adequately describe the observed transport characteristics over the first months after the eruption. Only in the interactive set-up, is the model able to simulate the initial southward cross-equatorial transport of the volcanic cloud, as well as a reduced northward and an enhanced meridional transport towards the south, consistent with satellite observations.

MAECHAM5-HAM simulations (*Niemeier et al., 2009)* could also show that depending on the location of the volcanic eruption, the initial transport direction changes due to the presence of volcanic fine ash. Volcanic fine ash (r<15 µm), which is usually located below the volcanic SO_2 cloud, leads to an additional radiative heating in the first days after the eruption. In the tropics, the local impact of the fine ash heating is too weak to interfere with the prevailing winds, but at 60 °N the situation is different because the local flow is weaker and the Coriolis- Force is stronger. There the additional heating leads to a vertical extension of the rotating volcanic cloud

and an increased uplift of the volcanic (sulfate) cloud. Changing wind directions with height together with increased wind speeds, leads then to changes in the transport direction of the volcanic sulfate cloud *(Niemeier et al., 2009).*

The global dispersal of the volcanic aerosol cloud is mainly controlled by the stratospheric large-scale circulation, and therefore depending on the eruption season and on the specific meteorological conditions at that time. *Timmreck and Graf* (2006) were the first, who pointed to the large impact of the eruption season on the hemispheric distribution of a NH midlatitude volcanic cloud. In winter, when the NH stratospheric circulation is dominated by westerlies, the volcanic cloud is transported east- and northward while for a summer eruption, the volcanic aerosol move west- and southward, driven by the Aleutian high pressure system. Hence, the aerosol cloud in the winter experiment remains mainly in the NH whereas in the summer experiment a significant part of the aerosol crosses the equator (Figure 6).

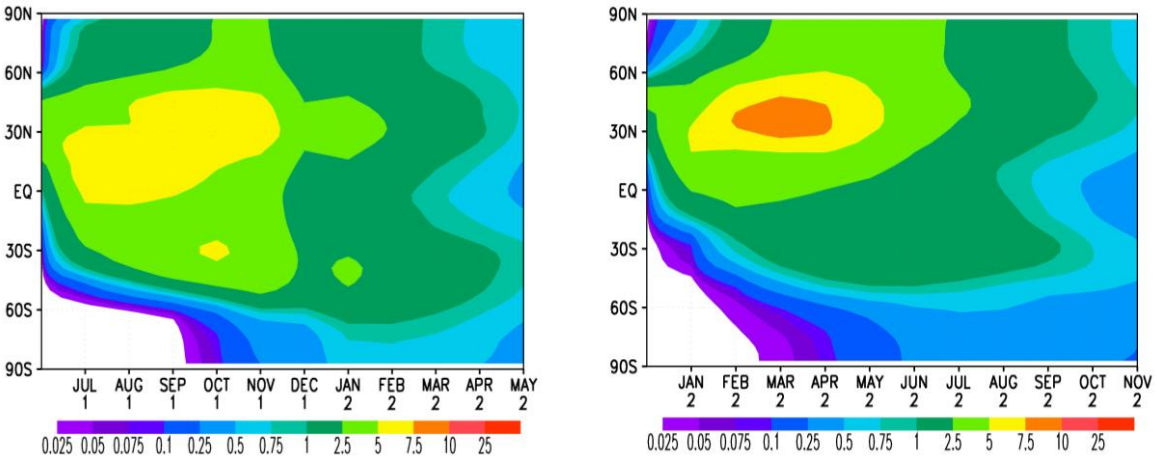

Figure 6: Aerosol optical depth at 0.5 µm for a Yellowstone type eruption in the summer (left) and winter (right). Numbers at the abscissae mark month and year after the eruption. Figure from *Timmreck and Graf (2006).*

Model studies of the seasonal influence of emission on the global aerosol distribution for a Mt. Pinatubo- size tropical volcanic eruption showed that the eruption season has a strong influence on the timing and strength of volcanic aerosol transport out of the tropics into the extra tropics *(Toohey et al., 2011).* Seasonal variations of the BDC lead, for example, to stronger volcanic aerosol transport to the NH after eruptions in October and January. Furthermore, the fact that the BDC is stronger in NH winter than in SH winter is reflected in the asymmetric aerosol dispersal with respect to hemisphere and season. Aquila et al. (2012) also showed that the initial cross-equatorial transport of the volcanic cloud arising from a Mount Pinatubo–like eruption is strongly dependent on the season of the eruption and is much stronger if the eruption takes place just prior to or during austral winter.

3. Radiative forcing

3.1 Volcanic radiative forcing

In terms of volcanic radiative forcing, here the instantaneous radiative forcing is discussed. The instantaneous radiative forcing is estimated by calling the radiation code twice in the model simulations: with volcanic aerosol and without. The radiative imbalance at the top of the atmosphere (TOA), which takes into account the response of the system via feedback processes, is slightly smaller as the radiative forcing (Figure 7). Klocke (2011) investigated the relationship between the maximum volcanic forcing strength and net radiaitive forcing and surface temperatures anomalies in MPI-ESM simulations of the last millennium for about 648 volcanoes and found that the normalized TOA forcing peaks about one year after the eruption with shortwave (SW) flux anomalies almost twice as large as the LW ones (Figure 7).

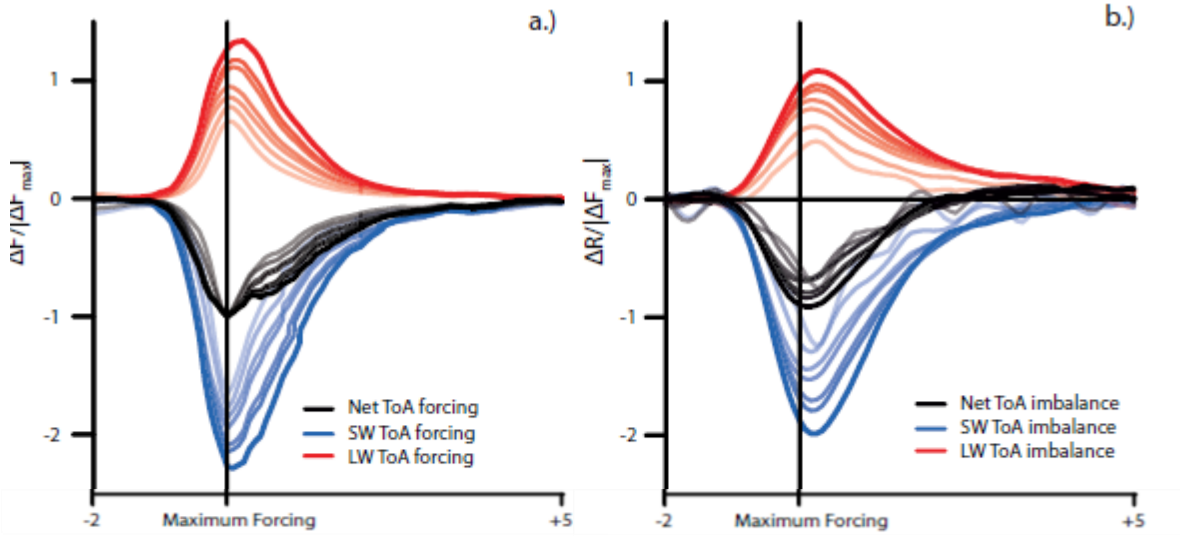

Figure 7: Composite statistics for large volcanic eruptions taken from 10 ensemble simulations of the last millennium (Jungclaus et al., 2010): (a) composite top-of-atmosphere radiative forcing, (b) as for Figure 7a but showing radiative imbalance. All quantities were normalized by the maximum net forcing of each eruption before the mean of all 10 simulations was calculated. Furthermore, the seasonal cycle was removed from all-time series. Color coding indicates the threshold of the minimum forcing for all considered volcanoes. Lightest color considers all volcanoes with a forcing larger than 0.1 W/m^2, and then the threshold increases in steps of 0.5 W/m^2 from 0.5 to 3.0 W/m^2 (Figure from *Kremser et al. (2016),* based on Klocke (2011).

For the Mt. Pinatubo eruption, information about the radiative forcing can be retrieved from satellite observations e.g. the Earth Radiation Budget Experiment (ERBE) data (Barkstrom, 1984; Minnis et al., 1993), which can be used to validate the model capabilities to simulate the volcanic radiative forcing. MAECHAM5-HAM model simulations (*Toohey et al., 2011*) which explicitly treat aerosol microphysical processes show for example excellent agreement with the ERBE observations in both, tropical and near-global mean, for the first one and a half years after the eruption (Figure 8). Heating rates are more difficult to observe. Here one needs to rely on

model results. For the Mt. Pinatubo eruption, for example, aerosol induced heating rates of more than 0.3 K/day are calculated in the tropical region for the first months after the eruption (e.g. Kinne et al., 1992; *Timmreck et al., 1999a; 2003*). Latitude and maximum values of the strongest perturbations vary between the months. In August 1991, the maximum calculated heating rates of 0.6 K/day are located in the SH tropics, while in October 1991 and in January 1992 peak values of 0.3-0.4 K/day and 0.2 K/day respectively, are found in the NH tropics.

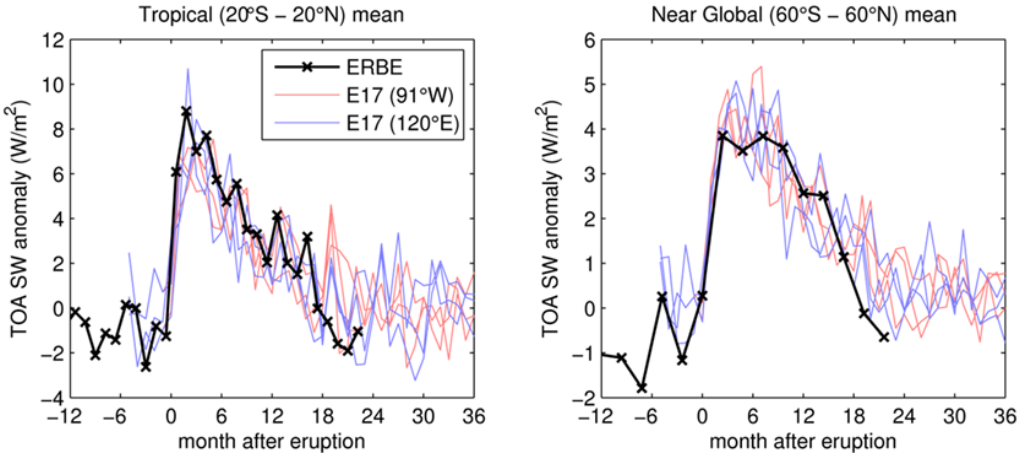

Figure 8: Tropical (20°S – 20°N) and near-global (60°S–60°N) reflected shortwave (SW) flux anomalies at the top of the atmosphere from Mt. Pinatubo eruption period, ERBE observations (black) and MAECHAM5-HAM simulations with eruptions at 15°N, 91°W (red) and 15°N, 120°E (blue). Model anomalies calculated with respect to a 20-yr control simulation, ERBE anomalies calculated with respect to the 1985–1989 mean. Figure from *Toohey et al. (2011).*

The global net volcanic TOA forcing after large volcanic eruptions is in general negative[8], but smaller over surfaces with high albedo, e.g. polar latitudes and deserts (*Timmreck et al., 1999a*). The effect of underlying clouds can also be clearly traced as reduction of the radiative effect, which could locally lead to a positive forcing anomaly in the tropics (*Timmreck et al., 1999a*). This feature can be explained with multiple scattering. At polar latitudes the TOA flux anomalies are also positive in winter. Then the absorption of terrestrial radiation during the polar night leads to a gain of radiative energy, while at lower latitudes the loss due to backscattering of shortwave radiation is dominant. *Toohey et al. (2011)* investigated the influence of the eruption season on the volcanic radiative forcing for a Mt. Pinatubo size tropical volcanic eruption. The model results indicate that global mean AOD and clear-sky surface SW anomalies are sensitive to the eruption season in the order of 15–20 %, which results from differences in the aerosol dispersal and in the aerosol effective radius for the different eruption seasons. But only the very large

[8]It is common e.g. in the MPI-M models to consider downward fluxes as positive and upward fluxes as negative.

volcanic eruptions affect the all-sky SW fluxes significantly. For the Mt. Pinatubo-magnitude eruption all-sky SW anomalies are found to be insensitive to the eruption season, due to the reflection of solar radiation by clouds in the mid to high latitudes.

Besides AOD, the effective radius of an aerosol size distribution is a crucial parameter for the estimation of the volcanic radiative forcing. The aerosol effective radius, r_{eff}, is an area weighted mean radius of the size distribution defined by the ratio of its third moment to its second moment. In a sensitivity study considering the large mid-13th century Samalas eruption[9], *Timmreck et al. (2009)* investigated the impact of the volcanic particle size on the radiative forcing and climate impact. Three experiments have been carried out under the assumption of aerosol mass conservation and constant aerosol lifetime. The most realistic aerosol size distribution with a maximum r_{eff} of 0.7 µm after nine months ($R_{0.7}$) is prescribed in the first experiment. In the second experiment it is assumed that the aerosol size remained constant at the background r_{eff} of 0.2 µm ($R_{0.2}$), and in the third one the increase in aerosol size above background of experiment $R_{0.7}$ is doubled reaching a maximum r_{eff} of 1.3 µm after nine months ($R_{1.3}$). Significant flux anomalies are visible for the first year after the Samalas eruption (Figure 9).

At the TOA the volcanic aerosol impacts the radiative energy balance by reflecting solar radiation back to space (albedo effect) and by trapping terrestrial radiation (greenhouse effect). Thus, by conserving aerosol mass and aerosol altitudes for the three simulations, no significant differences in the greenhouse effect are depicted (dotted lines, Figure 9a). In contrast, the albedo effect is strongly modulated by the prescribed aerosol size (dashed lines, Figure 9a). At the surface the albedo effect dominates, being largest for $R_{0.2}$ with a negative peak surface net flux anomaly of 10.5 W/m^2 in 1258 and smallest for $R_{1.3}$ with a surface flux anomaly of 4.1 W/m^2. The overall net effect of volcanic aerosol is a cooling with a 1.4 °C spread in the global mean surface temperature anomaly between the largest and the smallest assumed effective radius (Figure 8c). Comparing the surface temperature anomalies with temperature reconstructions from this period indicates that only aerosol particle sizes which are remarkably larger than measured after the Mt. Pinatubo eruption lead to temperature changes corresponding to continental NH summer temperature reconstructions (*Timmreck et al., 2009*).

[9]The very large mid 13th century has been recently identified as the Samals eruption of the Rinjani volcanic complex (8 °S) on Lombok Island, Indonesia which erupted between May and October A.D. 1257 (Lavigne et al., 2013). For a long time the eruption location and the eruption date were unknown. In my papers prior to 2013, I refer to this eruption as unkown 1258 eruption. In this thesis I use now the accepted notation Samalas, albeit the fact that the nomenclature is different to the cited references.

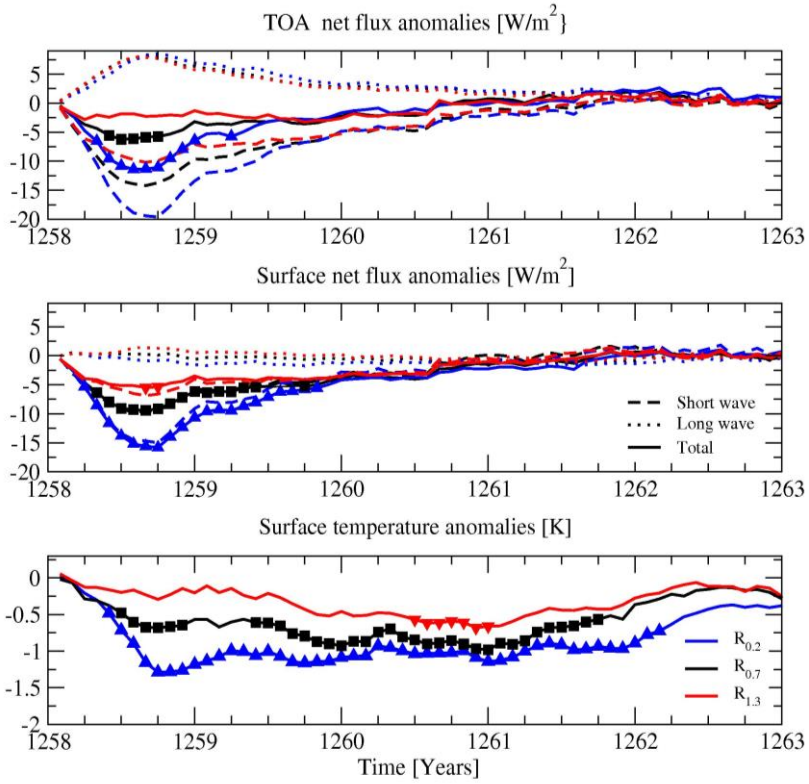

Figure 9: Globally averaged net radiative flux anomalies after the Samalas eruption (top) at the top of the atmosphere [W/m^2], (middle) at the surface, and (bottom) near surface temperature anomalies [K] in MPI-ESM simulations. Black line ($R_{0.7}$): original data set (maximum r_{eff}=0.7 µm); blue line ($R_{0.2}$): same mass as in $R_{0.7}$ but constant background effective radius (r_{eff}=0.2 µm); red line ($R_{1.3}$): same mass as in $R_{0.7}$ but higher effective radius (doubled the increase in size about background) (maximum r_{eff}= 1.3 µm). Solid symbols denote monthly mean values that are statistically significant at the 90% confidence level. Figure from *Timmreck et al. (2009).*

The importance of a temporally varying effective radius for the volcanic radiative forcing and the subsequent cooling is especially evident for very large volcanic eruptions. Incorporating aerosol microphysical processes in the Max-Planck-Institute Earth system model (MPI-ESM) simulations for a tropical super eruption (with an assumed volcanic sulfur emission of 100 times Pinatubo (850 Tg S)) *Timmreck et al. (2010)* obtained with their microphysical model a maximum r_{eff} of 1.1 µm, which is much larger than the observed Mt. Pinatubo effective radius of 0.5 µm (see also Figure 3). Similar results are obtained with the WACCM/CARMA model (English et al., 2013) with a peak r_{eff} of 1.6 µm for a slightly higher sulfur emission (1000 Tg S). The corresponding maximum AOD, which *Timmreck et al. (2010)* estimated in their simulations, is a factor of 3.5 smaller compared to the 100-times Pinatubo AOD (Sato et al., 1993) as used by Jones et al. (2005) and an e-folding AOD decay time reduced by a factor of two from 12 months to 6.8 months. As a result, *Timmreck et al. (2010)* simulated a global surface air temperature response about a factor of three smaller than in previous Toba studies, which used an effective radius as observed after the much smaller 1991 Mt. Pinatubo eruption (Robock et al., 2009) or which

simply scaled Mt. Pinatubo AOD (Jones et al., 2005; Harris et al., 2011; Frölicher et al., 2011). The latter implictely assume an effective radius consistent with that of the Mt. Pinatubo eruption.

3.2 Radiative forcing data sets

Unfortunately, direct atmospheric measurements of volcanic disturbances are only available for the past few decades. So volcanic forcing has to be reconstructed for the past from available optical measurements (Sato et al., 1993 Stothers, 1996; 2007) and/or best estimates of the potential atmospheric sulfur loading after a historical eruption, which can be obtained either from paleo volcanic ice core records (Gao et al., 2008; Crowley and Unterman, 2013, Sigl et al., 2014) or from the petrological method by analyzing eruption deposits (Devine et al., 1984). Optical measurements which take advantage of the ability of volcanic aerosols to change the refractive properties of the atmosphere and to alter the visual appearance of luminaries are best suited to give information about the volcanic radiative forcing. This approach is however limited in several ways. Satellite measurements, which nowadays could provide the best and exact measurements of volcanic AOD with global coverage, are only available for the last 30 years and might be supersaturated during times of the highest aerosol load as seen for SAGE II during the first year after the Mt. Pinatubo eruption (e.g. Russel et al., 1996). Based on pyrheliometric observations, stellar extinction observations and descriptions of total lunar eclipses in historical documents, a three hundred year climatology of volcanic AOD was reconstructed for the pre-satellite area (Stothers, 2007). An important caveat of these data is, however, that they are based on sparse local observations and random description of extraordinary weather phenomena. Petrological data, i.e. the chemical analysis of tephra, on the other hand provide only a lower estimate of the eruptive sulfur yield (Devine et al., 1984; Scaillet et al., 2003) because the total amount of the erupted magma is often not exactly known. In addition, estimates of the pre-eruptive sulfur content from melt droplets, which are included in the magma, are highly uncertain as reactions during the eruption phase could have altered the results.

Most commonly ice core records are used to reconstruct volcanic sulfur loading and volcanic radiative forcing, over millennial time scales (e.g. Crowley et al., 1993; Zielinski, 1995; Robock and Free 1995; Gao et al., 2008; Crowley and Unterman, 2013[10] Sigl et al., 2013; 2014; 2015). The accuracy of volcanic ice core records however drops back in time because the likelihood of

[10] A subset of this data set was described in a PAGES article (Crowley et al., 2008), which is often quoted instead of Crowley and Untermann (2013).

deformation processes increases with the depth of the ice cores (Oppenheimer, 2011). Local glaciology factors (e.g. deposition processes, snow accumulation rate) can substantially impact the interpretation of the records (Cole-Dai, 2010). Hence, it is necessary to combine records from different locations in order to retrieve a representative estimate of global volcanic forcing from ice cores (Gao et al., 2007; Cole-Dai, 2010; Crowley and Unterman, 2013; Sigl et al., 2013). Nowadays precise reconstructions of volcanic sulfate deposition are available for the past 2,000 years (Sigl et al; 2013), which allow a revision of the timing of past volcanic events. For example, the large bi-hemispheric deposition event ascribed to the Kuwae eruption in Vanuatu, previously thought to be 1452/1453, is placed now to the year 1458/1459. Using high precision ice core chronologies in combination with a multi-disciplinary approach, Sigl et al. (2015) could resolve inconsistencies between the reconstructed timing of volcanic sulfate deposition on the ice-sheets and tree-ring records for the last 2 thounds years.

Nevertheless, the relationship between polar ice sheet deposition and atmospheric stratospheric sulfate burden is a crucial factor for the interpretation of ice core volcanic sulfate signals. Originally, radioactive material during nuclear bomb tests of the 1950's and 1960's was used to derive scaling factors to relate polar ice sheet sulfate deposition to atmospheric burden assuming that the quantities are directly proportional (Clausen and Hammer, 1988; Hammer, 1977). MAECHAM5-HAM simulations for large tropical eruptions with SO_2 injections ranging from 8.5-700 Tg (*Toohey et al., 2013*) demonstrate that this is not the case. The model results suggest that the relationship between Antarctic and Greenland volcanic sulfate deposition is non-linear for eruptions of Tambora-magnitude and larger, with significantly less sulfate deposition to Antarctica than to Greenland. For large SO_2 injections, the aerosol particle size increases, this impacts aerosol sedimentation velocity and radiative properties and leads to strong dynamical changes including strengthening of the winter polar vortices. The latter inhibits the poleward transport of the volcanic aerosols and thereby modulating their deposition efficiency (Figure 10).

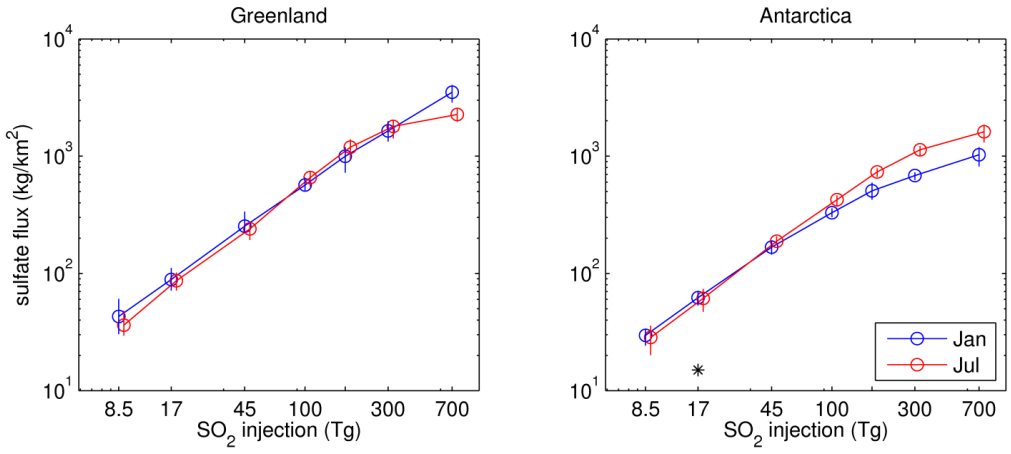

Figure 10: Modeled average sulfate deposition flux [kg/km^2] to Greenland and Antarctica for January and July eruptions as a function of SO_2 injection magnitude. Black star indicates the estimate of the average Antarctic sulfate flux from Pinatubo and Cerro Hudson eruptions derived from ice cores (Gao et al., 2007). Figure from *Toohey et al. (2013).*

In a next step, the volcanic sulfur emissions derived from ice cores had to be transformed into radiative forcing estimates. This is usually done by using empirical relationships between mass loading and AOD (Hyde and Crowley, 2000), or by simplified estimates based on model studies and atmospheric transport parameterizations. Often, a fixed aerosol effective radius is assumed for the optical calculations (Gao et al., 2007; Ammann et al., 2003; 2007). Combining global aerosol model simulations with observational based records of volcanic emissions, *Metzner et al. (2014)* produced a 2000 year time series of AOD and radiative forcing for application in large scale models for the Central American Volcanic Arc (CAVA). The conversion of observationally derived SO_2 emissions to the radiatively relevant AOD was achieved with two methods: 1) an approximate method based on simple parameterized relationships from past studies (e.g. Hyde and Crowley, 2000), and 2) based on results from the global aerosol model MAECHAM5-HAM (Stier et al., 2005; *Niemeier et al., 2009*). Comparing these AOD with global aerosol model results, *Metzner et al. (2014*) revealed that simple relationships between mass and AOD are accurate enough to describe the global maximum AOD, but are critical for the simulation of the temporal AOD evolution and decay rate.

Nevertheless, volcanic forcing estimates for eruptions of the past centuries have substantially improved over the last decade (*Timmreck, 2012*). Global annual mean data sets of TOA radiative forcing data (e.g. Crowley et al., 2003) are nowadays usually replaced by two- and three-dimensional data sets of monthly or higher time resolution (Amman et al., 2007; Gao et al., 2008; Crowley and Unterman, 2013), which also contain information about the particle size (Sato et al., 1993 (updated); Crowley and Unterman, 2013). Despite all recent improvements, the volcanic radiative forcing remains an important uncertainty. For example, the two

recommended volcanic forcing data sets (Gao et al., 2008; Crowley and Unterman, 2013) in the Paleoclimate Model Intercomparison Project 3 (PMIP3) protocol (Schmidt et al., 2011) show differences of about a factor of two in the forcing for the 1453 eruption (-12 W/m^2 and -5.4 W/m^2).

An important step is therefore the compilation of volcanic forcing with global stratospheric aerosol models. Arfeuille et al. (2014) calculated with a global microphysical aerosol model the global aerosol size distribution of the largest 26 volcanic eruptions over the last 400 years. Mills et al. (2016) developed a new prognostic capability for simulating stratospheric sulfate aerosols in the Community Earth System Model (CESM) to reconstruct global aerosol properties from 1990 to 2015. For CMIP6 some model centers plan to simulate the volcanic forcing online with global aerosol climate models. The use of global aerosol models has the great advantage that the global dispersal of the aerosol cloud and the aerosol forcing, is consistent with the simulated meteorological fields which is of particular importance for NH polar winter stratosphere (see section 4.3). Furthermore these models are also suitable for near-real time forecasting as the radiative forcing of future volcanic eruptions will probably considerably different from past ones in time, strength and location. However, interactive global aerosol simulations introduce more degrees of freedom into the model, which increase the range of uncertainties and which make a model intercomparison more difficult (see section 5). Driven by the motivation to have an easy and flexible forcing implementation strategy for volcanic aerosol, which is fast, model independent and which produces a consistent representation of eruptions over large historical time periods and a reasonable forecast for future events, *Toohey et al. (2016)* developed the Easy Volcanic Aerosol module (EVA) to use in global climate simulations. EVA consists of analytic formulations of wavelength dependent aerosol's radiative properties (aerosol extinction, single scattering albedo, and asymmetry factor), derived from an input list of eruption parameters (date, location and estimated stratospheric SO_2 emission and hemispheric asymmetry ratio). The structure of the prescribed forcing fields aims to reflect primary modes of spatial and temporal variability.

EVA is validated against satellite observations after the 1991 Mt. Pinatubo eruption (Figure 11) and scaled for larger eruption magnitudes consistent with the Crowley and Unterman (2013) forcing data set. The design of EVA allows for great flexibility, which makes it well suitable for idealized studies, but which cannot reproduce all observed features of aerosol forcing. EVA is, however, capable to address fundamental questions about the interactions of stratospheric aerosol and climate.

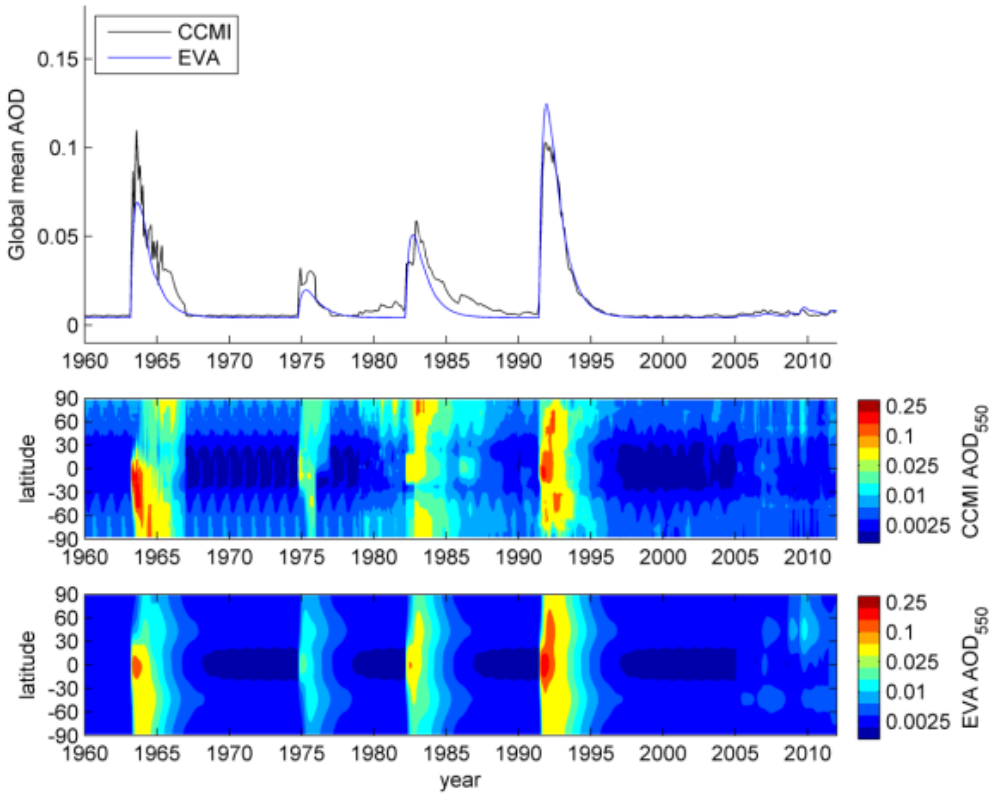

Figure 11: Global mean aerosol optical depth (AOD) at 0.550 µm between 1960-2015 from the Chemistry Climate Model Initiative (CCMI) data set (Eyring et al., 2013) and from EVA (upper panel). Zonal mean AOD at 0.55 µm as a function of latitude and time, with log color-scale or both reconstructions (middle and lower panel). Figure from *Toohey et al. (2016).*

Chemistry Climate models (CCMs) need, in addition to the radiative properties, information of the volcanic aerosol particle size to take into account also its impact on stratospheric ozone chemistry. CCM model intercomparison studies have shown substantial differences in the atmospheric response to volcanic eruptions, specifically in for temperature and ozone (Manzini and Matthes, 2010). The inter-model spread is mostly related to different and partially inconsistent parameterizations of the volcanic aerosol impact on radiative transfer and atmospheric chemistry. An internally consistent stratospheric aerosol data set was therefore compiled for the chemistry climate model initiative (CCMI) (Eyring et al., 2013; Arfeuille et al., 2013), which provides data for aerosol surface area density and for aerosol radiative parameters (extinction coefficient, asymmetry factor, and single scattering albedo) for the period 1960 – 2010 based on SAGEII and Cloud-Aerosol Lidar and Infrared Pathfinder Satellite Observations (CALIPSO) satellite data. The CCMI SAGE4λ data set has been updated and extended over the historical period (1850-2014) (Thomason et al., in prep.) for CMIP6 (Eyring et al., 2016).

4. Volcanic Impact on the Earth System

4.1 Surface climate response and climate sensitivity

Large volcanic eruptions lead in general to surface cooling and stratospheric warming (Robock, 2000), which are modulated by dynamical processes and internal variability. The surface temperature response is short-lived (a couple of years) and for Mt. Pinatubo size eruptions in the range of internal variability. Lehner et al. (2016) therefore emphasize the role sampling biases might play in the analysis and interpretation of volcanic signals in surface temperature anomalies. For example, the analysis of CMIP5 models shows an overestimation of the observed post-eruption global surface cooling (Marotzke and Forster, 2015), which decreases if the correct ENSO phase is taken into account (Lehner et al., 2016). Studying the relation between volcanic forcing and surface cooling in the MPI-ESM Millennium simulations (*Jungclaus et al., 2010*), Klocke (2011)) found that surface temperature response lags the forcing by 12 to 24 months depending on the strength of the forcing and adjusts back to the equilibrium temperature slower than the radiative flux perturbation decays. The adjustment time is strongly dependent on the strength of the volcanic eruption. Differences in the simulated global and regional surface air temperature response between a Mt. Pinatubo-size, a Tambora-size and and a Young Toba Tuff (YTT)-size volcanic eruption are shown in Figure 12.

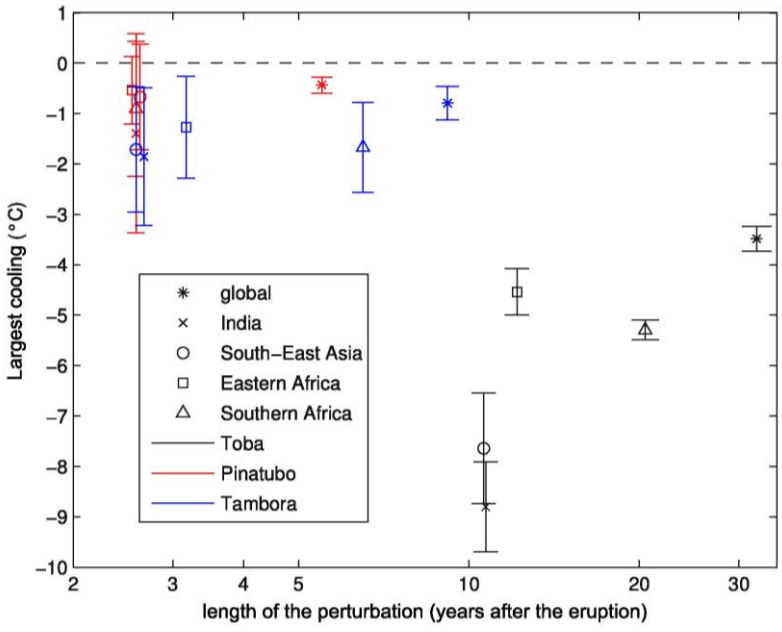

Figure 12: Scatter plot of ensemble-based monthly mean maximum cooling [K] versus length of perturbation (years) for the global average and four specific regions (indicated by different symbols) and for three different volcanoes (indicated by different colors) based on MPI-ESM ensemble simulations The length of perturbation indicates the time from the start of the eruption until the signal is within 0.5 of the standard deviation of the control run. A 61-month running average was used for the detection of the perturbation length. From *Timmreck et al. (2012).*

As expected, the cooling peak for the Tambora-size eruption is much weaker than for the YTT-size eruption, due to the difference in the estimated sulfur emission of more than one order of magnitude between the two simulations (Table 1). MPI-ESM results for the 1991 Mt. Pinatubo eruption match the observed maximum cooling of 0.4 K (e.g. Thompson et al., 2009) quite well, while the simulated global maximum cooling of 0.875 ± 0.3 K for the Tambora eruption is at the lower end of current estimates in the range of 0.8 K to 1.35 K (*Raible et al., 2016*). Nonetheless, the peak cooling does not increase linearly with the strength of the total stratospheric sulfur emission. For example, for the YTT eruption the global cooling is only a factor of 4.4 stronger than for the Tambora eruption. Multiple limiting effects are responsible for this, including those based on radiation transmission (Beer-Bouguer-Lambert) and the increase in particle size that was taken into account in the model simulations (*Timmreck et al., 2012*). The volcanic cooling is not only stronger for a YTT size eruption, but it also persists longer. The length of the global Mt. Pinatubo signal with six years appears to be consistent with the observed Mt. Pinatubo relaxation time. For all eruptions the volcanic signal persists much longer in the global temperature data than in the depicted regional averaged temperature data. This behavior can be explained with the long persistence of volcanic signal in the Arctic in the MPI-ESM due to the accompanying onset of an anomalously weak post-eruption oceanic heat transport in the North Atlantic and of sea ice-snow-albedo feedbacks (Zanchettin et al., 2012a, see section 4.3).

The climatic impact of past volcanic eruptions can be derived from climatic proxy data (tree rings, corals, subfossil-pollen, boreholes, lake and ocean sediments). Some of these methods, in particular tree rings, are extremely beneficial in constructing a volcanic chronology and provide an estimate of the climatic impact of historic eruptions, nevertheless, they are not direct signals of the eruption. Each of these proxy data provides specific different aspects of past climatic conditions with annual or seasonal resolution. In particular, certain characteristics of tree rings (narrow ring width and low maximum latewood density (MXD) have been found to correlate well with the volcanic activity (Briffa et al., 1998; D'Arrigo et al., 2006). However, for very large volcanic eruptions over the past millennium there is a mismatch between the simulated hemispheric cooling response and proxy reconstructions, which could either be related to model estimates, data reconstructions or both. One possible explanation might be the decreased enhancement of diffusive radiation (Robock, 2005) although observational tree ring data (Krakauer and Randerson, 2003) give no indication for it and model studies (*Timmreck et al., 2009*) indicate additionally that the loss in total radiation overweighs the gain in diffusive radiation (section 4.7, *Raddatz et al., EGU General Assembly 2009*)). Another reason is the

increase of the size of the volcanic aerosol particles. *Timmreck et al. (2009*) could show that if the temporal development of the aerosol size distribution is neglected in the radiative calculations the volcanic forcing of large volcanic eruptions is overestimated in the model (section 3.1, Figure 9). Mann et al. (2012; 2013) suggested that chronological errors in tree ring dating and reduced sensitivity to strong cooling in treeline records could be a possible reason for this discrepancy. This has however been refuted by the dendroclimate community (*Anchukaitis et al., 2012;* Esper et al., 2013; D'Arrigo et al., 2013), who stated that there is clear evidence that actual boreal tree ring chronologies are correctly dated. *Anchukaitis et al. (2012)* could also show that reconstructing simulated temperatures in the same manner as Mann et al. (2012) but using a well-tested tree-ring growth model and realistic parameters produced a good agreement between summertime temperatures reconstructed from pseudo proxies and those simulated with a climate model for the whole record. Recently Stoffel et al. (2015) pointed out that it is important to reconcile climate simulations and reconstructions on the hemispheric scale to resolve the discrepancies between proxy and model data.

The volcanic cooling signal was also used to constrain climate sensitivity, although feedback processes related to volcanic forcing and greenhouse gases might be fundamentally different in time and space. Global model studies (Wigley et al., 2005; Yokohata et al., 2005) show a strong relationship between the magnitude of the volcanic cooling signal and its decay time and climate sensitivity. However, a reasonable estimate of the climate sensitivity can only be obtained from the short-timescale responses to large volcanic eruptions (Wigley et al., 2005, Merlis et al., 2014) as the long-lasting response to volcanic eruptions is too small in comparison to internal variability. In addition, for the estimation of the equilibrium climate sensitivity information of the volcanic forcing and changes in the ocean heat content are necessary (Boer et al., 2007). Bender et al. (2010) analyzed radiative flux and surface temperature anomalies after the 1991 Mt. Pinatubo eruption in 10 CMIP3 models. They obtained for the equilibrium climate sensitivity a value in the range of 1.7–4.1 K, which corresponds to the 66% confidence interval from the Intergovernmental Panel on Climate Change (IPCC) Fourth Assessment Report (AR4) report (Hegerl et al., 2007b) (2.0 – 4.5 K). Merlis et al. (2014) pointed out that an observational constrain of transient climate sensitivity (TCS) from the Mt. Pinatubo eruption needs to consider various factors, e.g. asymmetry between warming and cooling, and dependence on the ocean state. Inferring the fast component of climate sensitivity from global models, simulations will therefore give only a lower bound of TCS (Merlis et al., 2014). Klocke (2011) neglects all complications associated with deriving climate sensitivity from volcanic eruptions, and assumed

that the response to volcanic forcing is linearly related to climate sensitivity. He could thereby demonstrate that even with this simplified assumption more than 10,000 years of volcanic activity similar to the last millennium are required to obtain from observations a narrower range of climate sensitivity than from IPCC AR4.

4.2 Impact on atmospheric chemistry

Volcanic emissions change the chemical composition of the atmosphere and can therefore affect the global biogeochemical cycle of many trace elements in several ways (*Textor et al., 2004;* Mather, 2015). A comprehensive overview of the impact of volcanic emissions in particular quiescent degassing on tropospheric chemistry is for example given by von Glasow et al. (2009). In the stratosphere, volcanic aerosols alter the chemical photolysis rates by reflecting and scattering incoming solar radiation (*Textor et al., 2004*). Furthermore, in the tropics chemical trace gases are transported to higher altitudes by increased upward motion that results from aerosol induced heating due to LW and near-infrared absorption (Kinne et al., 1992; *Timmreck et al., 2003*). Additionally, heterogeneous chemical reactions on the aerosol surfaces lead to a reduction of nitrogen oxides (NO_x) and chlorine activation (Solomon et al., 1996).

Tropical ozone profiles observed after the 1991 Mt. Pinatubo eruption (Grant et al., 1994) show decreases (up to 33%) between 16-28 km and small increases from 28 to 31.5 km. *Timmreck et al. (2003)* characterized the observed tropical ozone profile changes as a combined effect of heterogeneous chemistry, changes in photolysis rates and in heating rates. Tropical O_3 decreases between 20-30 km due to heterogeneous chemistry and upward transport, and increases above 30 km due to a decrease in NO_X (Figure 13). Below 20 km the simulated O_3 concentration slightly increases due to changes in the photolysis rates. *Timmreck et al. (2003)* performed the first fully coupled GCM simulation with respect to aerosol and ozone of the Mt. Pinatubo eruption. Prior to that only 2-dimensonal chemistry models (e.g. Tie et al., 1994 Rosenfield, 2003; Fleming et al., 2007) and two CCMs (Al-Saadi et al., 2001; Rozanov et al., 2002) had analyzed the impact of the Mt. Pinatubo eruption on the stratospheric trace gas concentration, but the CCMs prescribed the volcanic aerosol parameters (surface area density, extinction). In the last years the impact of the three largest volcanic eruptions of the last 60 years on atmospheric chemistry has been often discussed in the frame of the international chemistry climate model evaluation studies, e.g. the chemistry-climate model validation activity (CCMVal, Eyring et al., 2010) and the chemistry climate model Initiative (CCMI, Eyring et al., 2013, Hegglin et al., 2014). In these intercomparison studies a considerable spread has been found in the simulated temperature and ozone response to volcanic eruptions due to different parameterizations of the volcanic

aerosol in radiative transfer and atmospheric chemistry calculations (Manzini and Matthes, 2010), see also section 3.2.

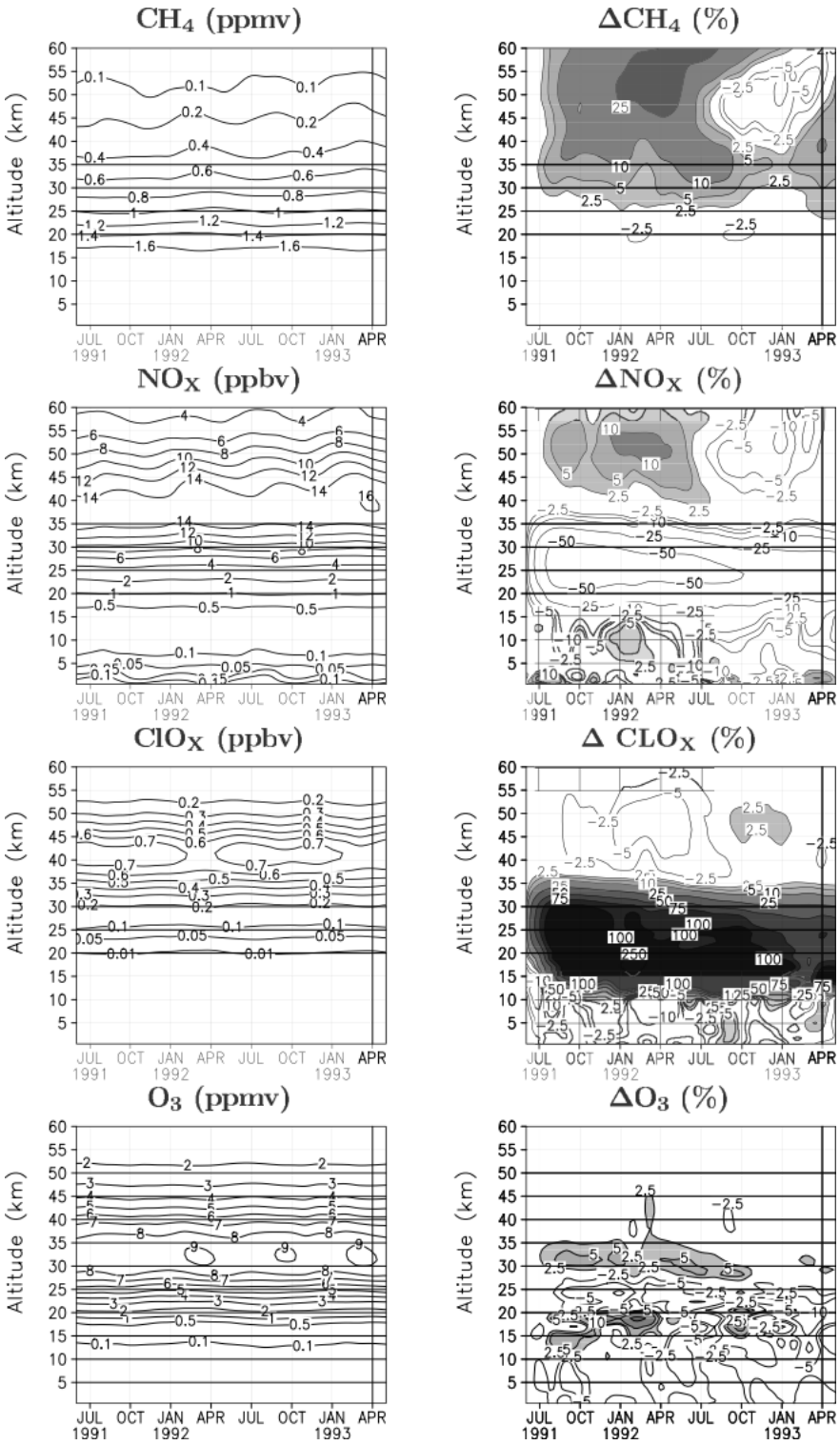

Figure 13: Altitude-height cross section of the tropical averaged (30°S–30°N) trace gas concentrations in an ECHAM4/CHEM simulation of the Mt. Pinatubo eruption: control run (left) and changes between the volcanically disturbed and the undisturbed run (right). From *Timmreck et al. (2003).*

An open question, which has been discussed for a long time in the stratospheric ozone community (e.g. WMO, 2011), was why in the aftermath of the Mt. Pinatubo eruption significant midlatitude column O_3 depletion was only observed in the NH, but not in the SH (e.g. Randel et al., 1995). Changes in the Brewer-Dobson Circulation arising from aerosol induced heating in the tropical stratosphere have been suggested to have counteracted chemical O_3 loss in the SH (Poberaj et al., 2011; Aquila et al., 2013). Dhomse et al. (2015) recently showed that smaller SH column O_3 loss can be attributed not only to dynamical variability but also to lower background stratospheric O_3 concentration in the SH.

Large volcanic eruptions are also a wild card in the future prediction of the ozone layer (*Timmreck*, 2012). Model studies indicate that a major volcanic eruption within the next decades, when there will still be substantial stratospheric concentrations of reactive Equivalent Effective Stratospheric Chlorine (EESC), will increase the ozone depletion and lead to a temporary delay in the recovery of the stratospheric ozone layer (Rosenfield, 2003; Bodeker and Waugh, 2006). Recently, Solomon et al. (2016) suggested that the southern Chilean Calbuco eruption in April 2015 was responsible for the record Antarctic ozone hole in 2015 and masked the ozone recovery. It is also possible that an ozone hole will occur over the Arctic in the upcoming decades if a large volcanic eruption coincides with a cold Arctic winter (Tabazadeh et al., 2002). Polar ozone loss in the first post-eruption winters leads to additional cooling and might therefore have an impact on atmospheric dynamics by strengthening the polar vortex with implications on the Arctic oscillation (AO) (Stenchikov et al., 2002). This is further discussed in section 4.3. However, in conditions with low EESC, a large volcanic eruption could slightly enhance the stratospheric O_3 concentration due to the suppression of nitrogen oxides (Tie and Brasseur, 1995). O_3 will also increase in the first days after an eruption at the top of the volcanic cloud due to the enhanced photo-dissociation of SO_2 (Crutzen and Schmailzl, 1983; Bekki, 1995). The simulated post-volcanic changes in the vertical ozone profile are reasonable but might change if other halogen components e.g. Br or iodine (I) are also taken into account. Recent studies (Kutterolf et al., 2013; Krüger et al., 2015) suggest that volcanic Br emissions could significantly impact stratospheric ozone levels following large eruptions. However, there are still gaps in the understanding of the volcanic halogen emissions to the stratosphere during large volcanic eruptions and their impacts on ozone (Mather, 2015). The effect of the short-term post-volcanic stratospheric water vapor increase on the total tropical ozone concentration seems to be neglible (Stenke and Grewe, 2005). A couple of model studies have also addressed the volcanic impact on other greenhouse gases (CH_4, N_2O) (e.g. Pitari and Mancini 2002; Considine et

al., 2001; Bandă et al., 2015; 2016) as well as on isoprene (Telford et al., 2010). The volcanic impact on the hydrological cycle is discussed in section 4.5 and on the carbon cycle in section 4.8.

4.3 Impact on atmospheric dynamics

One of the most prominent dynamical features after large tropical eruptions found in observational records is an abnormal surface warming in the first two post-eruption winters over the NH continents and anomalously cold winters over the Middle East and Greenland (Robock, 2000; Robock and Mao, 1992). This ”winter warming” pattern, see for example Figure 14a, has a large variability between individual eruptions (Shindell et al., 2004) and is the result of large-scale dynamical processes. It has been suggested (Graf et al., 1993;1994; Kodera, 1994; Graf et al., 2007) that the volcanic aerosol particles produce significant warming in the lower equatorial stratosphere thereby increasing the equator to pole temperature gradient and leading to an enhanced polar vortex and changing atmospheric circulation patterns.

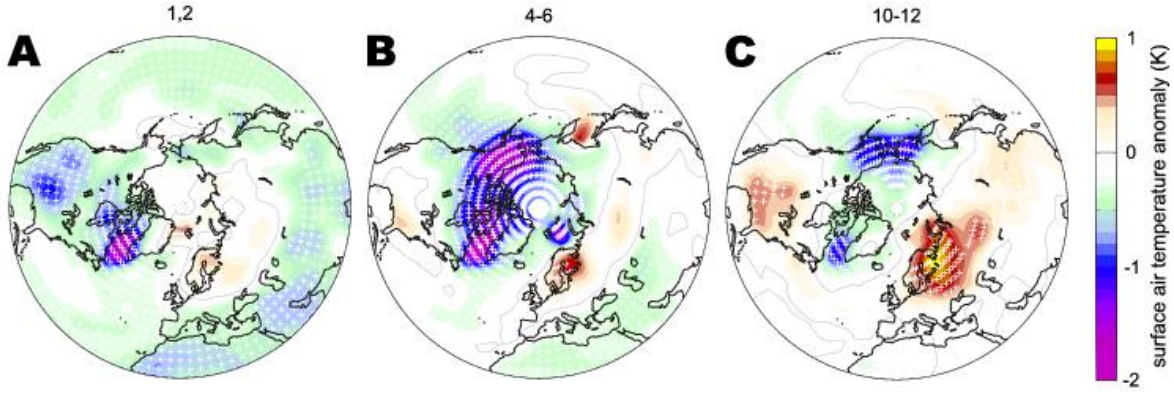

Figure 14: Ensemble-average simulated anomalies of winter Northern Hemisphere surface air temperatures for selected post-eruption winters (indicated by the numbers on the top of each panel) from the MPI-Earth system model simulations of the last Millennium (Jungclaus et al. 2010). Crosses indicate regions where changes are statistically significant at 95% confidence according to the Mann-Whitney U test. Figure from *Zanchettin et al. (2012a).*

This results in an anomalously positive phase of the AO, mostly expressed in the North Atlantic as an enhanced phase of the North Atlantic Oscillation (NAO). The response patterns are most prominent in the first two post-eruption boreal winters (Shindell et al., 2004; Stenchikov et al., 2002; 2006; Fischer et al., 2007). Monthly mean sea level pressure data from 1870 onwards also indicate that in most, but not in all, winters immediately following a volcanic eruption a positive AO and NAO phase were found (Christiansen, 2008). Work at MPI-M (*Zanchettin et al. 2012a; 2013a*) showed that coupled ocean-atmosphere processes lead also to a delayed winter warming pattern about a decade after the eruption (Figure 14c) which will be discussed in section 4.4.

Analysis of historical IPCC AR4 (Stenchikov et al., 2006) and CMIP5 runs (Driscoll et al., 2012) revealed that all climate models could reproduce the observed radiative response to volcanic eruptions (tropical stratospheric warming and surface cooling) but most of them have difficulties to capture the observed dynamical response following volcanic eruptions in the first two NH post-eruption winters. Although, for example, all analyzed CMIP5 models reproduce reasonably well the geopotential height increase in the lower stratosphere at low latitudes, none of the models simulate a sufficiently strong reduction in the geopotential height at high latitudes (Driscoll et al., 2012). In addition, the simulated mean sea level pressure and surface temperature anomaly fields show distinct differences with respect to the observed anomalies. The reasons for the model failures are still unclear and are related to various factors, e.g. a better spatial resolution of the volcanic aerosol distribution (Otterå, 2008; Marshall et al., 2009). To assess the influence of pattern and strength of the volcanic forcing on NH winter climate, *Toohey et al.* (2014) tested the simulated stratospheric dynamical response in winter to four different Mt. Pinatubo volcanic forcing data sets in the MPI-ESM-LR model. While tropical and midlatitude lower stratosphere temperatures are similarly affected in all experiments, significant differences occur in first NH post-eruption winter vortex dynamics (Figure 15). These results suggest that quite accurate aerosol forcing fields would be necessary to improve predictions of the dynamical response to stratospheric sulfate aerosol loading for a Mt. Pinatubo-magnitude eruption.

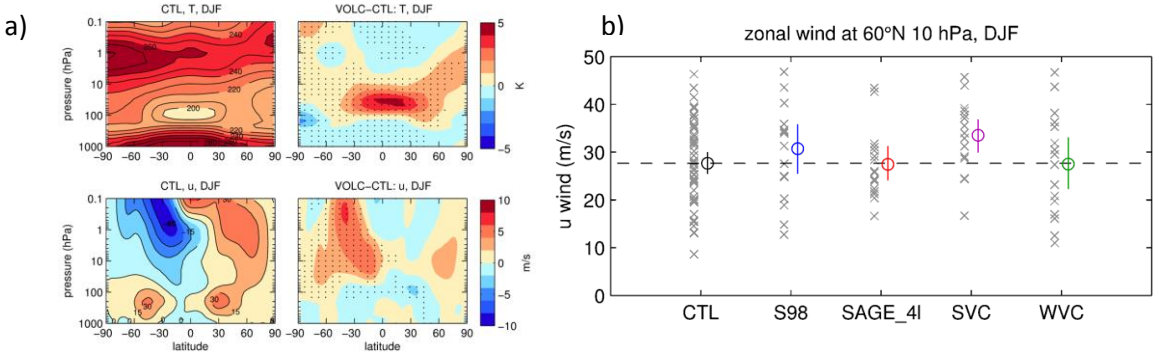

Figure 15: a) DJF temperature (top) and zonal wind (bottom) fields for the MAECHAM5/HAM control (CTL) ensemble (left) and anomalies for the Mt. Pinatubo ensemble (right). Anomalies which are significant at the 95% confidence level are hatched. b) DJF zonal wind at 60°N and 10 hPa for the CTL ensemble and the volcanically forced ensembles S98 (Stenchikov et al., 1998 and updates, SAGE-4α (Arfeuille et al., 2013), MAECHAM5/HAM composites according to strong (SVC) and weak (WVC) vortex states. Individual ensemble members are shown as gray symbols. Ensemble means shown in colored symbols, with vertical whiskers representing the 95% confidence interval of the ensemble mean. Dashed horizontal line shows the ensemble mean of the CTL ensemble. Figures from Toohey et al. (2014).

Other factors under debate are the applied model configurations, i.e., an insufficient vertical resolution in the stratosphere and/or a too low model top height (Shindell et al., 2004; Stenchikov et al., 2006). However, Marshall et al. (2009) found little impact in the Hadley Centre Global Environment Model (HadGEM1) model family on NH winter climate variability from an increasing vertical resolution in the stratosphere and an extended model domain near the mesopause. *Schmidt et al. (2013)* applied a multilinear regression method to study the response to volcanic forcing in CMIP5 historic simulations carried out with two different model versions of the MPI-ESM (LR/MR) model. Although quantitatively the responses to volcanic forcing seem more realistic in the MR configuration with a vertical atmospheric resolution almost twice of the LR model and its ability to interactively simulate the QBO, both MPI-ESM configurations underestimate the strong observed response of the NH winter stratosphere to volcanic forcing in comparison to observations (*Bittner et al.,* 3rd ICESM *2012*). Analysis of the average post-volcanic stratospheric response of high and low top CMIP5 models also revealed that for NH high latitudes in winter the difference in the post-volcanic response between both model types is insignificant and not as strong as observed (Charlton-Perez et al., 2013)

Important for the predictability of the climate response to large volcanic eruptions are the initial state and the history of the coupled atmosphere-ocean system prior to the eruptions. Hindcasts for the first post-volcanic NH winter (Marshall et al., 2009) indicate that an enhanced predictability of the European "winter warming" highly depends on the initialization of the stratospheric state at the beginning of the NH winter. The inability of most models to simulate of the observed dynamical response after e.g. the Mt. Pinatubo 1991 eruption, has therefore been related to the fact that the initial boundary conditions were not exactly the same as observed and that related factors are missing or incomplete, e.g. the post-volcanic stratospheric O_3 loss (section 4.2). By prescribing observed O_3 anomalies after the Mt. Pinatubo eruption, Stenchikov et al. (2002) could show that these post-volcanic O_3 anomalies strengthen and prolong the overall AO response to the volcanic forcing. Furthermore Muthers et al., (2014) could show that the simulated impact of a Tambora-like eruption on the NH winter warming is strongly depended on the prescribed O_3 climatology. Besides O_3 anomalies, the QBO has an impact on volcanically-induced atmospheric disturbances. Global model studies (Stenchikov et al., 2004; *Thomas et al., 2009b*) with a realistic QBO simulation demonstrated that the polar vortex strength and the AO response are modulated by the QBO phase. During the westerly QBO phase there is a tendency to simulate a strong NH polar vortex during and vice versa for easterly phase of the QBO. The QBO not only changes the volcanic imprint on atmospheric dynamics, the

oscillation itself will be altered after a volcanic eruption (Thomas et al, EGU Genral Assembly 2008; Giorgetta and Thomas EGU General Assembly 2009). Mt. Pinatubo simulations with the MAECHAM5 model, which simulates the QBO from resolved and parameterized wave mean-flow interactions, indicate that very likely the Mt. Pinatubo aerosols in the equatorial stratosphere caused the observed delay of 4 to 6 months in the descent of the easterly jet in 1991/1992 by increased tropical upwelling due to the aerosol radiative forcing (*Giorgetta et al., 2011 pers. com*) (Figure 16).

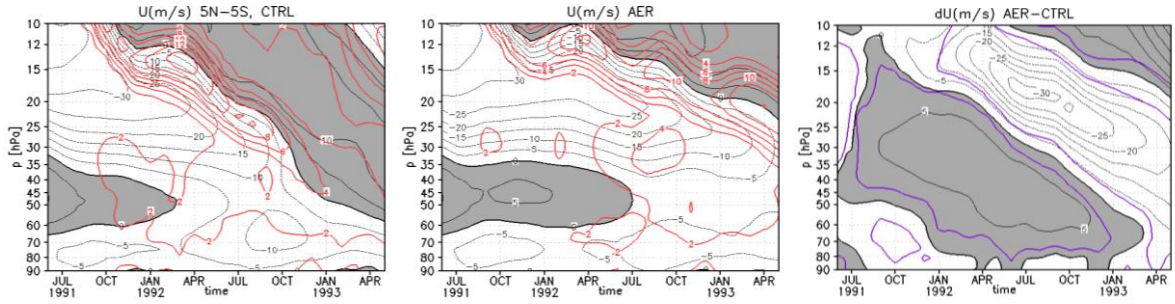

Figure 16: Zonal averaged zonal wind u (5°S-5°N) [m/s] ensemble average for the undisturbed case (left) for the volcanically perturbed case (mean), and the differences between both (right). Black line indicates the ensemble mean, the red line the standard deviation and the violet line 95% significance after the student T/-test. From *Giorgetta et al. pers. communication (2011).*

The question if El Niño-Southern Oscillation (ENSO) plays an important role for the volcanic imprint on the NH winter circulation is still not solved. A Mt. Pinatubo model study with the global middle atmosphere model MAECHAM5 (*Thomas et al., 2009a*) showed that the NH continental winter warming, although visible in some individual realizations, was not reproduced in the ensemble mean due to the strong El Niño Southern Oscillation (ENSO) variability in this model. However, reconstructions of monthly mean sea level pressure data for the NH from 1873 to 2000 indicate that the AO and the NAO modes are excited during the first NH post-volcanic winters independently of the ENSO phase (Christiansen, 2008). A possible explanation for this mismatch might be related to the El Niño type, (Central-Pacific and East-Pacific), which has a different effect on NH winter variability (Graf and Zanchettin, 2012). In addition, unresolved physical processes and systematic model biases could contribute to the poor performance of the climate models. Otterå (2008) argues that in general the simulated too weak AO response in many of these AR4 models could be related to the fact that most of them simulate an unrealistically strong polar vortex (Stenchikov et al., 2006) which potentially weakens any wave feedback and possibly the propagation of the stratospheric signals into the troposphere.

However, although the mean response of a positive NAO anomaly is statistically significant for the first two years following large tropical eruptions over much of the NH land area, the

standard deviation of the response is larger than the mean signal almost everywhere (Shindell et al., 2004). Due to a combination of natural forcing factors (volcanic aerosol, ENSO, QBO solar cycle) it is difficult to distinguish the dynamical effects caused by a volcanic eruption from those related to other forcing types. Given the capacity of the system to respond non-linearly to an imposed forcing (e.g. *Thomas et al., 2009a;b; Graf et al., 2014*) it is necessary to include all significant forcing types in simulations aiming to evaluate the climatic effects of volcanic eruptions. Indeed, despite the fact that the model response is too weak, not significant or missing in the ensemble mean, climate models are able to simulate the observed NH winter warming in individual ensemble members with increasing frequency for very strong volcanic eruptions. This poses general questions about the ratio between internal and externally forced variability and the capability of the climate models to simulate them (*Timmreck, 2012*). Hence, it seems that the internal variability in the climate model can mask the impact of a Mt. Pinatubo size eruption and the strength of the volcanic forcing turned out to be an important factor. Analysis of MPI-ESM-LR runs reveal that the ensemble variability of the simulated zonal mean wind and temperature anomalies in mid- and late winter in the northern polar stratosphere is significantly reduced under the strong forcing of a Tambora-like eruption in comparison to weaker eruptions in the historical runs and to internal variability in the control runs *(Bittner et al., 2016a*). For the Krakatau/Mt. Pinatubo eruptions for example, the ensemble variability of the zonal mean temperature anomalies are not discernible from internal variability. This implies that the confidence in some of the simulated regional response patterns after such eruptions is limited. The fact that a robust strengthening of the polar vortex is found in the historical MPI-ESM simulations only for the Tambora eruption (Figure 17) may hint to an imperfect representation of wave-mean flow interactions in the model. Since the dynamical response results, at least in part, from enhanced stratospheric wave activity it is therefore much less robust than it would be if it originated from direct radiative effects.

In a very recent study it has been demonstrated that the inconsistency in NH post-volcanic winter response between CMIP5 models and observational data might be more a matter of statistical sampling than a model error per se (Bittner et al., 2016b). Analyzing a large (100 member) ensemble of CMIP5 historical simulations (1850-2005) with the MPI-ESM-LR, Bittner et al. (2016b) could show that an ensemble larger than the average ensemble size provided in CMIP5 is needed to significantly detect the NH polar vortex strengthening. Furthermore, using more, but weak volcanic eruptions may make the identification of signals more difficult than using only a few larger ones.

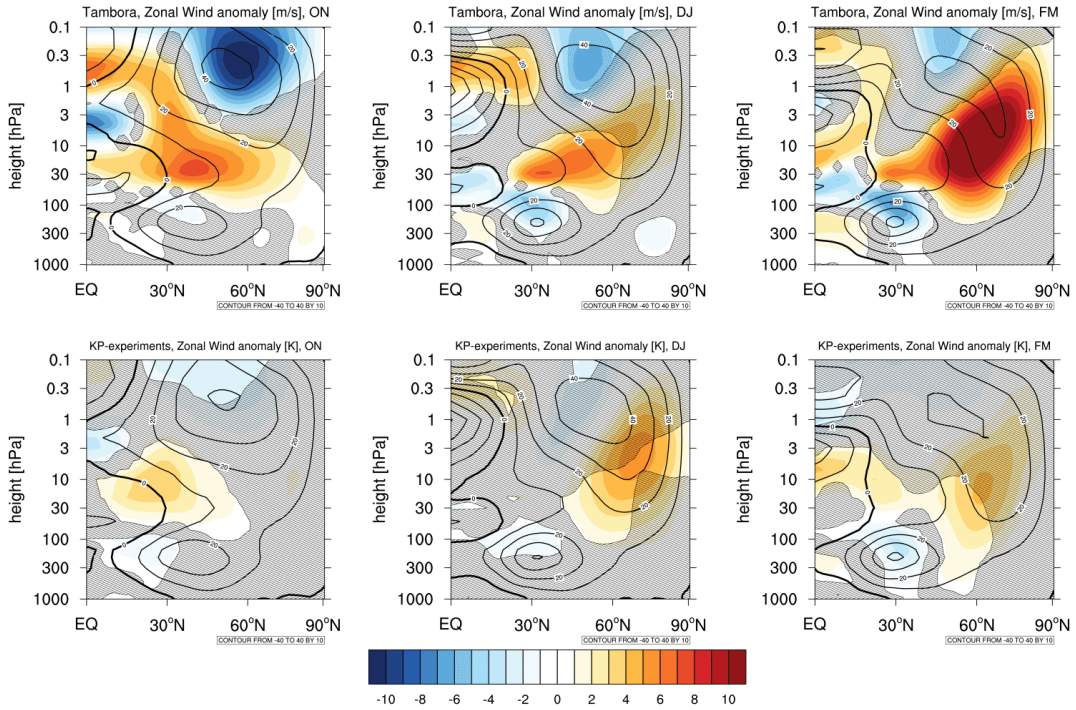

Figure 17: Ensemble average of the zonal mean zonal wind anomalies [m/s; colored] averaged over (left) October-November, (middle) December-January, and (right) February-March in the first Northern Hemisphere winter for the (top) Tambora and the (bottom) a composite of Krakatau and Pinatubo (KP) experiments. Positive wind anomalies are defined as eastward. Contour lines display the climatological background conditions of the reference periods. Signals not significant at the 95% confidence level are hatched. Figure from Bittner et al. (2016a).

When only the two strongest eruptions (Krakatau and Mt. Pinatubo) are considered, the mean of 15 CMIP5 models simulate a robust strengthening of the NH polar vortex. This indicates that the models do not in general fail to reproduce the dynamical response to volcanic eruptions as stated in previous papers (Driscoll et al., 2012; Carlton-Perez et al., 2013). On the other hand it also implies that the NH polar vortex response to volcanic eruptions in the real atmosphere is difficult to quantify due to the large internal variability and the limited number of observations. This is line with work *by Graf et al. (2014)* who demonstrated that caution has to be taken for over interpreting typical patterns derived from observational/reanalysis data as they not always provide sufficiently robust constraints of stratosphere-troposphere interactions in NH winter.

An important aspect is furthermore that still a scientifically sound understanding of the processes responsible for the post-volcanic NH winter warming is missing. Model studies (Stenchikov et al., 2002; Yoshimori et al., 2005) could, for example, reproduce a post-volcanic NH winter warming pattern without tropical stratospheric warming, although less pronounced than observed. Stenchikov et al. (2002) suggested as a possible explanation changes in tropospheric planetary waves forced by the reduced meridional tropospheric temperature gradient, while Yoshimori et al. (2005) explain this with changes in the transient eddy activity and its interaction with the mean flow. In a study with the MPI-ESM-LR, *Toohey et al. (2014)* showed that the post-

volcanic changes in the zonal wind in NH high latitudes are rather a result from a robust enhancement in the stratospheric residual circulation than from direct aerosol radiative heating. The high latitude effects are partly resulting from enhanced stratospheric wave activity and are therefore more variable than if they were resulting from aerosol heating only. *Bittner et al. (2016a)* could also demonstrate that the strongest change of the temperature-gradient is not located in the region of the polar vortex, but at approximately 30°N. Significant westerly zonal wind anomalies exist between 50– 10 hPa in early winter, which change the background conditions for wave propagation and lead to a deflection of planetary waves equatorward. As a consequence, wave-driven momentum deposition in the region of the NH polar vortex is reduced and wave-driven deceleration of the zonal wind at high latitudes is restrained. Figure 18 summarizes the recent understanding of the processes involved

The climate response to major volcanic eruptions in the Southern Hemisphere (SH) is still unclear. While observational and reanalysis data (Marshall, 2003; Crooks, 2005; Roscoe and Haigh, 2007) show a negative anomaly of the Southern Annular Mode (SAM) in response to volcanic forcing, give model results a quite diffuse picture dependent on the time period and the reference season. Simulations of the last 500 years with the NCAR Community Climate System Model, Version 3 (CCSM3) indicate a rather weak surface pressure response to volcanic eruptions, showing a SAM structure in the sector 90°E-120°W (Wilmes et al., 2012). No significant SAM response in SH winter is found for the Mt. Pinatubo eruption in Goddard Institute for Space Studies Model E (GISS model E) simulations (Robock et al., 2007) whereas CMIP3 models (Karpechko et al., 2010) shows significant dynamical changes in SH spring and autumn in the aftermath of the 1982 El Chichón and the 1991 Mt. Pinatubo eruptions (Karpechko et al., 2010). A positive SAM signal is found in the CMIP3 models for the last three volcanic eruptions, with a stronger stratospheric polar vortex and a weaker sea-level pressure over Antarctica in contrast to the reanalysis data. The disagreement between reanalysis data and CMIP3 models may be related to the sparse observational sample size and/or to a vertically poorly resolved stratosphere and to unresolved processes (ozone depletion, QBO, ENSO) (Karpechko et al., 2010). Recently the impact of large tropical eruptions on stratospheric circulation has been tested with the MPI-ESM-LR und MAECHAM5-HAM for different SO_2 emissions (Gleixner, 2012; *Krüger et al., EGU General Assembly 2011*). The model results show that the SH surface is impacted by tropical volcanic eruptions through direct radiative and indirect dynamical effects, i.e. stronger westerlies, shift of the storm tracks, colder and drier Antarctica. For extremely strong volcanic eruptions a significant positive SAM is simulated in the

stratosphere and at the surface. However, at the surface a stronger volcanic SO_2 emission strength is necessary to get a significant signal. The model results show for example for a Mt. Pinatubo size eruption a significant SAM signal at 50 hPa but not at the surface, which is in good correspondence with the aforementioned observations for the Mt. Pinatubo eruption.

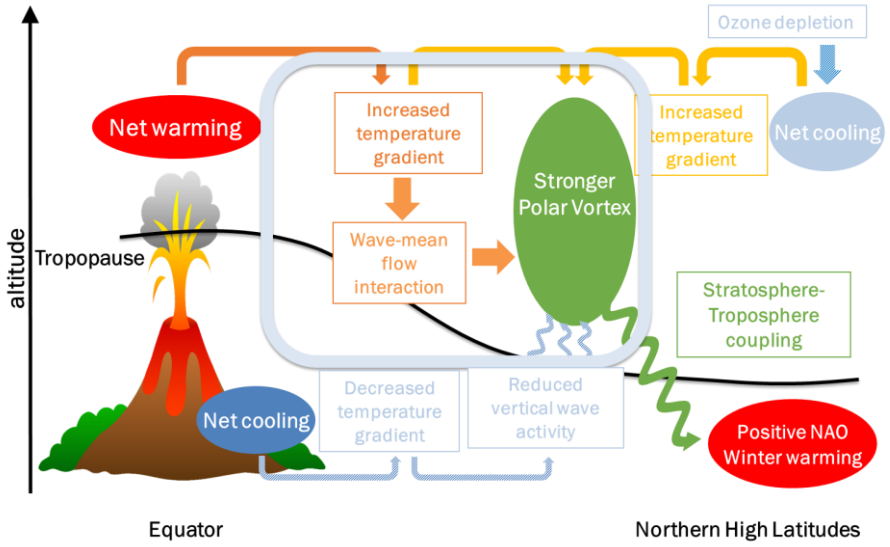

Figure 18: Schematic overview of the recent understanding of the processes which could be responsible for the dynamical effects after strong volcanic eruption adapted from the PhD thesis of M. Bittner (2015)[11] .

4.4 Impact on ocean dynamics

Due to the coincidence of the last major volcanic eruptions (Agung (1963), El Chichón (1982) and Mt. Pinatubo (1991)) with El Niño events, many questions have been raised if this simultaneous occurrence was by chance or if there exists a relation between El Niño events and explosive volcanic eruptions. Since the early eighties, many possible mechanisms and hypotheses were discussed but until the turn of the millennium no significant correlation between volcanoes and ENSO had been found (Robock, 2000). Analysis of proxy records propose now that El Niño events are not triggered by large volcanic eruptions but major eruptions could instead force the system to a state where the likelihood of El-Niño events is increased in the first post-eruption year (Adams et al., 2003; McGregor et al., 2010; Li et al., 2013). Model studies show however a quite diverse picture for the ENSO response in the first post-eruption year, indicating both an El Niño like (e.g. Emile-Geay, 2008; Ohba et al., 2013; Maher et al., 2015) or a La Niña type one (e.g. McGregor and Timmermann, 2011). Analyzing the CESM Last Millennium Ensemble simulations,

[11] Supervised by H. Schmidt and C. Timmreck.

Stevenson et al. (2016) further suggest that the direct ENSO response to volcanic eruptions has also a hemispheric component: the winter following a NH eruption tends toward El Niño, while SH volcanoes enhance the probability of La Niña events and tropical ones have only minor impact on ENSO dynamics.

To study the impact of a Mt. Pinatubo size eruption on the tropical Pacific, 10-member ensemble simulations for three different ENSO states (before the onset and during an El Niño event, and for a climatological mean) have been conducted with the ECHAM5/MPIOM model (Jungclaus et al., 2006) with and without prescribed volcanic aerosol starting in January and July (*Timmreck et al., Spring AGU 2007*). The simulated dynamical response in the tropical ocean appeared, however, to be highly variable and to differ between the selected cases. But also quite strong differences exist between the individual ensemble members, probably due to the fact that the Mt. Pinatubo forced surface temperature anomaly is within internal variability range. The situation could be different in the case of very large volcanic eruptions. As ocean thermostat model simulations for the last millennium point out, only volcanic eruptions larger than the size of Mt. Pinatubo can increase the likelihood and amplitude of an El Niño event (Emile-Geay et al., 2008).

Based on CCSM3 volcanic forcing experiments McGregor and Timmermann (2011) suggest that processes related to the zonal equatorial gradients of the mean cloud albedo, the mixed layer depth and Newtonian cooling ("atmospheric response"), could counteract the dynamical thermostat mechanism ("ocean response") which implies that anomalous upwelling in the equatorial ocean is capable of regulating tropical sea surface temperatures (Clement et al., 1996). Model simulations, where the "atmospheric response" is stronger than the "ocean response" will tend to an initial La-Niña-like response to volcanic forcing, while an El Niño type response will go along with a strong ocean response. Another mechanism was proposed by Ohba et al. (2013), who suggest that the land–sea cooling contrast (and a relatively rapid cooling of the Indian Ocean) is the dominant mechanism for an El Niño like response after tropical volcanic eruptions. On short time scales, volcanic eruptions can not only have an impact on ENSO dynamics but also on the positive Indian Ocean Dipole (IOD) phase events in the first post-eruption year (Maher et al., 2015).

In contrast to the atmosphere, the ocean responds to the volcanic forcing at longer time scales far beyond that of the atmospheric disturbance. In particular the North Atlantic is found to be quite sensitive to volcanic forcing. Climate model studies (Jones et al., 2005; Stenchikov et al., 2009; Otterå et al., 2010) indicate that large tropical volcanic eruptions lead to a significant

strengthening of the Atlantic Meridional Overturning Circulation (AMOC). However, Pausata et al. (2015b) could recently also show for a Laki type volcanic eruption that also high-latitude eruptions could lead to an AMOC strengthening for the first 25 years after the eruption, followed by a multidecadal weakening. The simulated AMOC changes with respect to the peak geographical location and strength are not only quite different for the individual climate models, but also for individual strong volcanic eruptions (*Zanchettin et al., 2012a*; Mignot et al., 2011).

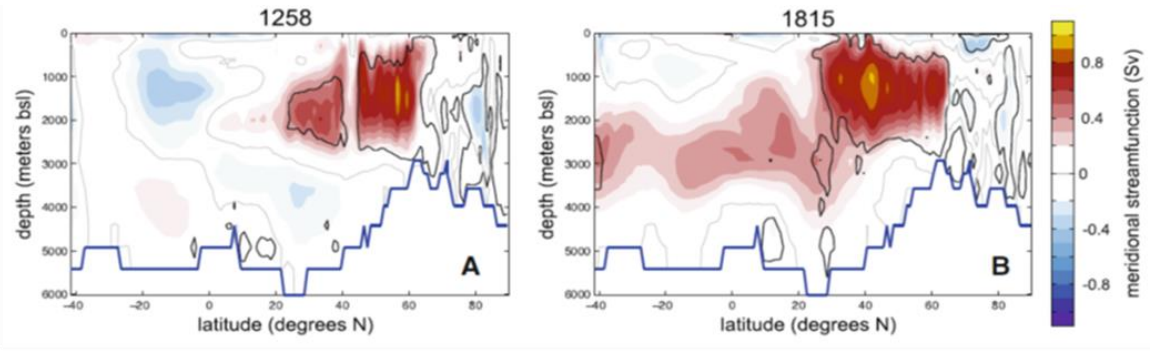

Figure 19: Ensemble-average simulated post-eruption anomalies of the annual, zonally-integrated Atlantic overturning stream function for the Samalas (1258) (panel A) and Tambora (panel B) eruptions. The thick black line individuates the 95% confidence level based on the Mann-Whitney U test. Figure from *Zanchettin et al. (2012a).*

The simulated post-eruption AMOC strengthening in the MPI-ESM Millennium runs peaks for example about one decade after the eruption, which is consistent with the characteristic time scale for ocean density anomalies propagation in the MPIOM ocean model (Jungclaus et al., 2006). The delayed AMOC peak response patterns for the two strongest volcanic eruptions (Samalas and Tambora), reveal the range of model variability in the MPI-ESM Millennium simulations (Figure 19). For the Samalas (Tambora) eruption, the peak location is displaced northward (southward) with respect to the ensemble-mean location, reflecting differences in the preferential sites of post-eruption deep convection (*Zanchettin et al., 2012a*). The post-eruption AMOC response in the MPI-ESM simulations of the last Millennium can be explained with a progressive strengthening of the AMOC at NH midlatitudes (30 °N–60 °N) and depths down to 2,500 m, which is primarily driven by enhanced deep convection in the central/eastern subpolar gyre region and, especially, in the Nordic Sea (*Zanchettin et al., 2012a*). This mechanism is different from the one proposed for the Bergen climate model, where the total heat flux response in the Labrador Sea is the main reason for the AMOC response to large volcanic eruptions (Otterå et al., 2010). Analysis of a subset of CMIP5 models further suggests that the impact of the moderate size Agung volcanic eruption on the North Atlantic ocean variability could explain the Great Salinity Anomalies in the 1970s (Swingedouw et al., 2015). The proposed mechanism is that increasing sea-ice cover in the Nordic Seas, could reduce the freshwater

export through the Denmark Strait which then leads to anomalously positive anomalies in the Labrador region.

Simulations and proxy reconstructions reveal that interactions between the AMOC and the North Atlantic gyre circulation lead to a strong and sustained decadal dynamical response to strong volcanic eruptions beyond the short-lived radiative forcing, which is closely linked to the NAO in NH winter (*Zanchettin et al., 2012a; 2013a;b*). Specifically, European seasonal climate reconstructions over the past 500 years (*Zanchettin et al., 2013a*) indicate a decadal-scale positive phase of the winter NAO accompanied by winter warming over Europe peaking approximately one decade after a major eruption; (Figure 14c). A dynamical framework to interpret this delayed winter warming was provided by Zanchettin et al. (2012a) based on the MPI-ESM Millennium simulations. The proposed processes include anomalously strong ocean heat release over the Arctic Ocean related to decadal modifications in the North Atlantic oceanic circulation and strong signal amplification in the Arctic influencing the westerly atmospheric circulation across the North Atlantic/European sector.

In a follow up MPI-ESM study, Zanchettin et al. (2013b) furthermore demonstrated that background conditions have the potential to quite substantially influence the aforementioned decadal climate response to strong tropical volcanic eruptions. Zanchettin et al. investigated in particular the response to the Tambora eruption in ensemble simulations of the early 19th century under I) full-forcing conditions, II) volcanic forcing-only conditions and III) volcanic forcing-only conditions excluding the 1809 eruption. While the simulated radiative perturbation induced by the Tambora eruption does not depend on the background conditions, the simulated near-surface temperature response and the post-volcanic decadal evolution of oceanic heat transport and sea ice in the North Atlantic/Arctic Ocean evolve significantly differently under different background conditions (Figure 20). The model results therefore show that multiple response pathways exist after strong volcanic eruptions, which depend on background conditions prior to the eruptions. Background conditions are therefore not merely a source of additive noise for post-eruption decadal climate variability, but actively influence the mechanisms involved in the post-eruption decadal evolution.

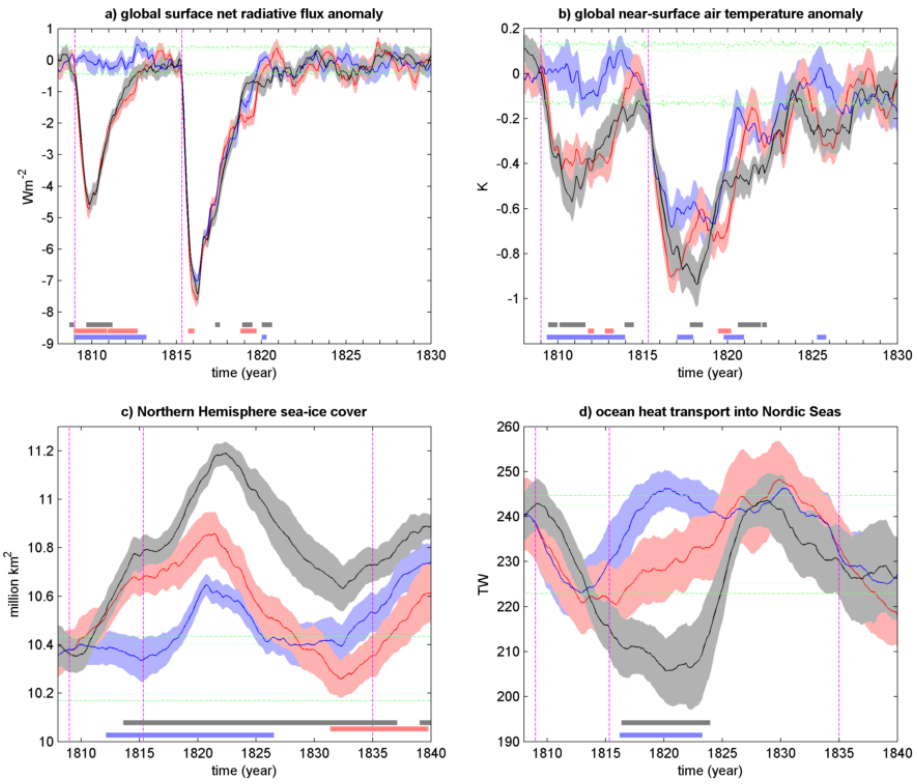

Figure 20: Global temporal evolution of different climate variables in a including all natural and anthropogenic forcing (black), with only volcanic forcing including the Tambora and the preceding 1808/1809 eruption (red), and with only volcanic forcing without the 1808/1809 eruption (blue). The all forcing simulations are started in 1751 from initial conditions taken from the COSMOS-Mil experiments (Jungclaus et al., 2010), the volcanic forcing only from a control run for 800 AD conditions. Lines indicate means of the 10 member ensemble of simulations and the shading one standard error of the mean. Green dashed lines are the 5th–95th percentile intervals for signal occurrence in the control run. The inner dotted lines are the 10th–90th percentile intervals. Magenta vertical lines indicate the occurrence of the 1808/1809, Tambora and Cosiguina eruptions. Bottom rectangles indicate periods when there is a significant difference between one ensemble and the other two. Positive surface net radiative flux anomalies correspond to increased downward flux. The units of the ocean heat transport are 1 TW = 10^{12} W. Original figure from *Zanchettin et al. (2013b),* modified in *Raible et al. (2016).*

Volcanically induced changes in the Southern Ocean are not so well exploited. Analyzing MPI-ESM simulations of the Los Chocoyos eruption, *Metzner et al.* (*AGU Chapman Conference on Volcanism and the Atmosphere, 2012*) found a significantly anomalous positive phase of the SAM which persists for at least one year after the eruption. The anomalous SAM anomaly is characterized by strong westerly winds over the Southern Ocean, which lead to significant changes in surface temperature, precipitation and wind fields associated with temporary modifications in the upper ocean circulation in the Antarctic Circumpolar Current region. Due to the propagation of the forced anomalies into the deep ocean layers, the anomalous oceanic state persists well beyond the atmospheric response timescale. Significant negative temperature anomalies in the SH ocean propagate down to ~2000 m during the first ~20-50 post-eruption years, and persist for the entire simulated 200 years (*Metzner et al., AGU Chapman Conference on Volcanism and the Atmosphere, 2012*). This is in good agreement with previous studies, which

show that the ocean heat content is significantly affected by large volcanic eruptions. Model results show a rapid fall of sea level (Stenchikov et al., 2009; Gregory et al.; 2006; Delworth et al., 2005) and a rapid drop in the global ocean heat content in the upper layers after large volcanic eruptions (Church et al., 2005; Delworth et al., 2005; Gleckler et al., 2006a; 2006b). For relative large volcanic eruptions, the cooling signal can penetrate even further down into the deeper ocean layers persisting there over multi-decadal or even centennial timescales (Delworth et al., 2005; Robock and Liu, 1994; Gregory, 2010). Omitting volcanic radiative forcing in control and spin-up experiments therefore leads to a negative bias in ocean heat uptake and global mean sea level rise due to thermal expansion in climate model simulations of the historical period (Gregory et al., 2013). For the CMIP6 pre-industrial control experiments it is now recommended to specify a background volcanic aerosol with a radiative forcing that matches the mean of the volcanic forcing during the historical simulation (Eyring et al., 2016).

4.5 Impact on the hydrological cycle

Climate model studies (e.g. Robock and Liu, 1994; Iles et al., 2013; Iles and Hegerl, 2014; Paik and Min, 2017) show significant reductions in global mean precipitation after large volcanic eruptions. Over the past 50 years, observed changes in global scale precipitation have been forced principally by volcanic aerosols as indicated by detection and attribution studies (Gillet et al., 2004). The response is, however, not always linear, since besides radiation changes, precipitation is also controlled by cloud microphysics processes and atmospheric dynamics on a variety of space and time scales. Analysis of the hydrological cycle in Mt. Pinatubo ensemble simulations with the ECHAM5/MPIOM (*Timmreck et al., SPARC General Assembly 2008*) also demonstrate the importance of the initial state of the tropical Pacific for volcanic induced changes in the hydrological cycle. Figure 21 shows for six different Mt. Pinatubo cases with 10 realizations each, a significant reduction in the ensemble mean in evaporation and integrated water vapor, in particular over the warm pool region, but no clear picture in cloud cover and runoff. Global precipitation is reduced for all cases, especially in the tropical belt, in agreement with Global Precipitation Climatology Project (GPCP) data which show roughly a 5% decrease of both tropical land and ocean precipitation as a response to the El Chichón and the Mt. Pinatubo eruption (Gu et al., 2007). This is a distinct volcanic signal, which clearly distinguishes the volcanic effect from the ENSO signal. The ENSO signal is more a less a shift between land (decrease) and ocean (increase) (Gu et al., 2007; Gu and Adler, 2011; Liu et al., 2012). Two cases, the case II – June and the case III – January simulations noticeably differ from the other cases in the integrated water vapor anomalies and related to temperature anomalies in the equatorial

Pacific (Figure 21). This different behavior is also seen in precipitation changes where the two cases mentioned above show the strongest reduction over the ocean close to the equator. Whether this behavior is by chance or if there is potential for deeper physical explanation has to remain unclear as the small number of cases does not permit a sound statistical analysis.

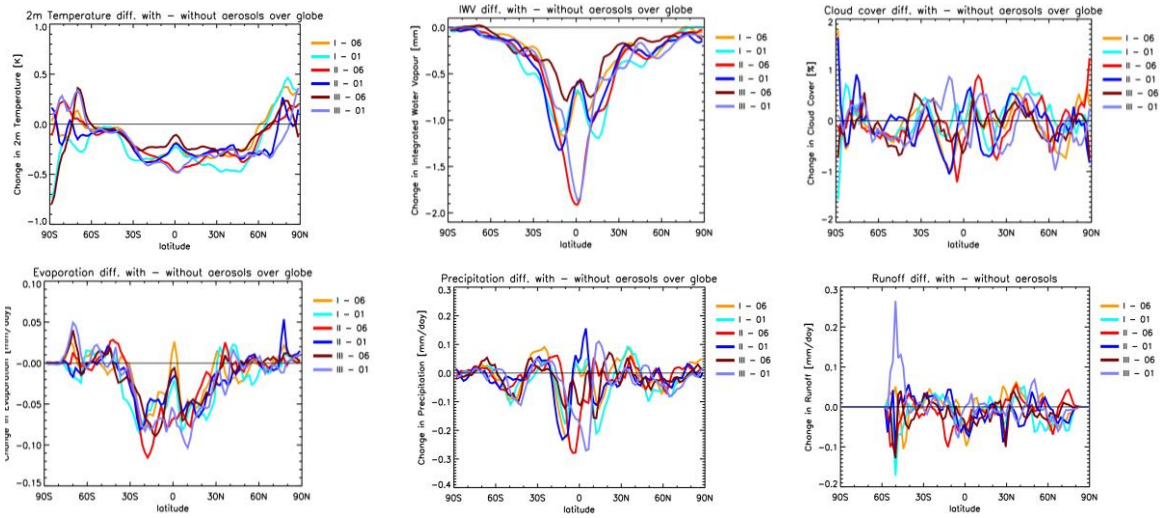

Figure 21: Zonal and annual (09/91-09/92) averaged anomalies between the volcanically perturbed and the unperturbed run (ensemble mean). The panels show (from left to right), 2m temperature [K], integrated water vapor (mm), cloud cover(%), evaporation/runoff (mm/day), precipitation over land and ocean (mm/day). The bluish curves denote the three cases starting in January; the reddish curves the ones starting in June. The three cases denote different states of the tropical Pacific: case I developing El Niño, case II ongoing El Niño and case III neutral conditions.

Low latitude precipitation anomalies are strongly affected by tropospheric circulation changes and associated shifts in the position of the Intertropical Convergence Zone (ITCZ). By changing the hemispheric temperature contrast, large volcanic eruptions could have a substantial impact on the ITCZ. Speleothem data from middle America over the last 450 years (Ridley et al., 2015) indicate that NH volcanic eruptions lead to a southward ITCZ shift, while volcanic eruptions located in the SH as the 1815 Tambora eruption, led to a Northward shift. Another Mesoamerican speleothem record reveals long-lasting (multi/decadal) reduction in local precipitation in combination with clusters of large tropical eruptions in the 19th and 20th century (Winter et al., 2015).

Major volcanic eruptions have also an impact on the Asian and African monsoon (e.g. Iles and Hegerl, 2014; Paik and Min, 2016). Model studies (Oman et al., 2005; Schneider et al., 2009; Fan et al., 2009) suggest significant reductions in precipitation in the Asian monsoon region in response to a NH high latitude eruption. However, the simulated post-volcanic changes of the Monsoon system deviate from paleo records: while some models predict less rain over Southeast Asia and more precipitation over central Asia, long-term paleo reconstructions

indicate an opposite behavior with more rain in Southeast Asia and drier conditions over central Asia in the aftermath of large volcanic eruptions (Anchukaitis et al., 2010). A model study by Oman et al. (2006b) also indicated that the Icelandic Laki eruption (1783-1784) led to a weakening of the African monsoon consistent with the recorded very low Nile flow in the post-volcanic years (Kondrashov et al., 2005). Climate reconstructions and model simulations for the last 400 years show not only a weakening of the Asian and African summer monsoons, but also an increase of south-central European summer precipitation in the first post-eruption year (Wegmann et al. 2014), which is consistent with reconstructions of the last 500 years (Fischer et al., 2007) and observations after the 1815 Tambora eruption (Auchmann et al., 2012; *Raible et al., 2016*). Wegmann et al. (2014) suggest that atmospheric circulation changes over the North Atlantic/European sector induced by a weakening of the northern branch of the Hadley circulation after the volcanic eruption lead to an increase of precipitation over Europe. Asian and African summer monsoons fail completely in the first two post-eruption years in MPI-ESM simulations of the extremely large YTT super eruption (*Timmreck et al., 2010*; *2012*). The initial precipitation reduction in response to the strong volcanic cooling is, however, followed by a notable increase of precipitation three to five years after the YTT eruption in many river catchment areas as a result of negative SSTs anomalies developing a few years after the eruption in the central equatorial Pacific (*Timmreck et al., 2012*). Iles and Hegerl (2015) demonstrate that large volcanic eruptions could have a substantial impact on water availability. Analyzing observational streamflow records from the last 150 years they found on average a decrease in streamflow across wet tropical and subtropical regions, but also in some river catchment an increase in flow (Southern South American, Southwestern North American).

The water vapor response after large volcanic eruptions e.g. the 1991 Mt. Pinatubo eruption provide a unique opportunity to test the capability of climate models to simulate humidity changes induced by external global-scale forcing (Randall et al., 2007). Soden et al. (2002) investigated the tropospheric water vapor response following volcanically induced surface temperature changes. They found that the simulated global temperature anomalies are only consistent with the observations if water vapor changes are included in the radiative calculations. Forster and Collins (2004) quantified the water vapor feedback after the Mt. Pinatubo eruption in observations and in global model simulations by using observed pattern of tropospheric water vapor changes in addition to detailed radiation calculations. The simulated water vapor feedback strength agrees in general with the observations with a mean value of 1.6 W/m^2 K, and an uncertainty range of 0.9 to 2.5 W/m^2 K, but models results and observations

notably differ in some cases i.e. in the upper troposphere and in the SH. Nevertheless, due to large variability in the observed and simulated values the long-term water vapor feedback could differ about a factor 2 to 3 between models and observations (Forster and Collins, 2004).

Stratospheric water vapor is increasing after large volcanic eruptions. Observations in the aftermath of the 1991 Mt. Pinatubo eruption show a short-term increase in stratospheric water vapor for example in the long-term Boulder record (Oltmans et al., 2000). The post-volcanic stratospheric water vapor increase is explained by two mechanisms: stratospheric injection of water vapor (Glaze et al., 1997; Joshi and Jones, 2009) and enhanced transport through the tropopause (Considine et al., 2001; Joshi and Shine, 2003). A model study (Joshi and Shine, 2003) suggests that the series of volcanic eruptions in the 2nd half of the 20th century could have contributed to the long-term trend in stratospheric water vapor.

The volcanic aerosol effect on cirrus clouds in the upper troposphere has been discussed controversially in the literature using the example of the 1991 Mt. Pinatubo eruption and is still not clear. Several observational studies point to an effect from volcanic eruptions on cirrus cloud formation (e.g. Sassen et al., 1995, Song et al., 1996, Wang et al., 1995). This is supported by detailed microphysical model simulations (Sassen, 1992; Jensen and Toon, 1992), which indicate that volcanic eruptions introduce larger and more abundant soluble aerosols into the upper troposphere leading to cirrus cloud formation at lower super saturations and to enhanced ice crystal number concentrations. On the other hand, ECHAM4 simulations suggest that effects from the Mt. Pinatubo eruption on clouds and climate, considering only homogeneous freezing are, small (*Lohmann et al., 2003*). These results are consistent with an analysis of three satellite based cirrus datasets produced by the International Satellite Cloud Climatology Project (ISCCP) (Luo et al., 2002), which suggest that the Mt. Pinatubo volcanic aerosol did not have a significant systematic effect on cirrus cloud coverage and brightness temperature difference. CALIPSO backscatter and extinction profiles after the 2011 Nabro eruption also indicate that the optical properties of ice and cirrus clouds are at most weakly dependent on the aerosol size distribution and droplet number density and, therefore, on the volcanic impact (Meyer et al., 2015).

Tropospheric volcanic sources are, however, one of the primary sources of cloud condensation nuclei (CCN) in the preindustrial atmosphere (Schmidt et al., 2012). Global model studies (Gettelman et al., 2015; Rap et al., 2013; Schmidt et al., 2012) and observations (McCoy and Hartmann, 2015) have shown the capacity of tropospheric volcanic emissions to affect low level cloud properties. After the Icelandic Bárðarbunga-Veiðivötnfissure eruption for example, the

cloud droplet radius over the North Atlantic was at the lowest value in the Moderate Imaging Spectroradiometer (MODIS) data record (Mc Coy and Hartmann, 2015).

4.6 Impact of Northern Hemisphere high latitude eruptions

In the last years, mid- and high- latitude volcanic eruptions especially from the NH raised more and more the interest of the scientific community. This interest has been fostered by both the fact that after the 1991 Mt.Pinatubo eruption no large tropical eruption happened and the significant volcanic activity in NH high latitudes e.g. the 2008 eruption of Kasatochi (52.1 °N) and the 2009 eruption of Sarychev (48.1 °N). Both eruptions were, however, not strong enough to have a climate impact (Kravitz et al., 2010; Haywood et al., 2010; Kravitz et al., 2011). The 2010 Icelandic Eyjafjallajökull (63.4° N) eruption, which stopped European air traffic for a couple of days, and the 2014-2015 Bárðarbunga-Veiðivötn fissure eruption at Holuhraun, which was the largest eruption in Iceland over the past 200 years (Schmidt et al., 2015), had also no climatic influence. They provide, however, valuable information of long-range transport (Stohl et al., 2011; Schmidt et al., 2015), air quality impacts (Schmidt et al., 2015) and aerosol-cloud interactions (Gettelman et al., 2015; McCoy and Hartmann, 2015).

While tropical volcanoes have the potential to affect the global climate system because the volcanic cloud can be transported into both hemispheres, mid to high latitude eruptions will primarily affect their own hemisphere. A good indicator that a large tropical eruption occurred during in the past are therefore a simultaneous occurrence of volcanic aerosol (sulfate/ash) signals in Arctic and Antarctic ice core records. However, if the volcanic source cannot be unambiguously identified another possible scenario would be possible that volcanic eruptions took place at the same in both hemispheres. Schneider et al. (2009) investigated these scenarios with the CCSM3 model and found significant NH summer cooling over the continents for both, which last longer-last for the tropical scenario. *Graf and Timmreck, (2001*) simulated the aerosol radiative effects of the Laacher See eruption (50 °N, 10,900 B.C.). Their model results indicate that a NH mid latitude eruption could reproduce a continental “winter warming” as observed after tropical eruptions, as an intensified cooling in polar night and a strengthening of the polar vortex is induced by the increased aerosol load in high latitudes. However, analyzing the NH winter response of NH high latitude eruptions in the MPI-ESM millennium simulations, *Zanchettin et al. (EGU General Assembly 2010)* could not find a significant signature on the NH extratropical stratospheric circulation. GCM simulations of the 1912 eruption of Katmai (58 °N) (Oman et al., 2005) also show no positive anomaly of the AO, but a significant cooling over southern Asia during boreal winter. The most prominent dynamical impact of the Katmai

eruption in their study is however found in boreal summer over Asia. The simulated strong cooling in NH summer over the NH continents leads to a weakening of the Asian monsoon with a notable decrease in cloud cover and, warming over northern India (Oman et al., 2005).

The latitude of the eruption also has an influence on the impact of fine volcanic ash during the initial spread of the volcanic cloud (*Niemeier et al., 2009*). While for tropical eruptions the influence of fine ash is marginal, it can change the transport direction of a high latitude volcanic aerosol cloud. Model studies (Kravitz and Robock, 2011, Meronen et al., 2012, *Toohey et al., to be submitted*) further indicate that the time of the year together with the strength of the eruption determine the climatic impact of a NH volcanic eruption. For NH high latitude eruptions with small SO_2 emissions, the climate impact is generally negligible independent of the eruption season, but is detectable for emissions >5 Tg SO_2 due to the seasonality in high latitude solar insolation and in the sulfate deposition rate (Kravitz and Robock, 2011). *Toohey et al. in prep.* challenges the general belief that extra-tropical or high latitude eruptions produce much smaller climate impacts than tropical eruptions of comparable magnitude. They find for MAECHAM5-HAM simulations of Mt. Pinatubo-like eruptions at different NH latitudes that the global mean radiative forcing from extratropical eruptions can be of comparable size to that of tropical ones and for NH mid-to-high latitudes even greater. The impact of extratropical eruptions is however quite sensitive to the injection height. Pausata et al. (2015b) could furthermore demonstrate that strong high latitude volcanic eruptions have the potential to lead to an El-Niño like response in the first 8-9 months after the eruption and to an AMOC strengthening for the first 25 years after an eruption followed by a multi-decadal weakening.

An especially well studied NH high latitude eruption is the 1783–1784 Laki eruption, which is the best-documented example of a historic long-lasting flood lava eruption in Iceland. Over the course of eight months, this eruption injected around 120 Tg SO_2 into the upper troposphere and lower stratosphere (Thordarson and Self, 2003) which caused a widespread sulfuric acid cloud ‘dry fog’ over Europe with serious negative health effects as seen in historical records (Durand and Grattan, 1999; Grattan et al., 2003). It was estimated that approximately 142,000 additional cardiopulmonary fatalities could occur in Europe from the increase in particulate air pollution during a future Laki-style eruption (Schmidt et al., 2011). Norwegian Earth System Model (NORESM) studies (Pausata et al., 2015a) could further demonstrate the importance of the initial background conditions for the short-term climatic effects of the Laki eruption, thereby extending the findings of Zanchettin et al. (2012a) to high latitude conditions. The total sulfur emission of the Laki eruption closely linked to the question of its emission height is still under debate. A first

climate model study of the Laki eruption (Highwood and Stevenson, 2003) showed only slight cooling in the NH annual mean temperature, since most of the emitted SO_2 (about 70%) was directly deposited to the surface before it could be transformed to sulfate aerosol. However, Oman et al. (2005) estimated for the Laki eruption about twice of the total sulfur yield (163-166 Mt) than used in Highwood and Stevenson (2003) (71 to 92 Mt). As a consequence, consistent with observations they simulated a stronger radiative impact resulting in an unusual cold summer over the NH continents and a weakening of the African and Asian monsoon circulation (Oman et al., 2006b. Sulfur isotopic measurements of the Laki sulfate (Lanciki et al., 2012) suggest that the Laki eruption did not reach altitudes of the stratospheric ozone layer. Further, the short aerosol lifetime of less than 6 months indicates that the bulk of the Laki plume was most likely confined to the middle and upper troposphere. These conclusions support the hypothesis of D'Arrigo and colleagues (2011) that the cold NH winter of 1783–1784 was not caused by Laki. This has been refuted by Schmidt et al. (2012), who claimed that the applicability of mass-independent sulfur isotopic composition measurements for interpreting the climatic impact of any high-latitude eruption has to be demonstrated.

4.7 Impact on decadal and centennial time scales/ volcanic super-eruptions

Although large volcanic eruptions, e.g. the 1991 Mt. Pinatubo or the 1815 Tambora eruption, have affected the atmospheric system for several years, the atmospheric life time of the aerosol cloud is too short to lead to decadal scale global surface cooling. Model studies (Pinto et al. 1989; *Timmreck et al. 2010*) reveal that self-limiting effects in volcanic aerosol clouds limit their atmospheric residence time. Only extremely large volcanic eruptions often referred to as “super-eruptions” might have the potential to have a longer term climate impact. One of the most famous and most studied super-eruptions is the YTT eruption 74 ± 2 kyr BP[12] (see special issue Quat. Int. eds. Petraglia et al., 2012). Due to the much debated hypothesis that this eruption led to a bottle-neck for modern human evolution (Ambrose, 1989), the YTT eruption has been in the scientific focus since several years. The genetic bottle-neck theory supposes that sever climate effects resulting from the YTT eruption lead to a significant decrease in human population. Climate model simulations suggested a 8-17K maximum global cooling and a decade of severe cooling (Robock et al., 2009; Jones et al., 2005). These studies, however, appear to be at odds

[12] Analysis of sanidine crystals extracted from Toba deposits in Malaysia, give an astronomically calibrated $^{40}Ar/^{39}Ar$ age of 73.88 ± 0.32 ka (Storey et al., 2012)

with the high survival rate of mammalian mega fauna in South East Asia (Louys, 2007) and modern humans in India (Petraglia et al., 2007).

A shorter and three times weaker temperature response (-3.5°C global maximum cooling) than previously estimated was obtained in MPI-ESM studies (*Timmreck et al., 2010; 2012*), which explicitly take into account aerosol microphysical processes. This leads to larger particle sizes and a faster fall out of the particles. Although in these simulations cooling reaches -12°C after one year in some mid-latitude continental regions, the temperature is back to internal variability within a decade (Figure 22). Since the "YTT bottle neck theory" discussion focuses on the conditions on the Indian subcontinent (Williams et al., 2009 and their associated comments; Balter, 2010; Haslam et al., 2010), *Timmreck et al. (2010; 2012)* specifically analyzed temperature and precipitation anomalies there (Figure 22). Temperature over the Indian subcontinent decreases during the first eight years after the eruption, but internal variability is exceeded only in the first five winters for all ensemble members. Variability of precipitation is small during the winter dry season, but very large for the summer monsoon season. Summer monsoon season precipitation anomalies during the first two years counteract the negative radiative flux anomalies since they lead to reduced evaporative cooling and to less reflection of solar radiation due to reduced cloudiness. Thus for the first two post-eruption years, summer temperature anomalies stay within the range of internal variability over India. Once the precipitation anomalies are no longer distinguishable from internal variability in year three, radiative cooling due to volcanic aerosol dominates with cooler summer conditions from year three onwards (Figure 22). The aforementioned simulations are based on assumptions of an initial SO_2 emission or an AOD comparable to 100 times the size of the 1991 Mt. Pinatubo eruption. Recent volcanological data based on the petrological method[13] suggest a much smaller sulfur release by the YTT eruption of about 5 times the Mt. Pinatubo strength, i.e. in the range of a Tambora eruption. This would even lead to a smaller volcanic cooling signal and a shorter duration of the perturbation, see section 3.3 (Figure 11).

[13] The petrological method (Chesner and Luhr, 2010) provides a minimum estimate of the emitted sulfur (Self and King, 1996).

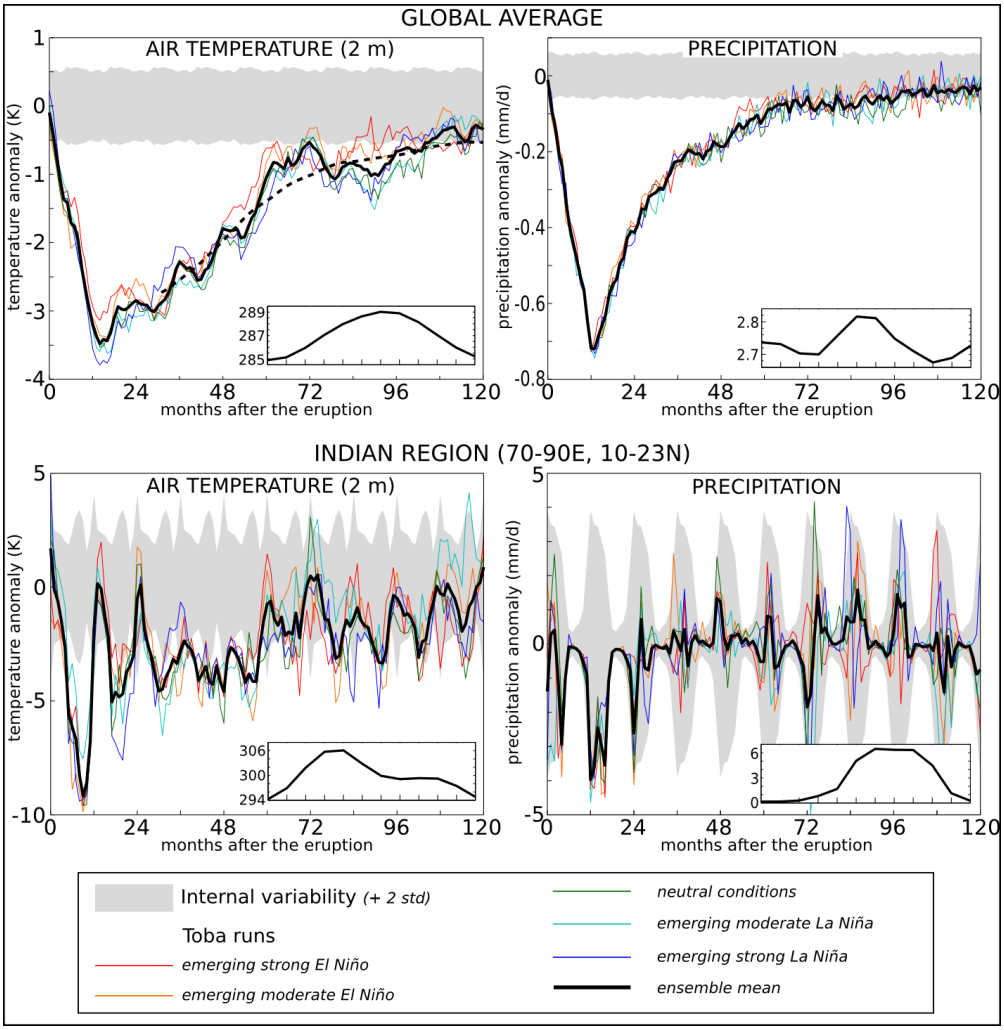

Figure 22: Mean temperature and (b, d) precipitation anomalies for the globe (a, b) and the Indian region (c, d) for the ensemble mean and individual simulations. The shaded areas denote ±1.96 standard deviations of the control run. The inserts are sketches of the respective climatological annual cycles of the control run. The dashed line in (a) depicts a 3-year running. Figure from *Timmreck et al. (2010).*

The Yellowstone volcanic system, with three known large caldera forming eruptions has also been addressed by several model studies (*Timmreck and Graf, 2006;* Jones et al., 2007; *Segschneider et al., 2012*). These eruptions s between 640,000 and 2.1 Ma years ago (Smith and Siegel, 2000) spread volcanic ash over large parts of the North American continent, covering up to one third of the continent with silicate ash of at least 10 cm depth. Large tephra deposits have a strong impact on vegetation and surface. They lead to dying of vegetation, changes of surface fluxes (canopy/ground - air), surface albedo, surface and soil hydrology. These changes will consequently have potentially large and long-lasting impacts on weather, climate and the CO_2 cycle on continental to hemispheric/global scales. Jones et al. (2007) were the first to investigate the climate effects of a continental-sized Yellowstone type volcanic ash deposit. They found no significant global climate changes by such a large ash blanket, but seasonal climatic variability is

increased and major teleconnection patterns (e.g., the Pacific/North American (PNA) are disturbed. However Jones et al. (2007) used a low resolution version of the HADCM3 model and prescribed a constant ash blanket with an assumed albedo of 0.47, which is at the upper end of recent estimates. To better understand the climatic impact of large tephra deposits, MPI-ESM simulations were carried out in the MPI-SV project with an interactive tephra layer. Tephra deposit was implemented in JSBACH similar to the treatment of snow in ECHAM in terms of depth and cover fraction, the latter is assumed to be a function of depth and orography. It is also differentiated between tephra on vegetation (interception, unloading due to wind and rain) and on ground (decay due to remobilization and re-distribution). The surface albedo depends on the fraction of a grid cell covered with tephra, with an estimated ash albedo of 0.35 according to observations (Black and Mack, 1986).

MPI-ESM model results show that the maximum tephra layer after four years is reduced from 50 m to 16 m, but the tephra cover fraction in the grid boxes close to Yellowstone is still 90% to 100%. The surface albedo is increased by up to 70% near the eruption center and about 5% at the east coast of the U.S in the years after the eruption (Figure 23)..

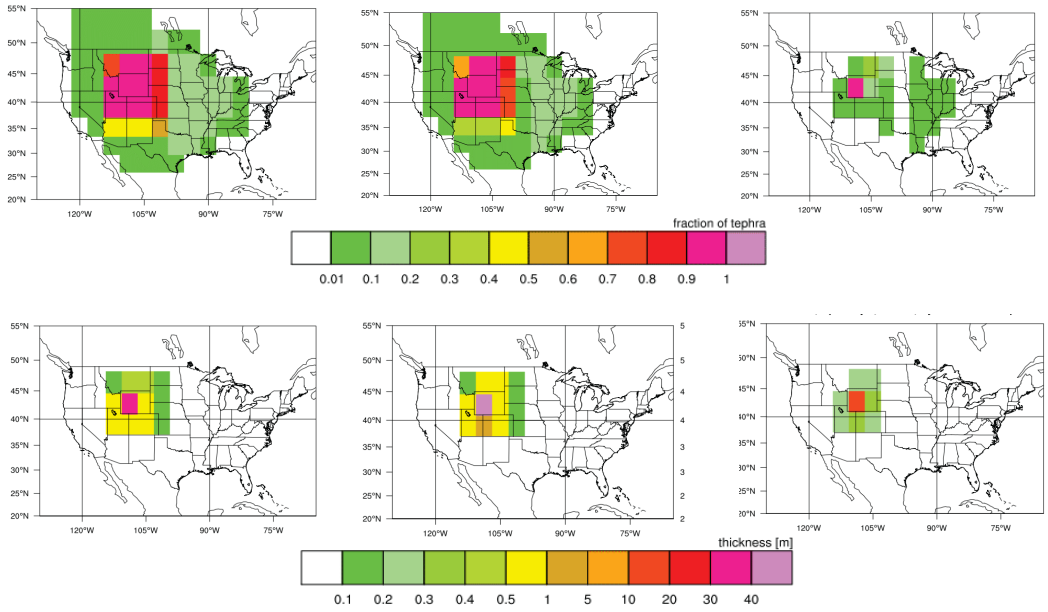

Figure 23: Tephra fraction (upper panel) and thickness (lower panel) after 1 day (left), 1 year (middle) and after 15 years.

The Leaf Area Index (LAI) is significantly reduced in the summer months in particular in a large area around the eruption center where the vegetation is destroyed by about 50% to 100%. After 15 years, the tephra cover fraction in the core grid cell is still 90% and its thickness is 1 m, while in the surrounding grid boxes the tephra thickness is below 10 cm and below 10% on average. Over the Yellowstone grid box the clear (all sky) surface flux is locally reduced by more than 20

(5) W/m2 in the first post-eruption years leading to a slightly larger local cooling of 1 K. Hence, the global climate impact of the tephra layer is not large enough to lead to long-lasting cooling, and therefore neglible in comparison to the one of the stratospheric volcanic aerosol

A series of volcanic eruptions can also enhance the AOD significantly over a long period and may therefore have the potential to modify climate on decadal to multi-decadal time scales. The coldest period in the historical record was the early 19th century, with the two large tropical volcanic eruptions of 1809 (unknown) and Tambora 1815, (Cole-Dai et al., 2009). Several studies discussed whether the increased volcanic activity in the second half of the 13th century contributed to the transition from the relatively warm medieval warm period to the cold one of the Little Ice Age. Schneider et al. (2009) calculated with the CCSM3 model a long-term Arctic cooling for a series of closely timely spaced multiple tropical eruptions, indicating a positive ocean-atmosphere-ice feedback process. With the same model, Zhong et al. (2011) could demonstrate for the mid-13th century that decadal-paced explosive tropical volcanism is able to produce a long-term Arctic cooling, caused by a multi-decadal-scale expansion of NH sea ice. This is in line with the reconstructed abrupt land ice growth from Iceland and Arctic Canada, and might also have triggered the Little Ice Age (Miller et al., 2012). However, in half of the CCSM3 simulations, the strong positive sea-ice-ocean feedback mechanism was absent, suggesting a strong sensitivity of this process to initial conditions (e.g. wind and ocean currents in the North Atlantic, stability of the seawater column). It is still uncertain which processes are the relevant and which states of the climate system are a prerequisite to establish this long-term coupled sea-ice-ocean feedback. Large volcanic eruptions also have an impact on decadal to multi-decadal SST variability via changes in atmospheric teleconnections patterns (*Zanchettin et al., 2012a*; 2012b; Wang et al., 2012).

MPI-ESM simulations of large volcanic eruptions with magnitudes ranging from the 1991 Mt. Pinatubo (historical) to 100-times Mt. Pinatubo (“super eruption”) show also a robust post-eruption sea-ice expansion in the Arctic in all ensembles, which last in the super volcano experiments for about two decades *(Zanchettin et al., 2014)*. Antarctic sea ice however responds only to “super eruptions”, undergoing at first an initial short-lived expansion and a subsequent prolonged contraction phase. Strong volcanic forcing therefore appears to be as potential source of inter-hemispheric interannual-to-decadal climate variability, although the inter-hemispheric signature is weak in the case of historically-sized eruptions. This inter-hemispheric decadal asymmetry in sea ice, which is found in the aftermath of extremely large volcanic eruptions appears therefore as a result of different exposure of Arctic and Antarctic regional climates to

induced meridional heat transport changes and of dominant local feedbacks within Antarctica (*Zanchettin et al., 2014*). After large volcanic eruptions, the global SST and the 2m temperature are almost back to the unperturbed climate state within one decade (Stenchikov et al., 2009; *Timmreck et al., 2010)*, but in the deep ocean the volcanic signal remains over multi-decadal to centennial time scales. The volcanic cooling signal from the late 19th and early 20th century eruptions is for example clearly detectable in the ocean heat content in historic CMIP3 simulations (Delworth et al., 2005; Gregory, 2010).

4.8 Impact on the carbon cycle and vegetation

Large volcanic eruptions can influence the global carbon cycle and biogeochemical processes, because both are sensitive to solar radiation, temperature, humidity and atmospheric and oceanic circulation changes. The volcanic impact on the global carbon cycle has been addressed by a variety of model studies (e.g. Bousquet et al., 2000; Lucht et al., 2002; Angert et al., 2004), but only a couple of research groups run ESMs with a fully coupled carbon cycle (e.g. *Brovkin et al., 2010*; Fröhlicher et al., 2011; Jones et al., 2001, Tjiputra and Otterå, 2011; *Segschneider et al., 2012;* Rothenberg et al., 2012). All studies suggest that the land component is the main driver of atmospheric CO_2 changes, but they differ in the proposed mechanisms (photosynthesis versus respiration) by which the land component drives an atmospheric CO_2 decrease and in the contribution of the different latitudinal distributions (tropics versus high latitudes). Several model studies (Jones et al., 2001; *Brovkin et al., 2010; Segschneider et al. 2012*; Tjiputra and Otterå, 2011) propose an atmospheric CO_2 decrease due to reduced heterotrophic respiration on land in response to surface cooling, which leads to increased carbon storage in soils mostly in tropical and subtropical regions. Other studies (Bousquet et al., 2000; Lucht et al., 2002) suggest more carbon uptake in NH high latitudes. Shortly after an eruption the ocean is a weak carbon sink due to the temperature-induced solubility (e.g. *Brovkin et al., 2010*). Analysis of carbon cycle changes after the Samalas eruption in last Millennium simulations (*Jungclaus et al., 2010; Brovkin et al., 2010*) indicate that after the temperature effect diminishes, the ocean quickly turns from a carbon sink to a carbon source compensating for atmospheric losses to soil, and thereby dampening the longer term atmospheric signal. An asymmetric response of atmospheric CO_2 to volcanic perturbation in general is characterized in the MPI-ESM studies by a fast drop followed by a slow recovery, which is explained by the combined effect of terrestrial and marine carbon pools (*Brovkin et al., 2010*). The magnitude of the atmospheric CO_2 anomaly is thereby primarily determined by the land carbon storage, while its duration is set by the marine carbon cycle (*Segchneider et al., 2013*). The response of the climate carbon cycle system to tropical

eruptions of different strengths was investigated by Frölicher et al. (2011), who could show that the carbon cycle-climate sensitivity γ[14], depends on the perturbation. Furthermore, the modeled γ is on decadal time scales several times larger for a Pinatubo-like eruption than for the industrial period and for a high emission, 21st century scenario.

Segschneider et al. (2013) were the first who studied the long term response of the global climate-carbon cycle system to a very large NH midlatitude (Yellowstone) volcanic eruption in MPI-ESM ensemble simulations of fifteen model integrations that are started at different pre-ENSO states of a control experiment. The long term time series of simulated annual mean carbon pool anomalies from these experiments (Figure 24) show that the response of the carbon cycle to the volcanic eruption can be divided into four phases: during the first two years, the land biosphere carbon pool is decreased in response to volcanic cooling and reduced SW radiation. During year 3, both ocean and soil carbon pool take up carbon in response to the cooling. Over years 4–20, the soil carbon pool further increases, but the ocean releases carbon to compensate for reduced atmospheric pCO_2 caused by the soil carbon pool increase. After two decades, when temperature are recovered, the soil carbon pool slowly releases carbon and the ocean slowly gains back previously released carbon. At the end of the simulations (after 200 years), the ocean and the land carbon pools are still slightly different from the pre-eruption state. The land carbon pools show some long-lasting local anomalies, which are only partly visible in the global signal. *Segschneider et al. (2013*) could also demonstrate the importance of considering different initial climate states for the estimate of the volcanic perturbation with ensemble simulations. For example, the spread of the volcanic perturbations in atmospheric pCO_2 is 4 ppm, compared to a signal of 3–7 ppm and an ensemble mean anomaly of about 5 ppm. Tjiputra and Otterå (2011) investigated the role of potential volcanic eruptions for future climate change projections and associated carbon cycle feedbacks and found that in the future, large volcanic eruptions could lead to increase of carbon uptake from the land and the ocean carbon pools, which is proportional to the frequency of the eruption events.

[14] The global carbon cycle-climate sensitivity γ is defined as change in atmospheric CO_2 per unit change in global mean surface temperature.

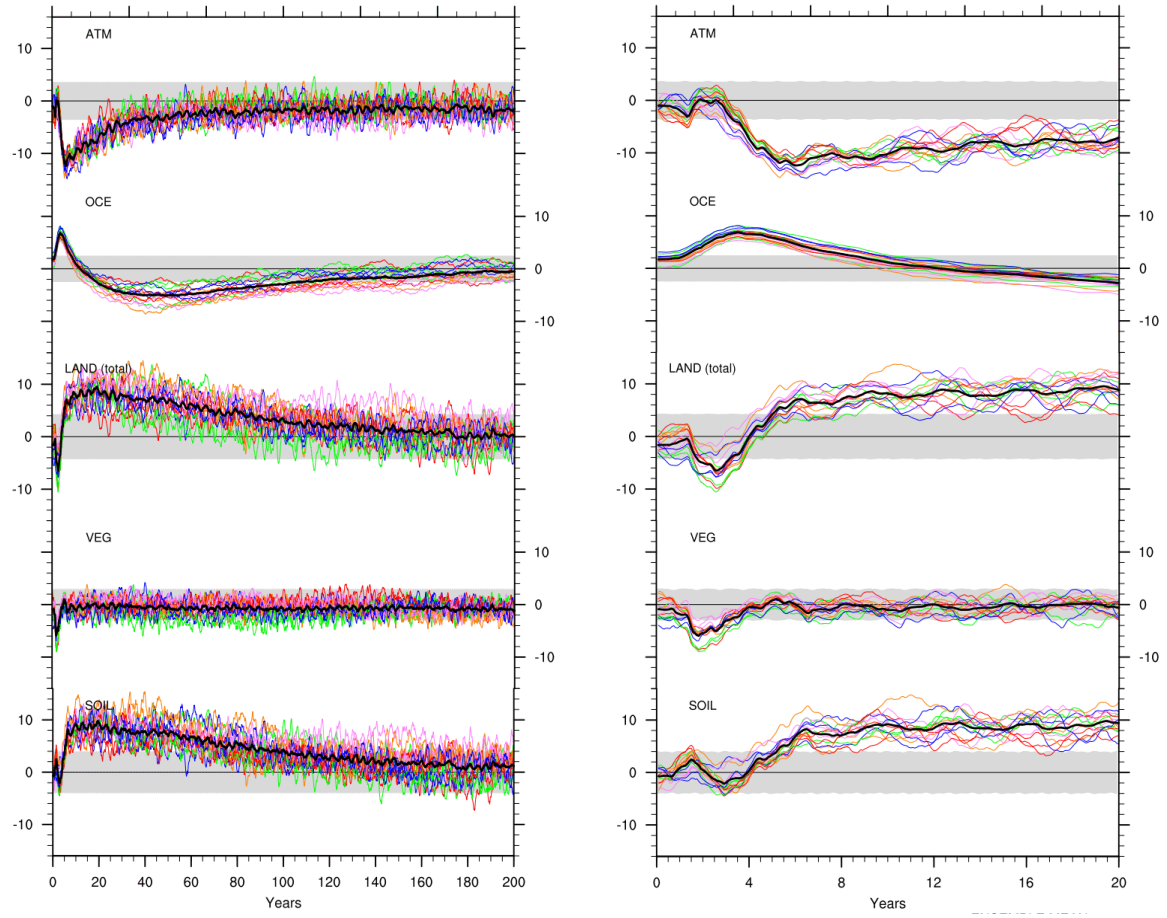

Figure 24: Time series of annual mean carbon pool anomalies in GtC for (from top to bottom) the atmosphere (ATM), ocean (OCE), land vegetation and soil (LAND), and land vegetation (VEG) and land soil (SOIL) separately. Left panel: the entire 200 years of the experiments, right panel: the first 20 years. The thick black line shows the ensemble mean, colors indicate individual ensemble members. The grey bars indicate the ±2σ interval from a 2000 yr control integration. The mean carbon pool inventories are: atmosphere 595 GtC, ocean 38102 GtC, land (total) 3004 GtC, vegetation 585 GtC, and soil 2419 GtC. From *Segschneider et al. (2013).*

However, two potentially important processes are ignored in all the aforementioned model studies which may have an impact on the global carbon cycle. One is the influence of the volcanic ash composition (iron) on the biological carbon pump (Duggen et al., 2010) and one the impact of volcanic induced diffusive radiation changes on the net primary production (Gu et al., 2003). Although recent observational evidence in the North Pacific Ocean indicates that the primary production in the ocean may be affected by nutrient addition from volcanic ash (Li et al., 2011; Hamme et al., 2010), the impact on global atmospheric CO_2 concentration is not necessarily significant (Hamme et al., 2010). Hence, open questions remain and need to be addressed in the future. It is also unclear if the 1991 Mt. Pinatubo eruption led to an enhancement in diffuse radiation and thereby to an increased CO_2 uptake by terrestrial ecosystems in the first 2 post-eruption years. While some model studies (Angert et al., 2004) indicate that the enhanced diffuse radiation to the land carbon sink anomaly is neglible, other studies (Mercado et al., 2009) rather found it to be a major influence. In addition, there is an

ongoing scientific debate if the post-volcanic increase in diffusive radiation could have biased the surface air temperature reconstruction from tree ring data to higher values which would give a smaller volcanic cooling signal. This bias could potentially explain differences in the NH cooling estimates after large tropical eruptions between climate model simulations and tree ring reconstructions (see section 4.1). In 2005, Robock raised the hypothesis that a significant cooling after large volcanic eruptions is missing in temperature reconstructions, because these are mainly based on tree-ring data and the effect of the low temperatures on tree growth is offset by the diffuse radiation effect on the net primary productivity (NPP) (Robock, 2005). Observational evidence from global tree ring data, however, did not show an enhanced NPP following volcanic eruptions, because in the open, conifer-dominated treeline environment from which most of the temperature-sensitive tree-ring chronologies are developed, this effect is less important for productivity (Krakauer and Randerson 2003). Furthermore, analysis of MPI-ESM simulations of the Samalas eruption (*Timmreck et al., 2009; Raddatz et al., EGU General Assembly 2009*) indicate that the reduction in global radiation is amplified more with increasing AOD than the gain in diffuse radiation (Figure 25, Table 3), which suggests that the diffuse radiation enhancement effect is of limited importance with respect to very large volcanic eruptions.

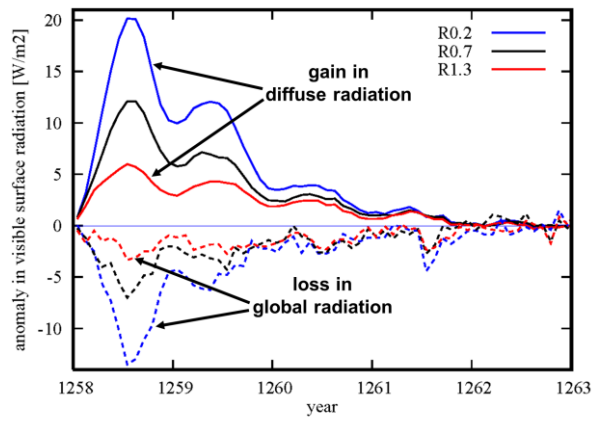

	$R_{0.2}$	$R_{0.7}$	$R_{1.3}$
vis,dif	19.5	11.7	5.72
$\Delta vis,glob$	-12.2	-6.2	-2.71
$-\Delta vis,dif / \Delta vis,glob$	1.59	1.89	2.11

Figure 25 and Table 3: Relation of direct to diffuse radiation. Signal in the diffuse surface visible flux (Δvis, dif, [W/m^2]) and the global surface visible flux (Δvis, glob, [W/m^2]) averaged over land (excluding glacier) and the first boreal summer (JJA) after the eruption. Denotations as in Figure 9. From *Timmreck et al. (2009).*

Distinct dynamical vegetation changes after very large volcanic eruptions have been found in lake sediments (Birks and Lotter, 1994) and marine sediments (Williams et al., 2009). In global climate model simulations a major influence on vegetation cover has so far only been addressed in the case of the YTT eruption. Robock et al. (2009) found in CCSM3 simulations with the Community Land Model Dynamic Global Vegetation Model (CLM-DGVM) that the vegetation distribution changed dramatically as a result of the reduction of sunlight and the following cooling induced by the large aerosol cloud. For example, broadleaf evergreen and tropical

deciduous trees almost disappear and midlatitude deciduous trees are substantially reduced. *Timmreck et al. (2012)* derived information about transient changes in vegetation types after the YTT eruption by forcing the offline dynamical global vegetation model LPJ (Sitch et al., 2002) with the climate anomalies simulated by the MPI-ESM[15].

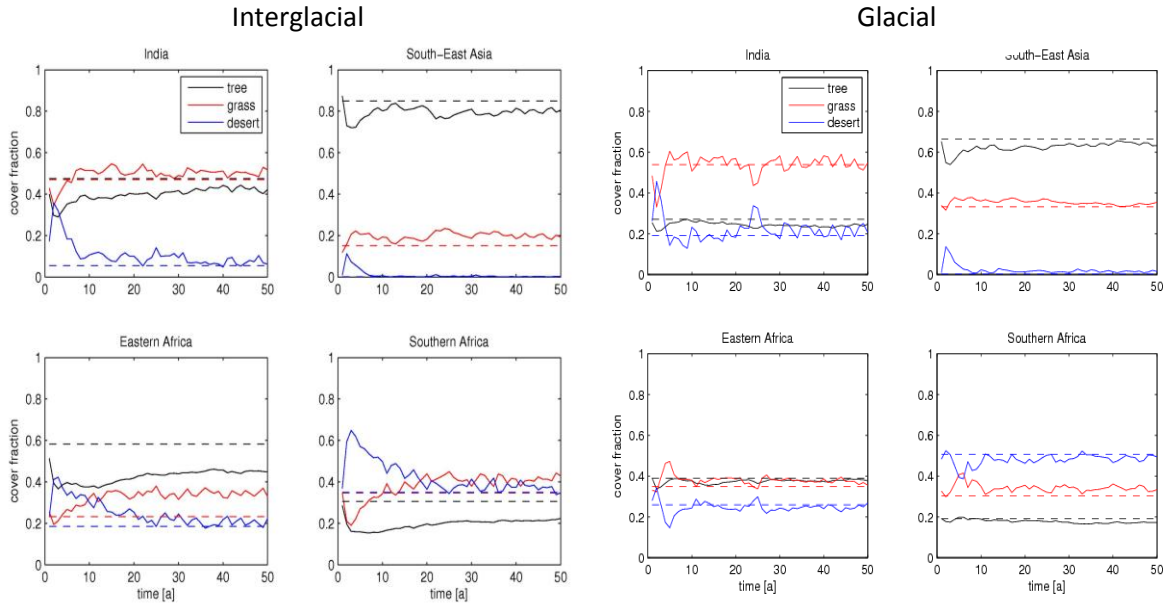

Figure 26: Time series of average vegetation cover fractions in four selected regions for interglacial (left) and glacial (right) conditions. Dashed lines show control experiment, solid lines Toba eruption. Figure from *Timmreck et al. (2012).*

The simulations were performed under both glacial and interglacial background climate conditions to take into account the uncertainties in the timing of the eruption (Figure 26). Under glacial background conditions effects on vegetation are only marginal. Tree and grass cover is reduced for about a decade in India, South East Asia, Southern and Eastern Africa. For interglacial background climate conditions the changes in vegetation changes are more prominent. Bare soil coverage is strongly increasing in Africa during the first few post-eruption years and the ratio between grasses and trees is disturbed for many decades with grasses becoming more dominant. In India and South East Asia the volcanic impact on vegetation is not as strong as in Africa. Grasses become more dominant in these regions for several decades, which agrees well with indications from proxy data. Changes in vegetation composition may therefore have created the biggest pressure on humans after the YTT eruption, who had to

[15] The super volcano experiments were run with the Millennium version of the MPI-ESM which has no dynamic vegetation included.

adapt to more open space with fewer trees and more grasses for some decades, especially in the African regions.

4.9 Impact on seasonal and decadal prediction

Future volcanic eruptions cannot be predicted, but as they could perturb the climate system significantly they could have a strong effect on climate predictions on different time scales. Volcanic eruptions are therefore a potential uncertainty source in seasonal and decadal predictions (Shiogama et al., 2010; Kirtman et al., 2013). Only a few studies have addressed their impact on climate and on multi-year seasonal and decadal climate predictability so far. Collins (2003) indicated that the El Chichón and Mt. Pinatubo eruptions significantly shifted the probability density functions of surface air temperature and mean sea level pressure with a more robust signal for larger eruptions and for continental-scale seasonal averages. Shiogama et al. (2010) studied the potential impact of a future Mt. Pinatubo-size eruption on decadal scale predictability and obtained an increase in variability of global mean surface and upper ocean temperature. Hindcasts with the atmosphere only HADGEM1 model (Marshall et al., 2009) showed that the climate anomalies in the first post-volcanic winter over Europe are strongly dependent on the stratospheric conditions in early winter. Recently, Meehl et al. (2O15) analyzed CMIP5 hindcasts and found that after a volcanic eruption the decadal hindcast skill over the Pacific can be reduced if the post-volcanic observed El Niño variability deviates from the multi-model forced response. However, it remains unclear how large the uncertainty will be for future decadal climate predictions if no volcanic aerosol is taken into account.

To understand how strong volcanic aerosol has affected decadal prediction skill on annual and multi-year seasonal scales over the CMIP5 hindcast period, the German MiKlip[16] prediction system (*Marotzke et al.,* 2016) was applied to perform CMIP5-type hindcasts without volcanic aerosol *(Timmreck et al., 2016*). Decadal hindcasts with the baseline1-LR version (b1-LR) (Pohlmann et al., 2013) are taken as reference. The results show that volcanic aerosols have a significant influence on the decadal prediction skill for global mean surface air temperature in the first pentad after large volcanic eruptions, but not on average over the whole hindcast period as the global warming trend dominates the prediction skill (Figure 27).

[16] The German medium term climate prediction program MiKlip is founded by the German Ministry for Education and Research (BMBF) with the aim to develop a system for decadal scale climate predictions. The MiKlIP prediction system is based on the MPI-M Earth System Model (MPI-ESM).

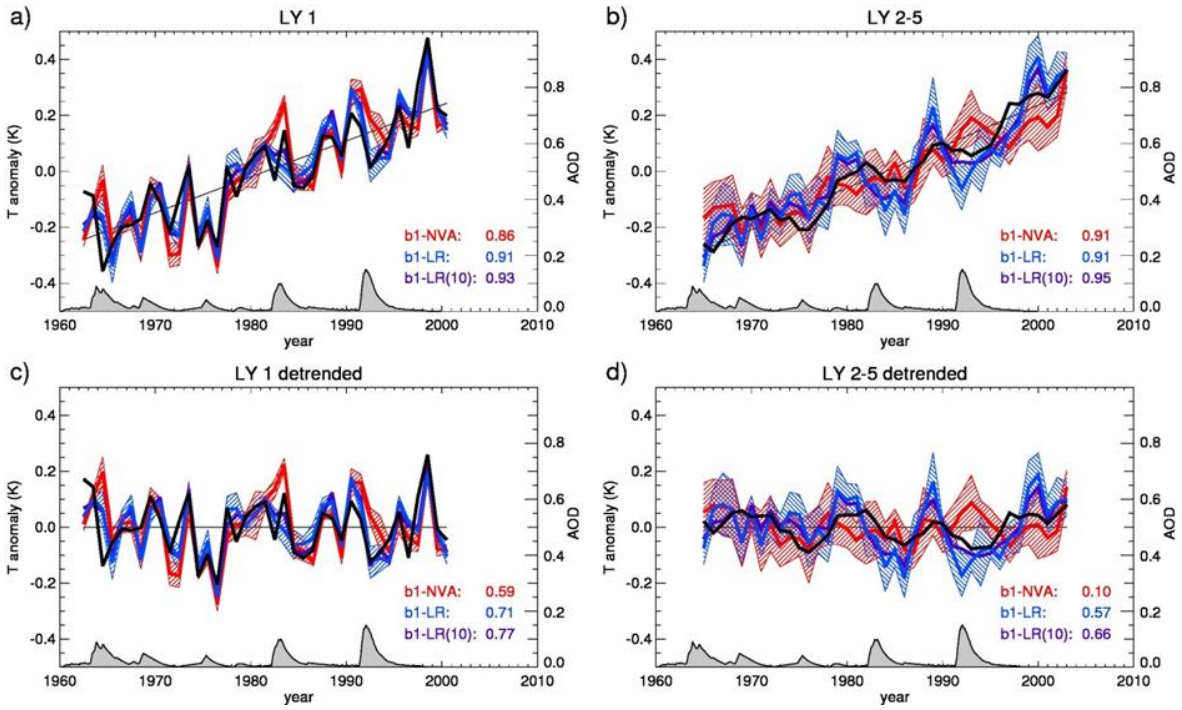

Figure 27: Time series of globally averaged surface temperature anomalies from 1962 to 2004 with respect to the mean of 1962-2004 for HadCRUT3 observations (Brohan et al., 2006) (black), b1-NVA (red) and b1-LR (blue, purple for the 10 ensemble mean). The standard deviation is indicated by the dashed areas. Left panels show the first prediction year (LY1), right panels the 2nd to 5th-year ensemble mean of the hindcasts (LY2-5). Numbers indicate the anomaly correlation coefficients between hindcasts and observations over the whole time period. The time series of annual averaged stratospheric aerosol optical depth (Stenchikov et al., 1998; and updates) is shown by the grey shaded regions. Figure from *Timmreck et al. (2016).*

If the global warming trend is removed from the model results a clear improvement is visible in the prediction skill of global mean surface air temperature due to volcanic aerosol. The low anomaly correlation coefficient of 0.1 between the hindcasts without volcanic aerosol and observed HADCRUT3 surface temperatures (Brohan et al., 2006) indicates that the MPI-ESM model has without external forcing nearly no prediction skill in global mean surface air temperature. Neglecting volcanic aerosol leads also on the regional scale to less skill over the tropical and subtropical Atlantic, Indic and West Pacific, but to an improvement over the tropical East-Pacific, where the model has a negative skill (Thoma et al., 2015).

Multi-seasonal differences in the prediction skill for seasonal-mean temperatures are apparent over Continental Europe with significant decrease in skill in NH winter over Scandinavia and central Europe and over south-eastern Europe and the East-Mediterranean in NH summer if volcanic aerosol is not considered. However, the results presented in *Timmreck et al. (2016*) are only valid for the applied model system and for the selected time period. Thus, the increase in the decadal prediction skill due to volcanic aerosol might be different over other time periods dependent on the strength, the frequency, the eruption season and the geographical location of the volcanic eruptions included.

5. Summary and Outlook

5.1 Summary of main research achievements

For 25 years I have studied the climate impact of large volcanic eruptions by developing the scientific basis and model tools necessary for the understanding of volcanic aerosols and their effects on the Earth system. In the first 15 years, I mostly focused on the volcanic impact on atmospheric chemistry, composition, dynamics and transport and their highly nonlinear interactions. From 2006 to 2011, I led the MPI-Super Volcano" (SV) project with the goal to better understand the climate effects of such extremely large eruptions on all components of the Earth system. Since 2011, I have coordinated the "Alert for LARge volcanic eruptions in Medium term climate prediction" (ALARM) project of the German national research project MiKliP with the focus on decadal scale predictability. My work on volcanoes and climate has been guided by the following questions:

- How do large volcanic eruptions impact atmospheric composition and radiation?
- Do nonlinearities in the climate system limit or enhance the impact of a huge volcanic disturbance and can a very large volcanic eruption or „super eruption" disturb the climate system over a longer time scale or even push the system into another climate state?
- What is the impact of large volcanic eruptions on seasonal and decadal predictability?

In the following, I briefly summarize my main research achievements for each of these research questions[17]:

Atmospheric impact of large volcanic eruptions

A prerequisite to understand the atmospheric impact of volcanic eruptions are suitable tools, for example global aerosol models capable of simulating the temporal and spatial development of the volcanic aerosol size distribution from the initial SO_2 emission and thereby also the relevant parameters for aerosol climate interactions. During my PhD thesis (*Timmreck, 1997; Timmreck and Graf; 2000*), I developed the first global three-dimensional stratospheric aerosol model, which calculates aerosol microphysical processes explicitly online in a GCM (*Timmreck, 2001*). In the following years, the *SAM model* has been updated, extended and further improved in a PhD thesis under my co-supervision (R. Hommel, 2008), resulting in a revised version *SAM2*

[17] As in the previous chapters, all of the publications to which I contribute as author or co-author are indicated in Italic but in addition I also indicate in this chapter, where I am second and third author.

(Hommel, 2008; *Hommel, Timmreck et al. 2011; 2015*). I also contributed to the adaption of a global tropospheric aerosol model to stratospheric processes and to the development of a volcanic ash module (*Niemeier et al., 2009*). In addition I performed the first fully coupled GCM simulation of the Mt. Pinatubo eruption with respect to aerosol and ozone (*Timmreck et al., 2003*). These developments have led to the following scientific highlights:

- In a volcanically undisturbed atmosphere the simulated stratospheric aerosol load is mainly determined by the sulfur flux from the troposphere (*Timmreck, 2001*) and modulated by QBO induced anomalies in the vertical advection (*Hommel, Timmreck at al., 2015*). Convective updraft in the Asian Monsoon region significantly contributes to both stratospheric aerosol load and size (*Hommel, Timmreck et al., 2011; Kremser et al., 2016*).
- The interactive coupling of the volcanic aerosol with the radiation scheme is a prerequisite to adequately describe the observed transport characteristics over the first months after the Mt. Pinatubo eruption (*Timmreck et al., 1999b*). Radiative heating from volcanic ash also influences the initial transport of the volcanic cloud for NH mid and high latitude eruptions (*Niemeier, Timmreck et al. 2009*).
- Post-volcanic ozone anomalies are a combined effect of different processes including aerosol induced heating, heterogeneous chemistry and changes in the photolysis rates (*Timmreck et al., 2003*). Between 20 km and 30 km, the tropical averaged O_3 concentration decreases due to heterogeneous chemistry and upward transport, and increases above 30 km due to a decrease in NO_x.
- An interactive treatment of aerosol microphysics is important for the volcanic impact on cloud microphysical/optical properties. Depending on the assumed scenario, a pronounced increase in ice water path and a notable effect on cloud radiative forcing were simulated (*Lohmann, Kärcher and Timmreck, 2003*).
- The evolution of volcanic aerosol, including its temporal and spatial dispersal, size distribution and the resulting aerosol optical parameters as well as its atmospheric impact, is sensitive to the season of eruption (*Timmreck and Graf, 2006; Toohey et al., 2011*).
- The high concentration of volcanic aerosol in high latitudes after a large NH midlatitude eruption leads to strongly intensified cooling in the polar night and to an intensified polar vortex which produces a midlatitude ``continental winter warming'' at the surface as observed after tropical eruptions (*Graf and Timmreck, 2001*).

- The stratospheric temperature response pattern can only be realistically simulated in MAECHAM5 if all known background conditions were included (M. Thomas, 2008; *Thomas, Timmreck et al.. 2009a*)
- The volcanic perturbation in the tropical and subtropical lower stratosphere is significantly modulated by the phase of the QBO (*Thomas, Giorgetta, Timmreck et al. 2009b*). Vice versa, Mt. Pinatubo simulations with a version of the MAECHAM5 model with higher vertical resolution, which simulates the QBO from resolved and parameterized wave mean-flow interactions, indicate that very likely the Mt. Pinatubo aerosols in the equatorial stratosphere caused the observed delay in the descent of the easterly jet of the QBO in 1991/1992 (Giorgetta and Thomas, EGU General Assembly 2009; *Giorgetta, Thomas, Timmreck et al. 2011 pers.com.*).

Nonlinearity

The question of the climate impact of very large volcanic eruptions and possible non-linearities associated with it has been addressed in the MPI-SV project under my guidance. MPI-ESM model simulations ranging from a recent eruption (Mt. Pinatubo in 1991) to super eruptions (YTT (74±2kyr BP), Yellowstone (most recent 640 kyr BP)) have been performed and analyzed together with MPI-ESM simulations of the last Millennium *(Jungclaus, Lorenz, Timmreck et al., 2010)* to address the question whether the post-volcanic climate response is linear with eruption strength or whether it is limited for extremely large ones. Key scientific achievements of the MPI-SV project are:

- The climate effects of extremely large volcanic eruptions are weaker and smaller than previously thought due to the nonlinear behavior of aerosol microphysical processes and aerosol optical properties (*Timmreck et al., 2009; 2010; 2012*). A more complex treatment of microphysical processes leads to much weaker radiative forcing due to larger particle sizes and a faster removal rate.
- No long-term shift in the climate system could be detected in the MPI-ESM simulations after a large volcanic eruption. The simulated surface air temperature is perturbed for a couple of decades after the YTT and Yellowstone eruptions but recovered after 75 years (*Timmreck et al., 2010*; *Segschneider, Beitsch, Timmreck et al., 2013*).
- Post-volcanic temperature and precipitation anomalies exceeded the range of natural variability after the YTT eruption but were not large enough to severely affect the survival of modern humans (*Timmreck et al., 2010; 2012*).
- The relatively weak temperature response after very large volcanic eruptions could partially also explain the inconsistencies between simulated and reconstructed post-

volcanic cooling for very large historic eruptions (*Timmreck et al., 2009; Anchukaitis et al., 2012*) and thereby substantially contribute to an intensive debate about chronological errors in tree-ring-based temperature reconstructions after large volcanic eruptions (e.g. Mann et al. 2012; 2013, D'Arrigo et al., 2013).

- Nonlinear aspects of volcanic aerosol growth and atmospheric transport lead to attenuated deposition of sulfate to Antarctica after very large eruptions. This implies that the strength of the largest eruptions of the Earth's history may be underestimated by analysis of Antarctic ice cores (*Toohey, Krüger and Timmreck, 2013*).
- Post-eruption sea ice anomalies show strong inter-hemispheric differences dependent on the magnitude of the eruption. This is the result of the different behavior of Arctic and Antarctic regional climates to induced meridional heat transport changes and of local feedbacks within the Antarctic subcontinent (*Zanchettin, Bothe, Timmreck et al., 2014*).
- Very large volcanic eruptions have a long-lasting impact on biogeochemical cycles, e.g. the carbon cycle is not in equilibrium after 200 years (*Segschneider, Beitsch, Timmreck et al., 2013*). On the short term post-eruption atmospheric CO_2 anomalies are explained mainly by changes in land carbon storage, on the longer term, the ocean compensates for the atmospheric carbon loss (*Brovkin et al., 2010; Segschneider, Beitsch, Timmreck et al., 2013*).
- Bare soil coverage is strongly increasing after a very large volcanic eruption with fewer trees and more grass compared to the pre-eruption phase (*Timmreck et al., 2012*).

Variability and Predictability

When the next large climate relevant volcano erupts, large changes in the Earth system are to be expected which will have an impact on seasonal and decadal climate predictability. It is therefore essential to ensure that current seasonal and decadal forecasts systems are prepared for future volcanic events. Therefore, I have set up a stand-by model system for a rapid, model-based assessment of the decadal scale climate impact of any major volcanic eruptions for the MiKlip forecast system (*Marotzke et al., 2016*) and tested it for a Mt. Pinatubo-like eruption in 2013 and 2015 (*Timmreck et al. in prep*). In addition, it is import that the main processes and pathways through which volcanic aerosol affects climate variability and predictability are fully understood and well represented in the model. This is in particular crucial for NH winter climate which is controlled largely by dynamical changes. Key findings with respect to the volcanic impact on climate variability and predictability are:

- Volcanic aerosol significantly affects the decadal prediction skill for global, annual and seasonal mean surface air temperature over the CMIP5 hindcast period in the first pentad after strong volcanic eruptions in the MiKlip prediction system (*Timmreck et al., 2016*). The MiKlip system has no prediction skill in global mean surface air temperature if global warming and volcanic forcing is neglected.
- The simulated stratospheric polar vortex in NH winter seems to react only weakly to external forcing (*Toohey et al., 2014; Bittner, Timmreck et al., 2016a*). This is relevant not only for the prediction potential for European/North Atlantic winter climate in the aftermath of large volcanic eruptions but also more generally for other external forcings as well.
- Post-volcanic changes in the zonal wind at NH high latitudes result from robust strengthening of the stratospheric residual circulation rather than from direct aerosol radiative heating (*Toohey et al., 2014*). The high latitude effects result in part from enhanced stratospheric wave activity and are therefore more variable than if they resulted from aerosol heating only.
- A new dynamical mechanism of the strengthening of the polar vortex in the first two post-volcanic NH winter has been identified *(*M. Bittner, 2015*; Bittner, Timmreck et al., 2016a).* Positive stratospheric zonal wind anomalies at 30°N, where the strongest change in the temperature gradient occurs, change the background conditions for wave propagation and lead to less wave-driven momentum deposition in the region of the NH polar vortex.
- Analyzing a 100-member ensemble of historical (1850-2005) MPI-ESM-LR simulations reveals that due to the high internal variability in NH high latitudes in boreal winter an ensemble larger than what is usually provided by CMIP5 is needed to significantly detect the NH polar vortex strengthening after volcanic eruptions (*Bittner, Schmidt, Timmreck et al., 2016b*).
- The strength of the volcanic eruption turns out to be an important factor, as the ensemble spread is significantly reduced under strong volcanic forcing (*Bittner, Timmreck et al., 2016a*). For the two strongest eruptions of the historical record, the mean of 15 CMIP5 models shows a robust strengthening of the NH polar vortex, which shows that the models do not fail to reproduce the dynamical NH winter response to volcanic eruptions (*Bittner, Schmidt, Timmreck et al., 2016b*).

- Post-eruption oceanic and atmospheric anomalies describe a decadal fluctuation in the coupled ocean–atmosphere system and lead to a second delayed NH winter warming (*Zanchettin, Timmreck et al., 2012a; 2013a*).
- A detailed knowledge of the background conditions is necessary for forecasting volcanically induced climate anomalies on seasonal and decadal time scales as background conditions add not only noise to the decadal climate response of a large volcanic eruption, but they also have an impact on the processes involved in the post-eruption decadal evolution (*Zanchettin et al., 2013b*).

In an invited overview paper for WIRE Climate change (*Timmreck, 2012*) I could demonstrate that understanding of volcanic climate effects had significantly advanced in the prior decade, in particular the knowledge about the influence of very large volcanic eruptions on other Earth system components other than the atmosphere. The MPI-SV project substantially contributed to this progress. An assessment of the climate impact of large volcanic eruptions can, however, not be achieved without a deep understanding of the variability of the stratospheric aerosol and the microphysical processes which determine the life cycle of the stratospheric aerosol (*Timmreck, 2012; Mann et al., 2015*) and post-volcanic climate variability (*Zanchettin, Timmreck et al., 2015*). These tasks can only be addressed in a multi-model framework. I am therefore strongly involved in the development and organization of two large model intercomparison projects: the Stratospheric Sulfur and its Role in Climate (SSiRC)[18] Interactive Stratospheric Aerosol Model Intercomparison Project (ISA-MIP[19]), which I coordinate together with Graham Mann, Univ. Leeds (*Timmreck et al. to be submitted*) and the CMIP6 endorsed Model Intercomparison Project on the climate response to Volcanic forcing (VolMIP[20]) together with Davide Zanchettin, Univ. of Venice, and Myriam Khodri, IPSL (*Zanchettin, Timmreck et al. 2015; Zanchettin, Khodri, Timmreck et al. 2016*). Both model intercomparison activities will be described in more detail in the next section in the light of future research questions.

5.2 Outlook/Avenues for future research

The simulation of volcanically-induced climate variability remains a challenging task for ESM and climate models. CMIP5 analyses have shown that climate models' capability to accurately and robustly simulate observed and reconstructed volcanically-forced climate behavior remains poor

[18] SSiRC is a SPARC initiative on Stratospheric Sulfur and its Role in Climate (SSiRC) (*Rex, Timmreck et al*., *2013*) aimed at facilitating an improved understanding of the role of stratospheric sulfur in climate http://www.sparc-ssirc.org
[19] http://www.sparc-ssirc.org
[20] http://volmip.org/

(*Zanchettin, Khodri, Timmreck et al., 2016*). In addition there is a lack of robust behavior in the climate simulations. The large inter-model spread in the CMIP5 models is critically determined by the internal variability and the imperfect knowledge of the background climate conditions before the instrumental period (e.g*., Zanchettin et al., 2013b*). Additionally, one has to deal with large uncertainties with the volcanic forcing itself (e.g *Timmreck, 2012*). On one hand, the volcanic radiative forcing has to be reconstructed mostly based on indirect evidence and are prone to partially substantial inconsistencies between available volcanological datasets (chapter 3), on the other hand past model intercomparison studies, have revealed significant discrepancies in the volcanic climate impact attributed to the treatment of the volcanic aerosols in the chemistry and radiation calculations (section 4.2). In summary, it is so far not clear whether the large inter-model spread in the simulated post-volcanic climate response mostly depends on uncertainties in the imposed volcanic forcing or on an insufficient representation of climate processes. To discriminate the individual uncertainty factors it is useful to develop standardized experiments/model activities that systematically address specific uncertainty factors. An approach I have followed in the last years is to focus separately on the two major aspects of uncertainties in the post-volcanic model response with two large international model intercomparison projects (Figure 28).

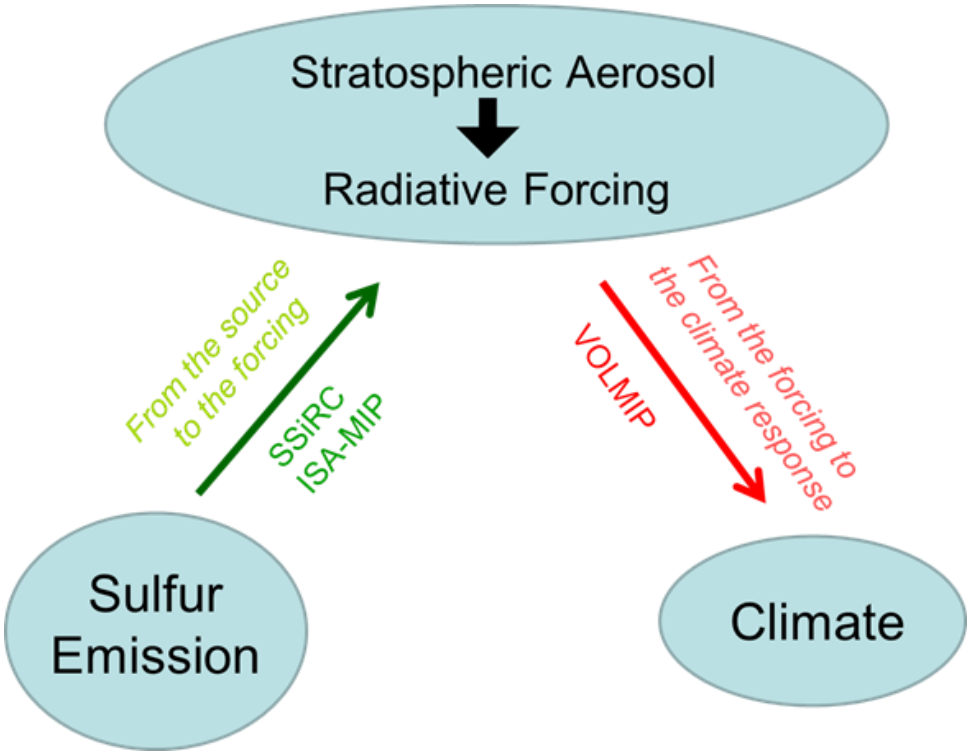

Figure 28: Schematic overview of the international model intercomparison activities I coordinate.

The SSiRC Interactive Stratospheric Aerosol Model Intercomparison project (ISA-MIP) covers the uncertainties in the pathway from the eruption source to the volcanic radiative forcing (*Timmreck et al., to be submitted*). The aim of ISA-MIP is to constrain and to improve global aerosol models by using a range of observations in order to reduce the forcing uncertainties. The experiments have been designed to investigate key processes which influence the formation and temporal development of stratospheric aerosol in different time periods of the observational record (background, the period 1998-2012, which is modulated by small to moderate eruptions and episodes of large volcanic eruptions). A detailed overview of the planned ISA-MIP experiments and the knowledge gaps to be addressed with them is found in the appendix table A1.

The CMIP6 Model Intercomparison Project on the climate response to Volcanic forcing (VolMIP) addresses the pathway from the forcing to climate response and the feedback, studying the uncertainties in the post-volcanic climate response to a well-defined volcanic forcing (*Zanchettin, Khodri, Timmreck* et al., 2016). The central idea of VolMIP is that all participating climate models apply the same volcanic forcing under a similar wide range of background climate conditions to assess the causes of an inter-model spread linked to the different treatment of physical processes. One key aspect of VolMIP is the consideration of the immediate short term scales changes, as for example the NH winter climate response in the aftermath of a large tropical eruption. The second focus of VolMIP is placed on volcanic induced decadal to multi-decadal changes e.g. the response of the oceanic circulations and associated long-term changes in heat transports and ocean-atmosphere coupling. A detailed overview of the planned experiments and their scientific questions is found in tables A2 and A3 in the appendix.

The upcoming model intercomparison projects cannot address all open questions and research needs. The large uncertainties that exist for the initial phase of the volcanic eruption with respect the amount of particulate and volatile matter released reaching the upper troposphere and lower stratosphere and their physical state (water vapor versus ice), are not tackled. Identifying synergies between different emission models, for example fire and volcanic eruption models, can help to better understand injection pathways (*Weil et al., 2012)*. In addition, cloud resolving three-dimensional model simulations of the volcanic plume (e.g. Herzog and Graf, 2010) which could link volcanological field data and global model simulations are needed. Differences between model and observations also exist for the dynamical response in the SH for the most recent eruptions. Post-volcanic changes in the Southern Annular Mode are important for stratospheric ozone and for the global carbon cycle. The volcanic impact on the global carbon

cycle has been investigated by a couple of model studies which indicate that land processes are the main driver of atmospheric CO_2 changes but the relative contribution of several processes is uncertain. In addition some important aspects have not been addressed in ESMs so far, e.g. volcanic ash fertilization. Another critical aspect is the simulation of the volcanic impact on the hydrological cycle, for example the spatial discrepancy between model and observations in the Asian monsoon regions (section 4.5). This is an important caveat, which needs to be resolved also in the light of reliability of geoengineering studies with respect to stratospheric aerosol, for which volcanic eruptions are often considered as an imperfect analogue (e.g. Robock et al. 2013). The model systems which are used are the same for both applications and forcing dependencies are similar; e.g. from the selected emission strategy (*Niemeier, Schmidt, Timmreck, 2011; Niemeier and Timmreck, 2015*).

Since the Mt. Pinatubo eruption in 1991, the stratosphere has not been disturbed by a large climate relevant volcanic eruption. Several small to moderate volcanic eruptions have, however, affected the lower stratosphere (e.g. Vernier et al., 2011), which rather than anthropogenic influences are the primary source of the observed increase in stratospheric aerosol in the early 21th century (Neely et al., 2013). Already in 1997, Graf et al. (1997) showed that the upper tropospheric sulfur load is dominated by volcanic sulfur, while anthropogenic sulfur dominates the sulfur concentrations in the lower troposphere. The effects of these small to moderate volcanic eruptions on climate are not so pronounced as for the big ones but are still evident in many aspects. Neglecting these changes could likely contribute to an over-estimation of global warming projected by climate models, compared to the observed global temperature record for the past decade (e.g. Solomon et al. 2011; Santer et al., 2014; Ridley et al. 2014; Brühl et al., 2015). The moderate 2015 eruption of the Calbuco volcano (19.6 °S) was also identified as the main reason why there was a record October Antarctic ozone hole in 2015 (Solomon et al., 2016). Hence, until the next large volcanic eruption happen, obervations of the moderate to smaller ones provide a good opportunity to learn more about the pathways through which volcanic aerosol could influence our climate, in particular aerosol microphysical and transport processes and the indirect effect of volcanic aerosol.

Large volcanic eruptions are rare and provide therefore only poor statistical constraints. This substantially affects the comparability of model results and the predictability of the climate effects of future eruptions. Current ESMs can be expected to reliably predict the global average temperature response to volcanic eruptions but the forecast skill for regional responses remains limited. Coordinated national and international efforts involving scientists from various fields

and with different expertise are necessary to get our society better prepared for the next large volcanic eruption. Our understanding of the impact of large volcanic eruptions on the Earth system has considerably improved over the last years, still the possibility of a large volcanic eruption introduces some of the largest uncertainty concerning the future evolution of the climate system on the time scale of a few years but also the greatest opportunity to learn more about the behavior of the climate system.

Acknowledgements

I am grateful for all the years I could work at the MPI of Meteorology (MPI-M). To do science in such a lively and inspiring atmosphere and together with such great colleagues is certainly not self-evident and I very much appreciate it. I would like to thank all the directors: Martin Claussen, Jochem Marotzke and Bjorn Stevens who made this possible and who supported me in several different ways. I am sincerely grateful not only to the current directors but also to their predecessors. I was priviledged to work with: Klaus Hasselmann, Hartmut Grassl and Lennart Bengtsson and I am especially obliged to Guy Brasseur who implemented the Super Volcano group as one of the cross-cutting projects of MPI-M. I had the pleasure to "lead" this project for a couple of years, which was a great experience and also a lot of fun. I also would like to thank my PhD supervisor Hans Graf for his continuous support and Tom Crowley, who left us far too early, for his advice and inspiring discussions.

My work would not have been possible without the support of many MPI-M institute members, not only from the scientific staff but also from the service and support groups and the administration who made and make my every day working life quite easy. In particular, I am obliged to my present and former colleagues in the Super Volcano and in the Middle and Upper Atmosphere group. Namely, I would like to thank (in alphabetical order): Alexander Beitsch, Matthias Bittner, Monika Esch, Marco Giorgetta, Rene Hommel, Johann Jungclaus, Stefan Kinne, Thomas Kleinen, Kicki Krüger, Stephan Lorenz, Elisa Manzini, Uwe Mikolajewicz, Ulrike Niemeier, Holger Pohlmann, Sebastian Rast, Hauke Schmidt, Jochen Segschneider, Natasha Sudarchikova, Manu Ana Thomas, Matt Toohey, Martin Wiesner and Davide Zanchettin for working with each other and learning from each other over all these years.I am also grateful for being part of the SSiRC and VolMIP communities. It is a privilege to work with a lot of great scientists at national and international levels and to learn from their expertise and experience. It is impossible to list all of them, so exemplary I would like to thank here my VolMIP and SSiRC co-chairs: Myriam Khodri, Stefanie Kremser, Markus Rex, Larry Thomason, Jean-Paul Vernier and again Davide Zanchettin for the succcesfull cooperation.

Last but not least, goes my deepest gratitude to my family and friends in particular to my son Johann, for bringing me always down to earth, and to my husband Hannes for his love, continuous support and patience (!)

While working on the thesis new ideas arised and new questions poped up which need to be answered. Hence, this will not be the end of my work on volcanoes and climate. I am still on my way.

References

Adams J, Mann ME, Ammann CM. Proxy evidence for an El Nino-like response to volcanic forcing. Nature 2003, 426: 274–278, doi: 10.1038/nature02101.

Al-Saadi J, Pierce R, Fairlie T, Kleb M, Eckman R, Grose W, Natarajan M, Olson J. Response of middle atmosphere chemistry and dynamics to volcanically elevated sulfate aerosol: Three-dimensional coupled model simulations. J Geophys Res 2001, 106: 27,255-27,276, doi: 10.1029/2000JD000185.

Ambrose SH. Late Pleistocene human population bottlenecks, volcanic winter, and differentiation of modern humans. J Hum Evol 1998, 34: 623–651,doi: 10.1006/jhev.1998.0219.

Ammann C, Meehl G, Washington W, Zender C. A monthly and latitudinally varying volcanic forcing dataset in simulations of 20th century climate. Geophys Res Lett 2003, 30: 1657, doi: 10.1029/2003GL016875.

Ammann CM, Joos F, Schimel DS, Otto-Bliesner BL, Tomas RA. Solar influence on climate during the past millennium: Results from transient simulations with the NCAR climate system model. Proc Natl Acad Sci 2007, 104:3713–3718, doi: 10.1073/pnas.0605064103.

Anchukaitis KJ, Buckley BM, Cook ER, Cook BI, D'Arrigo RD, Ammann CM. The influence of volcanic eruptions on the climate of the Asian monsoon region. Geophys Res Lett 2010, 37: L22703, doi: 10.1029/2010GL044843.

Anchukaitis K, Breitenmoser P , Briffa K, Buchwal A, Büntgen U, Cook E, D'Arrigo R, Esper J, Evans M, Frank D, Grudd H, Gunnarson B, Hughes M, Kirdyanov A, Körner C, Krusic P , Luckman B, Melvin T, Salzer M, Shashkin A, **Timmreck C**, Vaganov E, Wilson R. Tree-rings and volcanic cooling. Nat Geosci 2012, 5: 836-837, doi: 10.1038/ngeo1645.

Angert A, Biraud S, Bonfils C, Buermann W, Fung I. CO2 seasonality indicates origins of post-Pinatubo sink. Geophys Res Lett 2004, 31: L11103, doi: 10.1029/2004GL019760.

Arfeuille F, Luo BP, Heckendorn P, Weisenstein D, Sheng JX, Rozanov E, Schraner M, Brönnimann S, Thomason LW, Peter T. Modeling the stratospheric warming following the Mt. Pinatubo eruption: uncertainties in aerosol extinctions. Atmos Chem Phys 13: 11221-11234, doi: 10.5194/acp-13-11221-2013.

Arfeuille F, Weisenstein D, Mack H, Rozanov E, Peter T, Brönnimann S. Volcanic forcing for climate modeling: a new microphysics-based dataset covering years 1600–present. Clim Past 2014, 10: 359-375, doi:10.5194/cp-10-359-2014.

Aquila V, Oman LD, Stolarski RS, Colarco PR, Newman PA. Dispersion of the volcanic sulfate cloud from a Mount Pinatubo–like eruption. J Geophys Res 2012, 117: D06216, doi: 10.1029/2011JD016968.

Aquila V, Oman LD, Stolarski R, Douglass AR, Newman PA. The Response of Ozone and Nitrogen Dioxide to the Eruption of Mt. Pinatubo at Southern and Northern Midlatitudes. J Atmos Sci 2013, 70: 894–900, doi: 10.1175/JAS-D-12-0143.1.

Auchmann R, Brönnimann S, Breda L, Bühler M, Spadin R, Stickler A. Extreme climate, not extreme weather: the summer of 1816 in Geneva, Switzerland. Clim Past 2012, 8: 325-335, doi: 10.5194/cp-8-325-2012.

Balter M. Of two minds about Toba's impact. Science 2010, 23: 1187–1188, doi: 10.1126/science.327.5970.1187-a.

Barkstrom BR. The Earth Radiation Budget Experiment (ERBE). Bull Am Meteorol Soc 1984, 65: 1170-1185, doi: 10.1175/1520-0477(1984)065<1170:TERBE>2.0.CO;2.

Bândă N, Krol M, van Noije T, van Weele M, Williams JE, Le Sager P, Niemeier U, Thomason L, Röckmann R. The effect of stratospheric sulfur from Mount Pinatubo on tropospheric oxidizing capacity and methane. J Geophys Res Atmos 2015, 120: 1202–1220, doi: 10.1002/2014JD022137.

Bândă, N, Krol, M, van Weele, M, van Noije, T, Le Sager, P, Röckmann T. Can we explain the observed methane variability after the Mount Pinatubo eruption? Atmos Chem Phys 2016, 16: 195-214, doi: 10.5194/acp-16-195-2016.

Bender F, Ekman A, Rodhe H. Response to the eruption of Mount Pinatubo in relation to climate sensitivity in the CMIP3 models. Clim Dyn 2010, 35: 875–886, doi: 10.1007/s00382-010-0777-3.

Bekki, S. Oxidation of volcanic SO2: a sink for stratospheric OH and H2O. Geophys Res Lett 1995, 22: 913–916, doi: 10.1029/95GL00534.

Bekki S, Pyle JA, Zhong W, Toumi R, Haigh JD, Pyle DM. The role of microphysical and chemical processes in prolonging the climate forcing of the Toba eruption. Geophys Res Lett 1996 23: 2669-2672, doi: 10.1029/96GL02088.

Berdahl M, Robock A. Northern Hemispheric cryosphere response to volcanic eruptions in the Paleoclimate Modeling Intercomparison Project 3 last millennium simulations. J Geophys Res Atmos 2013, 118: 12,359–12,370, doi: 10.1002/2013JD019914.

Birks HJB, Lotter AE. The impact of the Laacher See Volcano (11000 yr B.P.) on terrestrial vegetation and diatoms. J Paleolimnol 1994, 11: 313-322, doi: 10.1007/BF00677991.

Bittner M, **Timmreck C**, Schmidt H. Impacts of Strong Volcanic Eruptions on the northern hemisphere winter in the CMIP5 MPI-ESM simulations. 3rd International Conference on Earth System Modelling Hamburg, Vol., 3rd ICESM-127, 2012.

Bittner, M. On the discrepancy between observed and simulated dynamical responses of Northern Hemisphere winter climate to large tropical volcanic eruptions. PhD Thesis Universität Hamburg 2015 (also Reports on Earth System Science Max Planck Institute for Meteorology, 173 doi: 10.17617/2.2239264).

Bittner, M, C. **Timmreck C**, Schmidt H, Toohey M, Krüger K. The impact of wave-mean flow interaction on the Northern Hemisphere polar vortex after tropical volcanic eruptions. J Geophys Res Atmos 2016a, 121: 5281–5297, doi: 10.1002/2015JD024603.

Bittner M,Schmidt H, **Timmreck C**, Sienz F. Using a large ensemble of simulations to assess the Northern Hemisphere stratospheric dynamical response to tropical volcanic eruptions and its uncertainty. Geophys Res Lett 2016b, 43: 9324–9332, doi: 10.1002/2016GL070587.

Black RA, Mack RN. Mount St. Helens: Recreating its effects on the steppe environment and ecophysiology. Ecology 1986, 67: 1289-1302, doi: 10.2307/1938685.

Bluth GJS, Rose WI, Sprod IE, Krueger AJ. Strato-spheric loading of sulfur from explosive volcanic eruptions. Journal of Geology 1997, 105: 671–683, doi: 10.1086/515972.

Bodeker GE, Waugh DW. The Ozone Layer in the 21st Century. Chapter 6 in Scientific Assessment of Ozone Depletion: 2006. Global Ozone Research and Monitoring Project—Report No. 50. World Meteorological Organization, Geneva, Switzerland.

Boer G, Stowasser M, Hamilton K. Inferring climate sensitivity from volcanic events. Clim Dyn 2007, 28: 481–502, doi: 10.1007/s00382-006-0193-x.

Boer GJ, Smith DM, Cassou C, Doblas-Reyes F, Danabasoglu G, Kirtman B, Kushnir Y, Kimoto M, Meehl GA, Msadek R, Mueller WA, Taylor KE, Zwiers F, Rixen,M, Ruprich-Robert Y, and Eade R. The Decadal Climate Prediction Project (DCPP) contribution to CMIP6. Geosci Model Dev 2016, 9: 3751-3777, doi: 10.5194/gmd-9-3751-2016.

Bourassa AE, Robock A, Randel WJ, Deshler T, Rieger LA, Lloyd NE, Llewellyn EJ, Degenstein DA. Large Volcanic Aerosol Load in the Stratosphere Linked to Asian Monsoon Transport. Science 2012, 337: 78-81, doi: 10.1126/science.1219371.

Bousquet P, Peylin PP, Ciais CLQ, Friedlingstein P, Tans P. Regional changes in carbon dioxide fluxes of land and oceans since 1980. Science 2000, 290: 1342–1346, doi: 10.1126/science.290.5495.1342.

Briffa KR, Jones PD, Schweingruber FH, Osborn TJ. Influence of volcanic eruptions on Northern Hemisphere summer temperature over the past 600 years. Nature 1998, 393: 450–455, doi: 10.1038/30943.

Brohan P, Kennedy JJ, Harris I, Tett SFB, Jones PD. Uncertainty estimates in regional and global observed temperature changes: a new dataset from 1850. J Geophys Res 2006, 111: D12106, doi: 12110.11029/12005JD006548.

Brovkin V, Lorenz SJ, Jungclaus J, Raddatz T, **Timmreck C,** Reick CH, Segschneider J, Six K. Sensitivity of a coupled climate-carbon cycle model to large volcanic eruptions during the last millennium. Tellus B 2010, 62:674–681, doi: 10.1111/j.1600-0889.2010.00471.x.

Brühl C, Lelieveld J, Crutzen PJ, Tost H. The role of carbonyl sulphide as a source of stratospheric sulphate aerosol and its impact on climate. Atmos Chem Phys 2012, 12: 1239-1253, doi: 10.5194/acp-12-1239-2012.

Brühl C, Lelieveld J,Tost H, Höpfner M, Glatthor N. Stratospheric sulfur and its implications for radiative forcing simulated by the chemistry climate model EMAC. J Geophys Res Atmos 2015, 120: 2103–2118, doi: 10.1002/2014JD022430.

Charlton-Perez AJ, Baldwin M, Birner T, Black RX, Butler AH, Calvo N, Davis A, Gerber EP, Gillett N, Hardiman S, Kim J, K Krüger K, Lee YY, Manzini E, McDaniel BA, .Polvani L, Reichler T, Shaw TA, Michael S.,Son SW, Toohey M, Wilcox L, Yoden S, Christiansen B, Lott F, Shindell D, Yukimoto SI, Watanabe S. On the lack of stratospheric dynamical variability in low-top versions of the CMIP5 models. J Geophys Res Atmos 2013, 118: 2494–25052 doi: 10.1002/jgrd.50125.

Chesner CA, Luhr J. Melt inclusion study of the Toba Tuffs, Sumatra, Indonesia. J Volcanol Geotherm Res 2010, 197: 259-278, doi: 10.1016/j.jvolgeores.2010.06.001.

Chipperfield MP, Fioletov VE. Global Ozone: Past and Present. Chapter 3 in Scientific Assessment of Ozone Depletion: 2006. Global Ozone Research and Monitoring Project—Report No. 50. World Meteorological Organization, Geneva, Switzerland, 2007.

Choi W, Grant WB, Park JH, Lee, Kwang-M L, Lee H, Russell III JM. Role of the quasi-biennial oscillation in the transport of aerosols from the tropical stratospheric reservoir to midlatitudes. J. Geophys Res 1998, 103: 2156-2202, doi: 10.1029/97JD03118.

Christiansen B. Volcanic Eruptions, Large-Scale Modes in the Northern Hemisphere, and the El Niño–Southern Oscillation. J Climate 2008, 21: 910–922, doi: 10.1175/2007JCLI1657.1.

Church J, White NJ, Arblaster JM. Significant decadal-scale impact of volcanic eruption and sea level and ocean heat content. Nature 2005, 438: 74–77, doi: 10.1038/nature04237.

Clausen HB, Hammer CU. The Laki and Tambora eruptions as revealed in Greenland ice cores from 11 locations. Annals of Glaciology 1988, 10: 16-22.

Clement AC, Seager R, Cane MA, Zebiak SE. An ocean dynamical thermostat. J Climate 1996, 9: 2190-2196, doi: 10.1175/1520-0442(1996)009<2190:AODT>2.0.CO;2.

Cole-Dai J, Ferris D, Lanciki A, Savarino J, Baroni M, Thiemens MH. Cold decade (AD 1810–1819) caused by Tambora (1815) and another (1809) stratospheric volcanic eruption. Geophys Res Lett 2009, 36: L22703 doi: 10.1029/2009GL04088.

Cole-Dai J. Volcanoes and climate. WIREs Clim Change 2010, 1:824-839, doi: 10.1002/wcc.76.

Collins M. Predictions of climate following volcanic eruptions. In: Robock A, Oppenheimer C (eds) Volcanism and the Earth's atmosphere, Washington, DC: AGU; 2003, 283 – 300, doi: 10.1029/139GM19.

Considine DB, Rosenfield JE, Fleming EL. An interactive model study of the influence of the Mount Pinatubo aerosol on stratospheric methane and water trends. J Geophys Res 2001, 106:27,711–27,728, doi: 10.1029/2001JD000331.

Crosweller HS, Arora B, Brown SK, Cottrell E, Deligne NI, Ortiz Guerrero N, Hobbs L, Kiyosugi K, Loughlin SC, Lowndes J, Nayembil M, Siebert L, Sparks RSJ, Takarada S,Venzke E. Global database on large magnitude explosive volcanic eruptions (LaMEVE). J Appl Volcanol 2012, 1:4, doi: 10.1186/2191-5040-1-4.

Crooks SA, Gray LJ. Characterization of the 11-year solar signal using a multiple regression analysis of the ERA-40 dataset. J Climate 2005, 18: 996–1015, doi: 10.1175/JCLI-3308.1.

Crowley TJ, Criste TA, Smith NR. Reassessment of Crete (Greenland) ice core acidity/volcanism link to climate change. Geophys Res Lett 1993, 20: 209-212, doi: 10.1029/93GL00207.

Crowley TJ. Causes of climate change over the past 1000 years. Science 2000, 289:270–277, doi: 10.1126/science.289.5477.270.

Crowley TJ, Baum SK, Kim KY, Hegerl GC, Hyde WT. Modeling ocean heat content changes during the last millennium. Geophys Res Lett 2003, 30: 1932, doi: 10.1029/2003GL017801.

Crowley TJ, Zielinski GA, Vinther B, Udisti R, Kreutz KJ, Cole-Dai J, Castellano E. Volcanism and the Little Ice Age. PAGES News 2008, 16:22–23.

Crowley TJ, Unterman MB. Technical details concerning development of a 1200-yr proxy index for global volcanism. Earth Syst Sci Data 2013, 5: 187-197, doi: 10.5194/essd-5-187-2013.

Crutzen PJ, Schmailzl U. Chemical budgets of the stratosphere. Planet Space Sci 1983, 31:1009-1032, doi: 10.1016/0032-0633(83)90092-2.

Decker RW. How often does a Minoan eruption occur? In Hardy DA, Keller J, Galanopoulos VP, Flemming NC, Druitt TH. eds. Thera and the Aegean World III, Volume II Earth Sciences, Proceedings of the Third International Congress, Santorini, Greece, 3-9 September 1989 The Thera Foundation, London, 1990 ISBN: 0950613355.

Delworth TL, Ramaswamy V, Stenchikov GL. The impact of aerosols on simulated ocean temperature, heat content, and sea level in the 20th century. Geophys Res Lett 2005, 32: L24709, doi: 10.1029/2005GL024457.

D'Arrigo R, Seager R, Smerdon JE, LeGrande AN, Cook ER. The anomalous winter of 1783–1784: Was the Laki eruption or an analog of the 2009–2010 winter to blame? Geophys Res Lett 2011, 38: L05706, doi: 10.1029/2011GL046696.

D'Arrigo R, Wilson R, Jacoby G. On the long-term context for late twentieth century warming. J Geophys Res 2006, 111: D03103, doi: 10.1029/2005JD006352.

D'Arrigo R, Wilson R, Anchukaitis KJ. Volcanic cooling signal in tree-ring temperature records for the past millennium. J Geophys Res Atmos 2013, 118: 9000–9010, doi: 10.1002/jgrd.50692.

Deshler T, Hofmann D, Johnson B, Rozier W. Balloonborne measurements of the Pinatubo aerosol size distribution and volatility at Laramie, Wyoming during the summer of 1991. Geophys Res Lett 1992, 19: 199–202, doi: 10.1029/91GL02787.

Deshler T, Johnson BJ, Rozier WR. Balloonborne measurements of Pinatubo aerosol during 1991 and 1992 at 41◦N:Vertical profiles, size distribution, and volatility. Geophys Res Lett 1993, 20: 1435–1438, doi: 10.1029/93GL01337.

Devine JD, Sigurdsson H, Davis AN, Self S. Estimates of sulfur and chlorine yield to the atmosphere from volcanic eruptions and potential climatic effect. J Geophys Res 1984, 89: 6309–6325, doi: 10.1029/JB089iB07p06309.

Dhomse SS, Emmerson KM, Mann GW, Bellouin N, Carslaw KS, Chipperfield MP, Hommel R, Abraham NL, Telford P, Braesicke P, Dalvi M., Johnson CE, O'Connor F, Morgenstern O, Pyle, JA, Deshler T, Zawodny, JM, Thomason LW. Aerosol microphysics simulations of the Mt. Pinatubo eruption with the UM-UKCA composition-climate model. Atmos Chem Phys 2014, 14: 11221-11246, doi: 10.5194/acp-14-11221-2014.

Dhomse SS, Chipperfield MP, Feng W, Hossaini R, Mann GW, Santee ML. Revisiting the hemispheric asymmetry in midlatitude ozone changes following the Mount Pinatubo eruption: A 3-D model study. Geophys Res Lett 2015, 42: 3038–3047, doi: 10.1002/2015GL063052.

Ding Y, Carton JA, Chepurin GA, Stenchikov G, Robock A, Sentman LT, Krasting JP. Ocean response to volcanic eruptions in Coupled Model Intercomparison Project 5 (CMIP5) simulations. J Geophys Res Oceans 2014, 119: 5622–5637, doi: 10.1002/2013JC009780

Driscoll S, Bozzo A, Gray LJ, Robock A, Stenchikov G. Coupled Model Intercomparison Project 5 (CMIP5) Simulations of Climate Following Volcanic Eruptions. J Geophys Res 2012, 117: D17105, doi: 10.1029/2012JD017607.

Duggen S, Olgun N, Croot P, Hoffmann L, Dietze H, Delmelle P, Teschner C. The role of airborne volcanic ash for the surface ocean biogeochemical iron-cycle: a review. Biogeosciences 2010, 7: 827-844, doi: 10.5194/bg-7-827-2010.

Durand M, Grattan J. Extensive respiratory health effects of volcanogenic dry fog in 1783 inferred from European documentary sources. Environ Geochem Health 1999, 21:371–376. doi: 10.1023/A:1006700921208.

Dutton EG, Christy JR. Solar radiative forcing at selected locations and evidence for global lower tropospheric cooling following the eruptions of El Chichón and Pinatubo. Geophys Res Lett 1992, 19: 2313-2316, doi: 10.1029/92GL02495.

Ellis BS, Mark DF, Pritchard CJ, Wolff JA. Temporal dissection of the Huckleberry Ridge Tuff using the 40Ar/39Ar dating technique. Quat Geochronol 2012, 9: 34-41, doi: 10.1016/j.quageo.2012.01.006.

Emile-Geay J, Seager R, Cane MA, Cook ER, Haug GH. Volcanoes and ENSO over the past millennium. J Climate 2008, 21: 3134–3148, doi: 10.1175/2007JCLI1884.1.

English JM, Toon OB, Mills, MJ, Yu F. Microphysical simulations of new particle formation in the upper troposphere and lower stratosphere. Atm Chem Phys 2011, 11: 9303-9322. doi: 10.5194/acp-11-9303-2011:

English JM, Toon OB, Mills, M J. Microphysical simulations of large volcanic eruptions: Pinatubo and Toba. J Geophys Res Atmos 2013, 118: 1880–1895, doi :10.1002/jgrd.50196.

Esper J, Schneider L, Krusic, PJ, Luterbacher J, Büntgen U, Timonen M, Sirocko F, Zorita, E. European summer temperature response to annually dated volcanic eruptions over the past nine centuries. Bull Volcanol 2013, 75: 736, doi: 10.1007/s00445-013-0736-z.

Eyring V, Shepherd TG, Waugh DW, eds. SPARC CCMVal Report on the Evaluation of Chemistry-Climate Models. SPARC Report No. 5, WCRP-132, WMO/TD-No. 1526, 2010.

Eyring V, Lamarque JF, Hess P, Arfeuille F, Bowman K, Chipperfield MP, Duncan B, Fiore A, Gettelman A, Giorgetta MA, Granier C, Hegglin M, Kinnison D, Kunze M, Langematz U, Luo B, Martin R, Matthes K, Newman PA, Peter T, Robock A, Ryerson T, Saiz-Lopez A, Salawitch R, Schultz M, Shepherd TG, Shindell D, Stähelin J, Tegtmeier S, Thomason L, Tilmes S, Vernier JP, Waugh DW, Young PJ et al. Overview of IGAC/SPARC Chemistry-Climate Model Initiative (CCMI) Community Simulations in Support of Upcoming Ozone and Climate Assessments. SPARC Newsletter 2013, 4: 48-66, 2013.

Eyring V, Bony S, Meehl GA, Senior CA, Stevens B, Stouffer RJ, Taylor KE. Overview of the Coupled Model Intercomparison Project Phase 6 (CMIP6) experimental design and organization. Geosci Model Dev 2016, 9: 1937-1958, doi: 10.5194/gmd-9-1937-2016.

Fairlie TDA. Three-dimensional transport simulations of the dispersal of volcanic aerosol from Mount Pinatubo. QJR Meteor Soc 1995, 121:1943-1980, doi: 10.1002/qj.49712152809.

Fan F, Mann ME, Ammann CM. Understanding changes in the Asian summer monsoon over the past millennium: Insights from a long-term coupled model simulation. J Climate 2009, 22: 1736–1748, doi: 10.1175/2008JCLI2336.1.

Feichter J, Kjellström E., Rodhe H, Dentener F, Lelieveld J, Roelofs GJ Simulation of the tropospheric sulfur cycle in a global climate model. Atmos Environ 1996, 30: 1693–1707, doi: 10.1016/1352-2310(95)00394-0.

Fleming E, Jackman C, Weisenstein D, Ko, M. The impact of interannual variability on multidecadal total ozone simulations. J Geophys Res 2007, 112: D10310, doi: 10.1029/2006JD007953.

Fischer EM, Luterbacher J, Zorita E, Tett SFB, Casty C, Wanner H. European climate response to tropical volcanic eruptions over the last half millennium. Geophys Res Lett 2007, 34: L05707, doi: 10.1029/2006GL027992.

Fontijn K, Costa F, Sutawidjaja I., Newhall CG, Herrin JS. A 5000-year record of multiple highly explosive mafic eruptions from Gunung Agung (Bali, Indonesia): implications for eruption frequency and volcanic hazards. Bull Volcanol 2015, 77: 59, doi: 10.1007/s00445-015-0943-x.

Forster PMD, Collins M. Quantifying the water vapour feedback associated with post-Pinatubo global cooling. Clim Dyn 2004, 23: 207-214, doi: 10.1007/s00382-004-0431-z.

Frölicher TL, Joos F, Raible CC. Sensitivity of atmospheric CO2 and climate to explosive volcanic eruptions. Biogeosciences 2011, 8: 2317-2339, doi: 10.5194/bg-8-2317-2011.

Frölicher TL, Joos F, Raible CC, Sarmiento JL. Atmospheric CO2 response to volcanic eruptions: The role of ENSO, season, and variability. Glob Biogeochem Cycl 2013, 27: 239-251, doi: 10.1002/gbc.20028.

Gao C, Robock A, Self S, Witter J, Steffenson JP, Clausen HB, Siggaard-Andersen M-L, Johnsen S, Mayewski PA, Ammann C: The 1452 or 1453 A.D. Kuwae eruption signal derived from multiple ice core records: Greatest volcanic sulfate event of the past 700 years. J Geophys Res 2006, 111: D12107, doi: 10.1029/2005JD006710.

Gao C, Oman L, Robock A, Stenchikov GL. Atmospheric volcanic loading derived from bipolar ice cores accounting for the spatial distribution of volcanic deposition. J Geophys Res 2007, 112: D09109, doi: 10.1029/2006JD007461.

Gao C, Robock A, Ammann C. Volcanic forcing of climate over the last 1500 years: An improved ice-core based index for climate models. J Geophys Res 2008, 113: 2517-2538, doi: 10.1029/2008JD010239.

Gerlach TM. Present-day CO2 emissions from volcanoes. Eos Trans. AGU 1991, 72: 249–255, doi: 10.1029/90EO10192.

Gettelman AE, Schmidt A, JE Kristjansson JE. Icelandic volcanic emissions and climate. Nat Geosci 2015, 8: 243, doi: 10.1038/ngeo2376.

Gillett NP, Weaver AJ, Zwiers FW, Wehner MF. Detection of volcanic influence on global precipitation. Geophys Res Lett 2004, 31: L12217, doi: 10.1029/2004GL020044.

Giorgetta MA, Thomas MA. Influence of the Mt. Pinatubo eruptions on the dynamics of the quasi-biennial oscillation (solicited) Geophysical Research Abstracts 2009, 11, EGU2009-9805.

Giorgetta MA, Thomas MA, **Timmreck C**. Influence of the Mt. Pinatubo Eruption on the Quasi-Biennial Oscillation. Poster presentation Institute evaluation 2011.

Glaze LS, Baloga SM, Wilson L. Transport of atmospheric water vapor by volcanic eruption columns. J Geophys Res 1997, 102: 6099–6108, doi: 10.1029/96JD03125.

Gleckler P, Wigley TML, Santer BD, Gregory JM, AchutaRao K, Taylor KE. Krakatoa's signature persists in the ocean. Nature 2006a, 439: 675, doi: 10.1038/439675a.

Gleckler PJ, AchutaRao K, Gregory JM, Santer BD, Taylor KE, Wigley TML. Krakatoa lives: The effect of volcanic eruptions on ocean heat content and thermal expansion. Geophys Res Lett 2006b, 33: L17702, doi: 10.1029/2006GL026771.

Gleixner S. Southern Annular Mode response to volcanic eruptions in the MPI-ESM. Master Thesis, Christian-Albrechts-Universität, Kiel 2012, 94 pp.

Graf HF, Kirchner I, Robock A, Schult I. Pinatubo eruption winter climate effects: model versus observations. Clim Dyn 1993, 9:81-93, doi: 10.1007/BF00210011.

Graf HF, Perlwitz J, Kirchner I. Northern Hemisphere tropospheric mid-latitude circulation after violent volcanic eruptions. Beitr Phys Atmos 1994, 67: 3–13.

Graf HF, Feichter J, Langmann B. Volcanic sulfur emissions: Estimates of source strength and its contribution to the global sulfate distribution. J Geophys Res 1997, 102: 10727–10738, doi: 10.1029/96JD03265.

Graf HF, **Timmreck C**. Aerosol radiative forcing of the Laacher See volcano eruption (10,900 B.C.). J Geophys Res 2001, 106: 14,747-14,756, doi: 10.1029/2001JD900152.

Graf HF, Li Q, Giorgetta MA. Volcanic effects on climate: Revisiting the mechanisms. Atmos Chem Phys 2007, 7: 183-200, doi: 10.5194/acp-7-183-2007.

Graf HF, Zanchettin D. Central Pacific El Niño, the "subtropical bridge" and Eurasian climate. J Geophys Res 2012, 117: D01102, doi: 10.1029/2011JD016493.

Graf HF, Zanchettin D, **Timmreck C**, Bittner M. Observational constraints on the tropospheric and near-surface winter signature of the Northern Hemisphere stratospheric polar vortex. Clim Dyn 2014, 43: 3245-3266, doi: 10.1007/s00382-014-2101-0.

Grant WB, Browell EV, Fishman J, Brackett VG, Veiga RE, Nganga D, Minga A, Cros B, Butler CF, Fenn M. et al. Aerosol-associated changes in tropical stratospheric ozone following the eruption of Mount Pinatubo. J Geophy Res 1994, 99: 8197-8211, doi: 10.1029/93JD03314.

Grattan J, Durand M, Taylor S. Illness and elevated human mortality in Europe coincident with the Laki fissure eruption. In: Oppenheimer C, Pyle DM, Barclay J eds. Volcanic Degassing, Geological Soc, London, Special Publications 2003, 213: 401-414, doi: 10.1144/GSL.SP.2003.213.01.24

Gregory JM, Lowe JA, Tett SFB. Simulated Global-Mean Sea Level Changes over the Last Half-Millennium. J Climate 2006, 19: 4576–4591, doi: 10.1175/JCLI3881.1.

Gregory JM, Long-term effect of volcanic forcing on ocean heat content. Geophys Res Lett 2010, 37: L22701, doi: 10.1029/2010GL045507.

Gregory, JM, Bi D, Collier MA, Dix MR, Hirst AC,Hu A, Huber M, Knutti R, Marsland SJ, Meinshausen M, Rashid HA, Rotstayn LD, Schurer A, Church JA. Climate models without preindustrial volcanic forcing underestimate historical ocean thermal expansion. Geophys Res Lett 2013, 40: 1600–1604, doi: 10.1002/grl.50339.

Gu LH, Baldocchi DD, Wofsy SC, Munger JW, Michalsky JJ, Urbanski SP, Boden TA. Response of a deciduous forest to the Mount Pinatubo eruption: enhanced photosynthesis. Science 2003, 299: 2035–2038, doi: 10.1126/science.1078366.

Gu G, Adler RF, Huffman GJ, Curtis S. Tropical rainfall variability on interannual-to-interdecadal/ longer-time scales derived from the GPCP monthly product. J Climate 2007, 20: 4033–4046, doi: 10.1175/JCLI4227.1.

Gu G., Adler RF. Precipitation and temperature variations on the interannual time scale: Assessing the impact of ENSO and volcanic eruptions. J Climate 2011, 24: 2,258–2,270, doi: 10.1175/2010JCLI3727.1.

Guevara-Murua A, Williams CA, Hendy EJ, Rust A C, Cashman KV. Observations of a stratospheric aerosol veil from a tropical volcanic eruption in December 1808: is this the Unknown ~1809 eruption? Clim Past 2014, 10: 1707-1722, doi: 10.5194/cp-10-1707-2014.

Guo S, Bluth GJS, Rose WI, Watson IM, Prata AJ. Re-evaluation of SO2 release of the 15 June 1991 Pinatubo eruption using ultraviolet and infrared satellite sensors. Geochem Geophys Geosyst 2004, 5: Q04001, doi: 10.1029/2003GC000654.

Hamill P, Jensen EJ, Russell PB, Bauman JJ. The Life Cycle of Stratospheric Aerosol Particles. Bull Amer Meteor Soc 1997, 78: 1395–1410, doi: 10.1175/1520-0477(1997)078<1395:TLCOSA>2.0.CO;2.

Hamme RC, Webley PW, Crawford WR, Whitney FA, DeGrandpre MD, Emerson SR, Eriksen CC, Giesbrecht KE, Gower JFR, Kavanaugh MT. et al. Volcanic ash fuels anomalous plankton bloom in subarctic northeast Pacific. Geophys Res Lett 2010, 37: L19604, doi: 10.1029/2010GL044629.

Hammer CU. Past volcanism revealed by Greenland Ice Sheet impurities. Nature 1977, 270: 482–486, doi: 10.1038/270482a0.

Harris BM, Highwood E. A simple relationship between volcanic sulfate aerosol optical depth and surface temperature change simulated in an atmosphere-ocean general circulation model. J Geophys Res 2011, 116: D05109, doi: 10.1029/2010JD01458.

Haslam, M. Clarkson C, Petraglia M, Korisettar R, Jones S, Shipton C, Ditchfield P, Ambrose SH. The 74 ka Toba super-eruption and southern Indian hominins: Archaeology, lithic technology and environments at Jwalapuram Locality 3. J Archaeol Sci 2010, 37: 3370–3384, doi: 10.1016/j.jas.2010.07.034.

Haslam M, Petraglia M. Comment on "Environmental impact of the 73 ka Toba super-eruption in South Asia" by M.A.J. Williams, S.H. Ambrose, S. van der Kaars, C. Ruehlemann, U. Chattopadhyaya, J. Pal and P.R. Chauhan [Palaeogeography, Palaeoclimatology, Palaeoecology 284 (2009) 295–314]. Palaeo, Palaeo, Palaeo 2010, 296: 199-203, doi: 10.1016/j.palaeo.2010.03.057

Haywood JA, Jones A, Clarisse L, Bourassa A, Barnes J Telford P, Bellouin N, Boucher O, Agnew P, Clerbaux C, et al. Observations of the eruption of the Sarychev volcano and simulations using the HadGEM2 climate model. J Geophys Res 2010, 115: D21212, doi: 10.1029/2010JD014447.

Hegerl GC, Crowley T, Allen M, Hyde WT, Pollack H, Smerdon J, Zorita E. Detection of human influence on a new, validated 1500-year temperature reconstruction. J Climate 2007a, 20: 650–666, doi: 10.1175/JCLI4011.1.

Hegerl GC, Zwiers FW, Braconnot P, Gillett NP, Luo Y, Orsini JAM, Nicholls N, Penner JE, Stott PA. Understanding and attributing climate change. In: Solomon S, Qin D, Manning M, Chen Z, Marquis M, Averyt KB, Tignor M, Miller HL, eds. Climate Change 2007: The Physical Science Basis Contribution of Working Group I to the Fourth Assessment Report of the Intergovernmental Panel on Climate Change. Cambridge, United Kingdom, and New York: Cambridge University Press; 2007b.

Hegglin MI, Lamarque J-F, V. Eyring V, Hess P, Young PJ, Fiore AM, Myhre G, Nagashima T, Ryerson T, Shepherd TG, Waugh DW. IGAC/SPARC Chemistry-Climate Model Initiative (CCMI) 2014 Science Workshop, SPARC Newsletter 2014, 43:32-35.

Herzog M, Graf HF. Applying the three-dimensional model ATHAM to volcanic plumes: Dynamics of large co-ignimbrite eruptions and associated injection heights for volcanic gases. Geophys Res Lett 2010, 37: L19807, doi: 10.1029/2010GL044986.

Highwood EJ, Stevenson DS. Atmospheric impact of the 1783–1784 Laki Eruption: Part II Climatic effect of sulphate aerosol. Atmos Chem Phys 2003, 3: 1177-1189, doi: 10.5194/acp-3-1177-2003.

Hofmann DJ. Increase in the stratospheric background sulfuric acid aerosol mass in the past 10 years. Science 1990, 248:996-1000, doi: 10.1126/science.248.4958.996.

Hommel, R.: Die Variabilität von stratosphärischem Hintergrund-Aerosol. Eine Untersuchung mit dem globalen sektionalen Aerosolmodell MAECHAM5-SAM2. Ph.D. thesis, Universität Hamburg, 2008.

Hommel R, **Timmreck C**, Graf HF. The global middle-atmosphere aerosol model MAECHAM5-SAM2: comparison with satellite and in-situ observations. Geosci Model Dev 2011, 4: 809-834, doi: 10.5194/gmd-4-809-2011.

Hommel R, **Timmreck C**, Giorgetta MA, Graf HF. Quasi-biennial oscillation of the tropical stratospheric aerosol layer layer. Atmos Chem Phys 2015, 15: 5557-5584, doi: 10.5194/acp-15-5557-2015.

Hyde WT, Crowley TJ. Probability of future climatically significant volcanic eruptions. J Climate 2000, 13: 1445–1450, doi: 10.1175/1520-0442(2000)013<1445:LOFCSV>2.0.CO;2.

Iles CE, Hegerl GC, Schurer AP, Zhang X. The effect of volcanic eruptions on global precipitation. J Geophys Res Atmos 2013, 118: 8770–8786, doi: 10.1002/jgrd.50678.

Iles CE, Hegerl GC. The global precipitation response to volcanic eruptions in the CMIP5 models. Environ Res Lett 2014, 9: 104012, doi: 10.1088/1748-9326/9/10/104012

Iles CE, Hegerl GC. Systematic change in global patterns of streamflow following volcanic eruptions. Nat Geosci 2015, 8: 838–842, doi: 10.1038/ngeo2545.

Jensen EJ, Toon OB. The potential effects of volcanic aerosols on cirrus cloud microphysics. Geophys. Res Lett 1992, 19: 1759 – 1762, doi: 10.1029/92GL01936.

Jones CD, Cox PM. Modeling the volcanic signal in the atmospheric CO2 record. Global Biogeochem Cy 2001, 15: 453–465, doi: 10.1029/2000GB001281.

Jones GS, Gregory JM, Stott PA, Tett SFB, Thorpe RB. An AOGCM simulation of the climate response to a volcanic super-eruption. Clim Dyn 2005, 25: 725–738, doi: 10.1007/s00382-005-0066-8.

Jones MT, Sparks RSJ, Valdes PJ. The climatic impact of supervolcanic ash blankets. Clim Dyn 2007, 29: 553–564, doi: 10.1007/s00382-007-0248-7.

Joshi MM, Jones GS. The climatic effects of the direct injection of water vapour into the stratosphere by large volcanic eruptions. Atmos Chem Phys 2009, 9: 6109-6118, doi: 10.5194/acp-9-6109-2009.

Joshi MM, Shine KP. A GCM study of volcanic eruptions as a cause of increased stratospheric water vapour. J Climate 2003, 16: 3525–3534, doi: 10.1175/1520-0442(2003)016<3525:AGSOVE>2.0.CO;2.

Jungclaus JH, Keenlyside N, Botzet M, Haak H, Luo JJ, Latif M, Marotzke J, Mikolajewicz U,. Roeckner E. Ocean circulation and tropical variability in the coupled model ECHAM5/MPI-OM. J Climate 2006, 19: 3952-3972, doi: 10.1175/JCLI3827.1.

Jungclaus JH, Lorenz SJ, **Timmreck C**, Reick CH, Brovkin V. Giorgetta MA, Raddatz TJ, Roeckner E, Segschneider J, Six K, Segschneider J, Giorgetta MA, Crowley TJ, Pongratz J, Krivova NA, Vieira LE, Solanki SK, Klocke D, Botzet M, Esch M, Gayler V, Haak H, Raddatz TJ, Roeckner E, Schnur R, Widmann H, Claussen M, Stevens B, Marotzke J. Climate and carbon-cycle variability over the last millennium. Clim Past 2010, 6: 723-737, doi: 10.5194/cp-6-723-2010.

Jungclaus JH, Bard E, Baroni M, Braconnot P, Cao J, Chini LP, Egorova T, Evans M, González-Rouco JF, Goosse H, Hurtt GC, Joos F, Kaplan JO, Khodri M, Klein-Goldewijk K, Krivova N, LeGrande AN, Lorenz SJ, Luterbacher J, Man W, Meinshausen M, Moberg A. Nehrbass-Ahles C, Otto-Bliesner BI, Phipps SJ, J. Pongratz J, Rozanov E, Schmidt GA, Schmidt H, Schmutz W, Schurer A., Shapiro AI, Sigl M, Solanki SK, Toohey M, **Timmreck C**, Usoskin IG, Wagner S, Wu CJ, Yeo KL, Zanchettin D, Zhang Q, Zorita E. The PMIP4 contribution to CMIP6 – Part 3: the Last Millennium, Scientific Objective and Experimental Design for the PMIP4 past1000 simulations. Geosci Model Dev Discuss 2016, doi: 10.5194/gmd-2016-278, in review for Geosci Model Dev.

Junge CE, Chagnon CW, Manson JE. Stratospheric aerosols. J Meteorol 1961,18:81-108, doi: 10.1175/1520-0469(1961)018<0081:SA>2.0.CO;2.

Kandlbauer J, Sparks RSJ. New estimates of the. 1815 Tambora eruption volume. J Volcanol Geotherm Res 2014, 286: 93–100, doi:10.1016/j.jvolgeores.2014.08.020.

Karpechko AY, Gillett NP, Dall'Amico M, Gray LJ. Southern Hemisphere atmospheric circulation response to the El Chichón and Pinatubo eruptions in coupled climate models. QJR Meteorol Soc 2010, 136: 1813–1822, doi: 10.1002/qj.683.

Kazil J, Lovejoy ER, Jensen EJ, Hanson DR. Is aerosol formation in cirrus clouds possible? Atmos Chem Phys 2007, 7: 1407-1413, doi: 10.5194/acp-7-1407-2007.

Kent GS, Wang PH, McCormick MP, Skeens KM. Multiyear Stratospheric Aerosol and Gas Experiment II measurements of upper tropospheric aerosol characteristics. J Geophys Res 1995, 100: 13875–13899, doi: 10.1029/95JD00017.

Kinne S, Toon OB, Prather MJ. Buffering of stratospheric circulation by changing amounts of tropical ozone a Pinatubo Case Study. Geophys Res Lett 1992, 19: 1927–1930, doi: 10.1029/92GL01937.

Kirtman B, Power SB, Adedoyin JA, Boer GJ, Bojariu R, Camilloni I, Doblas-Reyes FJ, Fiore AM, Kimoto M, Meehl GA, Prather M, Sarr A, Schär C, Sutton R, van Oldenborgh GJ, Vecchi G, Wang HJ, 2013: Near-term Climate Change: Projections and Predictability. In: Climate Change 2013: The Physical Science Basis. Contribution of Working Group I to the Fifth Assessment Report of the Intergovernmental Panel on Climate Change .In Stocker TF, Qin D, Plattner GK, Tignor M, Allen SK, Boschung J, Nauels A, Xia Y, Bex V, Midgley PM (eds.) Climate Change 2013: The Physical Science Basis. Contribution of Working Group I to the Fifth Assessment Report of the Intergovernmental Panel on Climate Change, Cambridge Univ. Press, Cambridge, U. K., and New York, 2013.

Klocke D. Assessing the uncertainty in climate sensitivity. Reports on Earth System Science, 95, Max Planck Institute for Meteorology ISSN 1614-1199, 87pp, PhD thesis, 2011.

Kodera, K. Influence of volcanic eruptions on the troposphere through stratospheric dynamical processes in the northern hemisphere winter. J Geophys Res 1994, 99: 1273–1282, doi: 10.1029/93JD02731.

Kokkola H, Korhonen H, Lehtinen KEJ, Makkonen R, Asmi A, Järvenoja S, Anttila T, Partanen, AI, Kulmala M, Järvinen H, Laaksonen A, Kerminen VM. SALSA – a Sectional Aerosol module for Large Scale Applications. Atmos Chem Phys 2008, 8: 2469-2483, doi: 10.5194/acp-8-2469-2008.

Kokkola H, Hommel R, J. Kazil J, Niemeier U, Partanen A-I, Feichter J, **Timmreck C.** Aerosol microphysics modules in the framework of the ECHAM5 climate model – intercomparison under stratospheric conditions. Geosci Model Dev 2009, 2: 97-112, doi: 10.5194/gmd-2-97-2009.

Kondrashov D, Feliks Y, Ghil M. Oscillatory modes of extended Nile River records (A.D. 622–1922). Geophs. Res Lett 2005, 32: L10702, doi: 10.1029/2004GL022156.

Krakauer NY, Randerson JT. Do volcanic eruptions enhance or diminish net primary production? Evidence from tree rings. Global Biogeochem Cycles 2003, 17: 1118, doi: 10.1029/2003GB002076.

Kravitz B, Robock A. Climate effects of high-latitude volcanic eruptions: Role of the time of year. J Geophy Res 2011, 116: D01105, doi: 10.1029/2010JD014448.

Kravitz B, Robock A, Bourassa A. Negligible climatic effects from the 2008 Okmok and Kasatochi volcanic eruptions. J Geophys Res 2010, 115: D00L05, doi: 10.1029/2009JD013525.

Kravitz B, Robock A, Bourassa A, Deshler T, Wu D. Mattis I, Finger F, Hoffmann A, Ritter C, Bitar L, et al. Simulation and observations of stratospheric aerosols from the 2009 Sarychev volcanic eruption. J Geophys Res 2011, 116: D18211, doi: 10.1029/2010JD015501.

Kremser S, Thomason LW, von Hobe M , Hermann M, Deshler T, **Timmreck C**, M. Toohey M, Stenke A, Prata F, Schwarz J, Weigel R, Fueglistaler S, Vernier JP, Luo B , Schlager H, Barnes J, Antuna-Marrero JC, Fairlie D, Palm M, Mahieu E, Notholt J, Rex M, Neely R, Bingen C, Bourassa A, Plane J, Klocke D, Carn S, Lieven C, James A, Borrmann S, Rieger L, Trickl T, Wilson C, Meland B. Stratospheric aerosol - Observations, processes, and impact on climate. Rev Geophys 2016, 54: 278–335, doi: 10.1002/2015RG000511.

Krüger K, Toohey M, Zander S, **Timmreck C**. Do tropical volcanic eruptions influence the Southern Annular Mode? Geophysical Research Abstracts 2011, 13, EGU2011-9761.

Krüger K., Kutterolf S, Hansteen TH. Halogen release from Plinian eruptions and depletion of stratospheric Ozone. In Schmidt A et al., ed. Volcanism and global environmental change, Cambridge University Press, 2015, 244-259, ISBN: 9781107058378.

Kulmala M, Pirjola L, Mäkelä JM. Stable sulphate clusters as a source of new atmospheric particles, Nature 2000, 404: 66– 69, doi: 10.1038/35003550.

Kutterolf S, Hansteen T, Appel K, Freundt A, Krüger K, Peréz W, Wehrmann H. The combined Bromine and Chlorine release from large explosive volcanic eruptions: a threat to stratospheric ozone? Geology 2013: 41, 707-710, doi: 10.1130/G34044.1.

Labitzke K, McCormick MP. Stratospheric temperature increases due to Pinatubo aerosols. Geophys Res Lett 1992, 19: 207-210, doi: 10.1029/91GL02940.

Lanciki A, Cole-Dai J, Thiemens MH, Savarino J. Sulfur isotope evidence of little or no stratospheric impact by the 1783 Laki volcanic eruption. Geophys Res Lett 2012, 39: L01806, doi: 10.1029/2011GL050075.

Lavigne F, Degeaia JP, Komorowski JC, Guillet S, Roberta V, Lahitte P, Oppenheimer C, Stoffeld M, Vidalc CM, Suronoh, Indyo Pratomoi I, Wassmera P, Hajdask I, Hadmoko DS, de Belizala E. Source of the great A.D. 1257 mystery eruption unveiled, Samalas volcano, Rinjani Volcanic Complex, Indonesia. Proc Natl Acad Sci 2013, 110 ,42: 16742–16747, doi: 10.1073/pnas.1307520110.

Lehner F, Schurer AP, Hegerl GC, Deser C, Frölicher TL. The importance of ENSO phase during volcanic eruptions for detection and attribution. Geophys Res Lett 2016, 43: 2851–2858, doi: 10.1002/2016GL067935.

Li II, Hu C, Li YH, Ho TY, Fischer T, Wong GT, Wu J, Huang CW, Chu DA, Ko DS, Chen JP Fertilisation potential of volcanic dust in the low nutrient low chlorophyll western North Pacific Subtropical Gyre: satellite evidence and laboratory study. Global Biogeochem Cycles 2011, 25: GB1006, doi: 10.1029/2009GB003758.

Liu C, Allan RP, Huffman GJ. Co-variation of temperature and precipitation in CMIP5 models and satellite observations. Geophys Res Lett 2012, 39: L13803, doi: 10.1029/2012GL052093.

Lohmann U, Kärcher B, **Timmreck C**. Impact of the Mount Pinatubo eruption on cirrus clouds formed by homogeneous freezing in the ECHAM4 GCM. J Geophys Res 2003, 108: 4568, doi: 10.1029/2002JD003185.

Long C, Stowe L. Using the NOAA/AVHHR to study stratospheric aerosol optical thickness following the Mt. Pinatubo eruption. Geophys Res Lett 1994, 21: 2215–2218, doi: 10.1029/94GL01322

Louys J. Limited effect of the Quaternary's largest super-eruption (Toba) on land mammals from Southeast Asia. Quat Sci Rev 2007, 26: 3108–3117, doi: 10.1016/j.quascirev.2007.09.008

Lovejoy ER, Curtius J, Froyd KD. Atmospheric ioninduced nucleation of sulfuric acid and water. J Geophys Res 2004, 109: D08204, doi: 10.1029/2003JD004460.

Lucht W, Prentice IC, Myneni RB, Sitch S, Friedlingstein P, Cramer W, Bousquet P, Buermann W, Smith B. Climate control of the high-latitude vegetation greening trend and Pinatubo effect. Science 2002, 296:1687–1689, doi: 10.1126/science.1071828.

Luo Z, Rossow WB, Inoue T, Stubenrauch CJ. Did the eruption of the Mt. Pinatubo volcano affect cirrus properties? J. Climate 2002, 15: 2806–2820, doi: 10.1175/1520-0442(2002)015<2806:DTEOTM>2.0.CO;2.

Maher N, McGregor S, England MH, Sen Gupta A. Effects of volcanism on tropical variability. Geophys Res Lett 2015, 42: 6024–6033, doi: 10.1002/2015GL064751.

Mann, G, Dhomse S, Schmidt A, Neely R**, Timmreck C,** Deshler T, Thomason L. Realistic global particle size evolution key to improved volcanic forcings. Past Global Changes Magazine 2015, 23: 2, 52-53, doi: 10.22498/pages.23.2.52.

Mann ME, Fuentes JD, Rutherford S. Underestimation of volcanic cooling in tree-ring based reconstructions of hemispheric temperatures. Nat Geosci 2012, 5: 202–205, doi: 10.1038/ngeo1394.

Mann ME, Rutherford S, Schurer A, Tett SFB. Discrepancies between the modeled and proxy-reconstructed response to volcanic forcing over the past millennium: Implications and possible mechanisms, J Geophys Res Atmos 2013, 118: 7617–7627, doi: 10.1002/jgrd.50609.

Manzini E, Matthes K. Natural Variability of Stratospheric Ozone. In Eyring V, Shepherd TG, Waugh DW, eds. SPARC CCMVal Report on the Evaluation of Chemistry-Climate Models. SPARC Report No. 5, WCRP-132, WMO/TD-No. 1526 2010.

Marotzke J, Forster PM. Forcing, feedback and internal variability in global temperature trends. Nature 2015, 517: 565-570, doi: 10.1038/nature14117.

Marotzke J, Müller WA, Vamborg F, Becker P, Cubasch U, Feldmann H, Kaspar F, Kottmeier C, Marini C, Polkova I, Prömmel K, Rust H, Stammer D, Ulbrich U, Kadow C, Köhl A, Kröger J. Kruschke T, Pinto JG, Pohlmann H, Reyers M, Schröder M, Sienz F, **Timmreck C**, Ziese M. MiKlip – a National Research Project on Decadal Climate Prediction. Bull Am Meteorol Soc 2016, 97: 2379–2394, doi: 10.1175/BAMS-D-15-00184.

Marshall GJ. Trends in the Southern Annular Mode from observations and reanalyses. J Climate 2003, 16: 4134–4143, doi: 10.1175/1520-0442(2003)016<4134:TITSAM>2.0.CO;2.

Marshall AG, Scaife AA, Ineson S. Enhanced seasonal prediction of European winter warming following volcanic eruptions. J Climate 2009, 22: 6168–6180, doi: 10.1175/2009JCLI3145.1.

Mason BG, Pyle DM, Oppenheimer C. The size and frequency of the largest explosive eruptions on Earth. Bull Volcanol 2004, 66: 735-748, doi: 10.1007/s00445-004-0355-9.

Mather, TA. Volcanoes and the environment: Lessons for understanding Earth's past and future from studies of present-day volcanic emissions. J Volcanol Geotherm Res 2015, 304: 160–179, doi: 10.1016/j.jvolgeores.2015.08.016.

McCormick MP, Thomason LW, Trepte CR. Atmospheric effects of the Mt. Pinatubo eruption. Nature 1995, 373:399-404, doi: 10.1038/373399a0.

McCoy DT, Hartmann DL Observations of a substantial cloud-aerosol indirect effect during the 2014–2015 Bárðarbunga-Veiðivötn fissure eruption in Iceland. Geophys Res Lett 2015, 42: 10,409–10,414, doi: 10.1002/2015GL067070.

McGregor S, Timmermann A, Timm O. A unified proxy for ENSO and PDO variability since 1650. Clim Past 2010, 6: 1-17, doi: 10.5194/cp-6-1-2010.

McGregor S, Timmermann A. The effect of explosive tropical volcanism on ENSO. J Climate 2011, 34: 2178–2191, doi: 10.1175/2010JCLI3990.1.

Meehl GA, Teng H, Maher N, England MH. Effects of the Mount Pinatubo eruption on decadal climate prediction skill of Pacific sea surface temperatures. Geophys Res Lett 2015, 42: 10,840–10,846, doi: 10.1002/2015GL066608.

Mercado LM, Bellouin N, Sitch S, Boucher O, Huntingford C, Wild M, Cox PM. Impact of changes in diffuse radiation on the global land carbon sink. Nature 2009, 458: 1014-1017, doi: 10.1038/nature07949;

Merlis TM; Held IM; Stenchikov GL; Zeng F; Horowitz, LW. Constraining Transient Climate Sensitivity Using Coupled Climate Model Simulations of Volcanic Eruptions. J Climate 2014, 27: 7781-7795, doi: 10.1175/JCLI-D-14-00214.1.

Meronen H, Henriksson SV, Raisanen P, Laaksonen A. Climate effects of northern hemisphere volcanic eruptions in an Earth System Model. Atm Res 2012, 114: 107-118 12, doi: 10.1016/j.atmosres.2012.05.011

Metzner D, Kutterolf S, Toohey M, **Timmreck C**, Niemeier U, Freundt A, Krüger K. Radiative forcing and climate impact resulting from SO2 injections based on a 200,000 year record of Plinian eruptions along the Central American Volcanic Arc. Int J Earth Sci 2014, 103: 2063-2079, doi: 10.1007/ s00531-012-0814-z.

Metzner D., Krüger K., Zanchettin D, Toohey M, **Timmreck, C.** Southern Hemisphere Climate Response to an extremely large tropical Volcanic Eruption: Simulations with the MPI-ESM. AGU Chapman Conference on Volcanism and the Atmosphere 2012, 10.-15.06.2012, Selfoss, Iceland.

Meyer A., Vernier JP, Luo B, Lohmann U, Peter T. Did the 2011 Nabro eruption affect the optical properties of ice clouds? J Geophys Res Atmos 2015, 120: 9500–9513, doi: 10.1002/2015JD023326.

Mignot J, Khodri M, Frankignoul C, Servonnat J. Volcanic impact on the Atlantic Ocean over the last millennium. Clim Past 2011, 7: 1439-1455, doi: 10.5194/cp-7-1439-2011.

Miller GH, Geirsdóttir Á, Zhong Y, Larsen DJ, Otto-Bliesner BL, Holland MM, Bailey DA, Refsnider KA, Lehman SJ, Southon JR, et al. Abrupt onset of the Little Ice Age triggered by volcanism and sustained by sea-ice/ocean feedbacks. Geophys Res Lett 2012, 39: L02708, doi: 10.1029/2011GL050168.

Mills MJ, Schmidt A, Easter R, Solomon S, Kinnison DE, Ghan SJ, Neely III RR, Marsh DR,. Conley A, Barden CG, Gettelman A. Global volcanic aerosol properties derived from emissions, 1990-2014, using CESM1 (WACCM). J Geophys Res Atmos 2016, 121: 2332-2348, doi: 10.5065/D6S180J.

Minnis P, Harrison EF,Stowe LL, Gibson GG, Denn PM, Doelling DR, Smith Jr. WL. Radiative climate Forcing by Mount Pinatubo Eruption. Science 1993, 259:1411-1415, doi: 10.1126/science.259.5100.141.

Muthers S., Anet JG, Raible CC, Brönnimann S, Rozanov E, Arfeuille F, Peter T, Shapiro AI, Beer J, Steinhilber F , Brugnara Y, Schmutz W, Northern hemispheric winter warming pattern after tropical volcanic eruptions: Sensitivity to the ozone climatology. J Geophys Res Atmos 2014, 119: 1340–1355, doi: 10.1002/2013JD020138.

Neely III RR, Toon OB, Solomon S, Vernier JP, Alvarez C, English JM, Rosenlof KH, Mills MJ, Bardeen CG, Daniel JS, Thayer JP, Recent anthropogenic increases in SO2 from Asia have minimal impact on stratospheric aerosol. Geophys Res Lett 2013, 40: 999-1004, doi: 10.1002/grl.50263.

Newhall CG*,* Self *S.* The volcanic explosivity index (VEI) an estimate of explosive magnitude for historical volcanism. J Geophys Res 1982*,* 87: 1231–1238, doi: 10.1029/JC087iC02p01231.

Niemeier U, **Timmreck C**, Graf HF, Kinne S, Rast S, Self S. Initial fate of fine ash and sulfur from large volcanic eruptions. Atmos Chem Phys 2009, 9: 9043-9057, doi: 10.5194/acp-9-9043-2009.

Niemeier U, Schmidt H, **Timmreck C**. The dependency of geoengineered sulfate aerosol on the emission strategy. Atmos Sci Lett 2011, 12: 189–194, doi: 10.1002/asl.304.

Niemeier U, **Timmreck C.** What is the limit of climate engineering by stratospheric injection of SO2? Atmos Chem Phys 2015, 15: 9129-9141, doi: 10.5194/acp-15-9129-2015.

Ohba M, Shiogama H, Yokohata T, Watanabe M. Impact of strong tropical volcanic eruptions on ENSO simulated in a coupled GCM. J Climate 2013, 26: 5169–5182, doi: 10.1175/JCLI-D-12-00471.1.

Oltmans SJ, Vömel H, Hoffman DJ, Rosenlof KH, Kley D. The increase in stratospheric water vapor from balloon borne frostpoint hygrometer measurements at Washington, DC and Boulder, Colorado. Geophys Res Lett 2000, 27: 3453–3456, doi: 10.1029/2000GL012133.

Oman L, Robock A, Stenchikov G, Schmidt GA, Ruedy R. Climatic response to high-latitude volcanic eruptions. J Geophys Res 2005, 110: D13103, doi: 10.1029/2004JD005487.

Oman L, Robock A, Stenchikov GL, Thordarson T, Koch D. Shindell DT, Gao C. Modeling the distribution of the volcanic aerosol cloud from the 1783-1784 Laki eruption. J Geophys Res 2006a, 111: D12209 doi: 10.1029/2005JD006899.

Oman L, Robock A, Stenchikov GL, Thordarson T. High-latitude eruptions cast shadow over the African monsoon and the flow of the Nile. Geophys Res Lett 2006b, 33: L18711, doi: 10.1029/ 2006GL027665.

O'Neill BC, Tebaldi C, van Vuuren DP, Eyring V, Friedlingstein P, Hurtt G, Knutti R, Kriegler E, Lamarque J.-F, Lowe J, Meehl GA, Moss R, Riahi K, Sanderson BM: The Scenario Model Intercomparison Project (ScenarioMIP) for CMIP6. Geosci Model Dev 2016, 9: 3461-3482, doi: 10.5194/gmd-9-3461-2016.

Oppenheimer C. Limited global change due to the largest known Quaternary eruption, Toba 74 kyr BP? Quat Sci Rev 2002, 21: 1593–1609, doi: 10.1016/S0277-3791(01)00154-8.

Oppenheimer C. Eruptions that shook the world. Cambridge University Press, Cambridge, 2011, 408 pp 392, ISBN: 9780521641128.

Otterå OH. Simulating the effects of the 1991 Mount Pinatubo volcanic eruption using the ARPEGE atmosphere general circulation model. Adv Atmos Sci 2008, 25: 213–226, doi: 10.1007/s00376-008-0213-3.

Otterå OH, Bentsen M, Drange H, Suo L. External forcing as a metronome for Atlantic multidecadal variability. Nat Geosci 2010, 3: 688–694, doi: 10.1038/ngeo955

Paik S, Min SK. Climate responses to volcanic eruptions assessed from observations and CMIP5 multi-models. Clim Dyn 2017, 48: 1017–1030, doi: 10.1007/s00382-016-3125-4.

Pausata FSR, Grini A, Caballero R, HannachiA, Seland Ø. High-latitude volcanic eruptions in the Norwegian Earth System Model: the effect of different initial conditions and of the ensemble size. Tellus B 2015a, 67, 26728, doi: 10.3402/tellusb.v67.26728

Pausata FSR, Chafik L, Caballero R, Battisti D. Impacts of high-latitude volcanic eruptions on ENSO and AMOC. Proc Natl Acad Sci 2015b, 112: 13784-13788, doi: 10.1073/pnas.1509153112.

Petraglia MD, Korisettar R, Pal JN (eds). The Toba Volcanic Super-eruption of 74,000 Years Ago: Climate Change, Environments, and Evolving Humans. Quat Int 2012, 258: 1-4, doi: 10.1016/j.quaint.2011.12.001

Petraglia M, Korisettar R, Boivin N, Clarkson C, Ditchfield P, et al. Middle Paleolithic assemblages from the Indian subcontinent before and after the Toba Super-Eruption. Science 2007, 317: 114–116, doi: 10.1126/science.1141564.

Pinto JR, Turco RP, Toon OB. Self-Limiting Physical and Chemical Effects in Volcanic Eruption Clouds. J Geophys Res 1989, 94: 11165-11174, doi: 10.1029/JD094iD08p11165.

Pitari G, Mancini E. Short-term climatic impact of the 1991 volcanic eruption of Mt. Pinatubo and effects on atmospheric tracers. Nat Hazards Earth Syst Sci 2002, 2: 91-108, doi: 10.5194/nhess-2-91-2002.

Pyle DM Sizes of volcanic eruptions. In Sigurdsson H, Houghton B, McNutt SR, Rymer H, Stix J eds. The Encyclopedia of Volcanoes. Academic Press, London, 2000, 1: 263-269, eBook ISBN: 9780080547985

Poberaj, C.S, Staehelin J, Brunner D. Missing stratospheric ozone decrease at Southern Hemisphere middle latitudes after Mt. Pinatubo: A dynamical perspective. J Atmos Sci 2011, 68: 1922–1945, doi: 10.1175/JAS-D-10-05004.1.

Pohlmann, H., et al., Improved forecast skill in the tropics in the new MiKlip decadal climate predictions, Geophys Res Lett 2013, 40: 5798–5802, doi: 10.1002/2013GL058051.

Raddatz TJ, **Timmreck C,** Lorenz S. Volcanic aerosol size distribution, diffuse radiation and vegetation productivity. Geophys Res Abstracts 2009, 11, EGU2009-9720.

Raible CC, Brönnimann S, Auchmann R, Brohan P, Frölicher TL, Graf HF, Jones P, Luterbacher J, Muthers S, Neukom R, Robock A, Self S, Sudrajat A, **Timmreck C**, Wegmann M. Tambora 1815 as a test case for high impact volcanic eruptions: Earth system effects. WIREs Clim Change 2016, 7: 569-589, doi: 10.1002/wcc.407.

Randall DA, Wood RA, Bony S, Colman R, Fichefet T, Fyfe J, Kattsov V, Pitman A, Shukla J, Srinivasan J, et al. Cilmate models and their evaluation. In: Solomon S, Qin D, Manning M, Chen Z, Marquis M, Averyt KB, Tignor M,Miller HL, eds. Climate Change 2007: The Physical Science Basis Contribution of Working Group I to the Fourth Assessment Report of the Intergovernmental Panel on Climate Change. Cambridge, United Kingdom, and New York: Cambridge University Press; 2007.

Randel WJ, Wu F, Russell III JM, Waters J, Froidevaux L. Ozone and temperature changes in the stratosphere following the eruption of Mt. Pinatubo. J Geophys Res 1995, 100: 16,753-15,764, doi: 10.1029/95JD01001

Randel WJ, Park M, Emmons L, Kinnison D, Bernath P, Walker K, Boone C, Pumphrey H. Asian monsoon transport of pollution to the stratosphere. Science 2010, 328: 611, doi: 10.1126/science.1182274.

Rap A., Scott CE, Spracklen DV, Bellouin N, Forster PM, Carslaw KS, Schmidt A, Mann G. Natural aerosol direct and indirect radiative effects. Geophys Res Lett 2013, 40: 3297–3301, doi: 10.1002/grl.50441.

Read WG, Froidevaux L, Waters JW. Microwave limb sounder measurements of 25 stratospheric SO2 from the Mt. Pinatubo volcano. Geophys Res Lett 1993, 20: 1299–1302, doi: 10.1029/93GL00831.

Rex M, **Timmreck C**, Kremser S, Thomason L, Vernier JP. Stratospheric sulphur and its Role in Climate (SSiRC). SPARC Newsletter 2012, 39 p. 37.

Ridley H, Asmerom Y, Baldini JUL, Breitenbach SFM,Aquino VV,Prufer KM, Culleton BJ, Polyak V, Lechleitner FA, Kennett DJ, Zhang M,Marwan N, Macpherson CG, Baldini LM, Xiao T, PeterkinJL, Awe J, Haug GH. Aerosol forcing of the position of the intertropical convergence zone since AD 1550. Nat Geosci 2015,8: 195–200, doi: 10.1038/ngeo235.

Ridley DA, Solomon S, Barnes JE, Burlakov VD , Deshler T, Dolgii SI, Herber AB, Nagai T,. Neely III RR, Nevzorov AV, Ritter C, Sakai T, Santer BD, M. Sato M, Schmidt A, Uchino O, Vernier JP Total volcanic stratospheric aerosol optical depths and implications for global climate change. Geophys Res Lett 2014, 41: 7763–7769, doi: 10.1002/2014GL061541.

Robock A, Mass C. The Mount St. Helens volcanic eruption of 18 May 1980: Large short-term surface temperature effects. Science 1982, 216: 628-630, doi: 10.1126/science.212.4501.1383.

Robock A, Mao J. Winter warming from large volcanic eruptions. Geophys Res Lett 1992, 19: 2405-2408, doi: 10.1029/92GL02627.

Robock A, Liu Y. The volcanic signal in Goddard Institute for Space Studies three-dimensional model simulations. J Climate 1994, 7: 44–55, doi: 10.1175/1520-0442(1994)007<0044:TVSIGI>2.0.CO;2.

Robock A, Free MP. Ice cores as an index of global volcanism from 1850 to the present. J Geophys Res 1995, 100: 11549–11567, doi: 10.1029/95JD00825.

Robock A. Volcanic eruptions and climate. Rev Geophys 2000, 38: 191–219, doi: 10.1029/1998RG000054.

Robock A. Cooling following large volcanic eruptions corrected for the effect of diffuse radiation on tree rings. Geophys Res Lett 2005, 32: L06702, doi: 10.1029/2005GL023287.

Robock A, Adams T, Moore M, Oman L, Stenchikov GL. Southern Hemisphere atmospheric circulation effects of the 1991 Mount Pinatubo eruption. Geophys Res Lett 2007, 34: L23710 doi: 10.1029/2007GL031403.

Robock A, Ammann CM, Oman L, Shindell D, Levis S, Stenchikov GL. Did the Toba volcanic eruption of ~74 ka B.P. produce widespread glaciation? J Geophys Res 2009, 114: D10107, doi: 10.1029/2008JD011652.

Robock A, MacMartin DG, Duren R, Christensen MW. Studying geoengineering with natural and anthropogenic analogs. Climatic Change 2013, 121: 445-458, doi: 10.1007/s10584-013-0777-5.

Rothenberg D, Mahowald N, Lindsay K, Doney SC, Moore JK, Thornton P. Volcano impacts on climate and biogeochemistry in a coupled carbon-climate model. Earth Syst Dynam 2012, 3: 121-136, doi: 10.5194/esd-3-121-2012.

Roscoe HK, Haigh JD. Influences of ozone depletion, the solar cycle and the QBO on the Southern Annular Mode. QJR Meteorol Soc 2007, 133: 1855–186, doi: 10.1002/qj.153.

Rose WI, Chesner, CA. Worldwide dispersal of ash and gases from earth's largest known eruption: Toba, Sumatra, 75 kyr. Palaeo Palaeo Palaeo 1990, 89: 269–275,doi: 10.1016/0031-0182(90)90068-I.

Rosenfield JE, Effects of volcanic eruptions on stratospheric ozone recovery. In: Robock A, Oppenheimer C, eds. Volcanism and the Earth's Atmosphere. Washington, DC: AGU; 2003, 227-236, doi: 10.1029/139GM14.

Rozanov EV, Schlesinger ME, Andronova NG, Yang F, Malyshev SL, Zubov VA, Egorova TA, Li B. Climate/Chemistry Effects of the Pinatubo volcanic eruption by the UIUC stratosphere/troposphere GCM with interactive photochemistry. J Geophys Res 2002, 107: 4594 doi: 10.1029/2001JD000974.

Russel PB, Livingston JM, Pueschel RF, Hughes JJ, Pollack JB, Brooks SL, Hamill P, Thomason LW, Stowe LL, Dutton EG, Bergstrom RW. Global to microscale evolution of the Piinatubo volcanic aerosol, derived from diverse measurements and analyses. J Geophys Res 1996, 101: 18745—18763, doi: 10.1029/96JD01162.

Santer BD, Wehner MF, Wigley TML, Sausen R, Meehl GA, Taylor KE, Ammann C, Arblaster J, Washington WM, Boyle JS, et al. Contributions of anthropogenic and natural forcing to recent tropopause height changes. Science 2003, 301: 479-483, doi: 10.1126/science.1084123.

Santer BD, Bonfils C, Painter JF, Zelinka MD, Mears C,Solomon S, Schmidt GA, Fyfe JC, Cole JNS, Nazarenko L, Taylor KE, Wentz FJ. Volcanic contribution to decadal changes in tropospheric temperature. Nat Geosci 2014 7: 185–189, doi:10.1038/ngeo2098.

Sassen K. Evidence for liquid-phase cirrus cloud formation from volcanic aerosols: Climatic implications. Science 1992, 257: 516–519, doi:10.1126/science.257.5069.516.

Sassen K, O' C. Starr D, Mace GG, Poellot MR, Melfi SH, Eberhard WL, Spinhirne JD, Eloranta EW, Hagen DE, Hallett J. The 5–6 December 1991 FIRE IFO II jet stream cirrus case study: Possible influences of volcanic aerosols. J Atmos Sci 1995, 52: 97–123, doi: 10.1175/1520-0469(1995)052<0097:TDFIIJ>2.0.CO;2.

Sato M, Hansen J, McCormick M, Pollack J. Stratospheric aerosol optical depths. J Geophys Res 1993, 98:22,987–22,994, doi: 10.1029/93JD02553, updated version.

Scaillet B, Clemente B, Evans BW, Pichavant M. Redox control of sulfur degassing in silicic magmas. J Geophys Res 1998, 103: 23937–23949, doi: 10.1029/98JB02301.

Scaillet B, Luhr JF, Carroll MR. Petrological and volcanological constraints on volcanic sulfur emissions to the atmosphere, In: Robock A, Oppenheimer C, eds. Volcanism and the Earth's Atmosphere. Washington, DC: AGU; 2003, 213-225, doi: 10.1029/139GM02.

Schneider DP, Ammann CM, Otto-Bliesner BL, Kaufman DS. Climate response to large, high-latitude and low-latitude volcanic eruptions in the Community Climate System Model. J Geophys Res 2009, 114: D15101, doi: 10.1029/2008JD011222.

Schmidt A, Ostro B, Carslaw KS, Wilson M, Thordarson T, Mann GW, Simmons AJ. Excess mortality in Europe following a future Laki-style Icelandic eruption. Proc Natl Acad Sci 2011, 108: 15710-15715, doi: 10.1073/pnas.1108569108.

Schmidt A, Carslaw KS, Mann GW, Rap A, Pringle KJ, Spracklen DV, Wilson M, and Forster PM. Importance of tropospheric volcanic aerosol for indirect radiative forcing of climate. Atmos Chem Phys 2012, 12: 7321-7339, doi: 10.5194/acp-12-7321-2012.

Schmidt, A., Thordarson T, Oman LD, Robock A, Self S. Climatic impact of the long-lasting 1783 Laki eruption: Inapplicability of mass-independent sulfur isotopic composition measurements. J Geophys Res 2012, 117: D23116, doi: 10.1029/2012JD018414.

Schmidt A, Leadbetter S, Theys N, Carboni E, Witham CS, Stevenson JA, Birch CE, T. Thordarson T, Turnock S, Barsotti S, et al. Satellite detection, long-range transport, and air quality impacts of volcanic sulfur dioxide from the 2014–2015 flood lava eruption at Bárðarbunga (Iceland). J Geophys Res Atmos 2015, 120: 9739–9757, doi: 10.1002/2015JD023638.

Schmidt GA, Jungclaus JH, Ammann CM, Bard E, Braconnot P, Crowley TJ, Delaygue G, Joos F, Krivova NA, Muscheler R, Otto-Bliesner BL. et al. Climate forcing reconstructions for use in PMIP simulations of the Last Millennium (v1.0). Geosci Model Dev 2011, 4: 33-45, doi: 10.5194/gmd-4-33-2011.

Schmidt H, Rast S, Bunzel F, Esch M, Giorgetta M, Kinne S, Krismer T, Stenchikov G , **Timmreck C**, Tomassini L, Walz M. The response of the middle atmosphere to anthropogenic and natural forcing in the CMIP5 simulations with the MPI-ESM. Journal of Advances in Modeling Earth Systems (JAMES) 2013, 5: 98-116, doi: 10.1002/jame.20014.

Segschneider J, Beitsch A, **Timmreck C**, Brovkin V, Ilyina T, Jungclaus J, Lorenz S, Six K, Zanchettin D. Impact of an extremely large magnitude volcanic eruption on the global climate and carbon cycle estimated from ensemble Earth System Model simulations. Biogeosciences 2013, 10: 669-687, doi: 10.5194/bg-10-669-2013.

Self S, King AJ. Petrology and sulfur and chlorine emissions of the 1963 eruption of Gunung Agung, Bali, Indonesia. Bull Volcanol 1996, 58:263-285, doi: 10.1007/s004450050139.

Self S, Gertisser R, Thordarson T, Rampino MR, Wolff AJ. Magma volume, volatile emissions, and stratospheric aerosols from the 1815 eruption of Tambora. Geophys Res Lett 2004, 31: L20608. doi: 10.1029/2004GL020925.

Self S. The effects and consequences of very large explosive volcanic eruptions. Phil Trans R Soc A 2006, 364:1845, 2073-2097. doi: 10.1098/rsta.2006.1814 1471.

Self S, Blake S. Effects and consequence of super-eruptions. Elements 2008, 4:29-34, doi: 10.2113/GSELEMENTS.4.1.41

Sheng, J-X, Weisenstein DK, Luo B-P, Rozanov E, Stenke A, Anet J, Bingemer H, Peter T. Global atmospheric sulfur budget under volcanically quiescent conditions: aerosol–chemistry–climate model predictions and validation. J Geophys Res Atmos 2015, 120: 256–276. doi:10.1002/2014JD021985.

Shindell D, Schmidt GA, Mann ME, Falugevi G. Dynamic winter climate response to large tropical volcanic eruptions since 1600. J Geophys Res 2004, 109: D05104, doi: 10.1029/2003JD004151.

Shiogama H, Emori S, Mochizuki T, Yasunaka S, Yokohata T, Ishii M, Nozawa T, Kimoto M. Possible Influence of Volcanic Activity on the Decadal Potential Predictability of the Natural Variability in Near-Term Climate Predictions. Advances in Meteorology 2010,657318. doi: 10.1155/2010/657318.

Sigl M, McConnell JR, Layman L, Maselli O, McGwire K, Pasteris D, Dahl-Jensen D, Steffensen JP, Edwards R, Mulvaney R. A new bipolar ice core record of volcanism from WAIS Divide and NEEM and implications for climate forcing of the last 2000 years. J Geophys Res Atmos 2013, 118: 1151–1169. doi: 10.1029/2012JD018603.

Sigl M, McConnell JR, Toohey M, Curran M, Das SB, Edwards R, Isaksson E, Kawamura K, Kipfstuhl S, Krüger K, Layman L, Maselli OJ, Motizuki Y, Motoyama H, Pasteris DR, Severi M. New insights from Antarctica on volcanic forcing during the Common Era'. Nat Clim Change 2014, 4:693–697, doi: 10.1038/nclimate2293.

Sigl M, Winstrup M, McConnell JR, Welten KC, Plunkett G, Ludlow F, Büntgen U, Caffee MW, Chellman NJ, Dahl-Jensen D, Fischer H, Kipfstuhl S, Kostick C, Maselli OJ, Mekhaldi F., Mulvaney R, Muscheler R, Pasteris DR, Pilcher JR, Salzer M, Schüpbach S, Steffensen JP, Vinther B, Woodruff TE. Timing and climate forcing of volcanic eruptions for the past 2,500 years. Nature 2015, 523:543–549, doi: 10.1038/nature14565.

Smith RB, Siegel L. Windows into the Earth: The Geologic Story of Yellowstone and Grand Teton National Park. Oxford University Press, New York, 2000, 242, ISBN: 9780195105971.

Sitch S, Smith B, Prentice IC, Arneth A, Bondeau A, Cramer W, Kaplan JO, Levis S, Lucht W, Sykes MT, Thonicke K, Venevsky, S. Evaluation of ecosystem dynamics, plant geography and terrestrial carbon cycling in the LPJ dynamic global vegetation model. Global Change Biology 2003, 9: 161-185, doi: 10.1046/j.1365-2486.2003.00569.x.

Soden BJ, Wetherald RT, Stenchikov GL, Robock A. Global cooling after the eruption of Mount Pinatubo: A test of climate feedback by water vapor. Science 2002, 296: 727-730 doi: 10.1126/science.296.5568.727.

Solomon S, Portmann RW, Garcia RR, Thomason LW, Poole LR, McCormick M. The role of aerosol variations in anthropogenic ozone depletion at northern midlatitudes. J Geophys Res 1996, 101: 6713–6727, doi: 10.1029/95JD03353.

Solomon S, Daniel JS, Neely RR, Vernier JP, Dutton EG, Thomason LW. The Persistently Variable ”Background” Stratospheric Aerosol Layer and Global Climate Change, Science 2011, 333:866–870, doi: 10.1126/science.1206027.

Solomon S, Ivy DJ, Kinnison D, Mills MJ, Neely III RR, Schmidt A. Emergence of healing in the Antarctic ozone layer. Science 2016, 353: 269-274. doi: 10.1126/science.aae0061.

Song N, O’C. Starr D, Wuebbles DJ, Williams A, Larson S. Volcanic aerosols and interannual variation of high level clouds, Geophys Res Lett 1996, 23: 2657–2660, doi: 10.1029/96GL02372.

Stratosphere-troposphere Processes and their Role in Climate (SPARC), Assessment of Stratospheric Aerosol Properties (ASAP), Thomason L, Peter T (eds.) SPARC Report 2006, 4, WCRP-124, WMO/TD - No. 1295.

Stenchikov GL, Kirchner I, Robock A, Graf HF, Antuña JC, Grainger RG, Lambert A, Thomason *L.* Radiative forcing from the 1991 Mount Pinatubo volcanic eruption. J Geophys Res 1998, 103*:* 13837–13857, doi: 10.1029/98JD00693.

Stenchikov GL, Robock A, Ramaswamy V, Schwarzkopf MD, Hamilton K, Ramachandran S. Arctic Oscillation response to the 1991 Mount Pinatubo eruption: Effects of volcanic aerosols and ozone depletion. J Geophys Res 2002, 107: 4803, doi: 10.1029/2002JD002090.

Stenchikov GL, Hamilton K, Robock A, Ramaswamy V, Schwarzkopf MD. Arctic Oscillation response to the 1991 Pinatubo eruption in the SKYHI general circulation model with a realistic quasi-biennial oscillation. J Geophys Res 2004, 109:D03112, doi: 10.1029/2003JD003699.

Stenchikov G, Hamilton K, Stouffer R, Robock A, Ramaswamy V, Santer,B, Graf HF. Arctic Oscillation response to volcanic eruptions in the IPCC AR4 climate models. J Geophys Res 2006, 111: D07107, doi: 10.1029/2005JD006286.

Stenchikov G, Delworth, TL, Ramswamy V, Stouffer RJ, Wittenberg A, Zeng F. Volcanic signals in oceans. J Geophys Res 2009, 114: D16104, doi :10.1029/2008JD011673.

Stenke A, Grewe V. Simulation of Stratospheric Water Vapor Trends: Impact on Stratospheric Ozone Chemistry. Atmos Chem Phys 2005, 5: 1257-1272, doi: 10.5194/acp-5-1257-2005.

Stevenson S, Otto-Bliesner B, Fasullo F, Brady E. "El Niño Like" Hydroclimate Responses to Last Millennium Volcanic Eruptions. J Climate 2016, 29: 2907–2921, doi: 10.1175/JCLI-D-15-0239.1.

Stier P, Feichter J, Kinne S, Kloster S, Vignati E, Wilson J, Ganzeveld L, Tegen I, Werner M, Balkanski Y, Schulz, M, Boucher O, Minikin A, Petzold A. The aerosol climate model ECHAM5-HAM. Atmos Chem Phys 2005, 5: 1125– 1156, doi: 10.5194/acp-5-1125-2005.

Stoffel M, Khodri M, Corona C, Guillet S, Poulain V, Bekki S, Guiot J, Luckman BH, Oppenheimer C, Lebas N, Beniston M, Masson-Delmotte V.Estimates of volcanic-induced cooling in the Northern Hemisphere over the past 1,500 years. Nat Geosci 2015, 8: 784–788, doi: 10.1038/ngeo2526.

Stohl A, Prata AJ, Eckhardt S, Clarisse L, Durant A, Henne S, Kristiansen NI, Minikin A, Schumann U, Seibert P, et al. Determination of time- and height-resolved volcanic ash emissions and their use for quantitative ash dispersion modeling: the 2010 Eyjafjallajökull eruption. Atmos Chem Phys 2011, 11: 4333-4351, doi: 10.5194/acp-11-4333-2011.

Storey M, Roberts RG, Saidinc M. Astronomically calibrated 40Ar/39Ar age for the Toba supereruption and global synchronization of late Quaternary records. Proc Natl Acad Sci 2012, 109: 18684–18688, doi: 10.1073/pnas.1208178109.

Stothers RB. Major optical depth perturbations to the stratosphere from volcanic eruptions: Pyrheliometric period, 1881-1960. J Geophys Res 1996, 101: 3901-3920, doi: 10.1029/-95JD03237.

Stothers RB. Three centuries of observation of stratospheric transparency. Clim Change 2007, 83: 515–521, doi: 10.1007/s10584-007-9238-3.

Swingedouw D, Ortega P, Mignot E, Guilyardi E, Masson-Delmotte V, Butler PG., Khodri M., Seferian R. Bidecadal North Atlantic ocean circulation variability controlled by timing of volcanic eruptions. Nature Communications 2015, 6: 6545, doi: 10.1038/ncomms7545.

Tabazadeh A, Turco RP. Stratospheric chlorine injection by volcanic eruptions: HCl scavenging and implications for ozone. Science 1993, 260: 1082-1086, doi: 10.1126/science.260.5111.1082.

Tabazadeh A, Drdla K, Schoeberl MR, Hamill P, Toon OB. Arctic "ozone hole" in cold volcanic stratosphere. Proc Natl Acad Sci 2002, 99: 2609–2612, doi: 10.1073/pnas.052518199.

Taylor, KE, Stouffer RJ, Meehl GA. An Overview of CMIP5 and the experiment design. Bull Amer Meteor Soc 2012, 93: 485-498, doi: 10.1175/BAMS-D-11-00094.1.

Telford PJ, Lathière J, Abraham NL, Archibald AT, Braesicke P, Johnson CE, Morgenstern O, O' Connor FM, Pike RC, Wild O, et al. Effects of climate-induced changes in isoprene emissions after the eruption of Mount Pinatubo. Atmos Chem Phys 2010, 10: 7117-7125, doi: 10.5194/acp-10-7117-2010.

Textor C, Graf HF, Herzog M, Oberhuber JM. Injection of gases into the stratosphere by explosive volcanic eruptions. J Geophys Res 2003, 108: 4606, doi:10.1029/2002JD002987.

Textor C, Graf HF, **Timmreck C**, Robock A. Emissions from volcanoes. In Granier, C, Artaxo PE, Reeves CE, eds. Emissions of Atmospheric Trace Compounds, Advances in Global Change Research 2004, 18:269-303, doi: 10.1007/978-1-4020-2167-1_7.

Thoma M, Greatbatch RJ, Kadow C, Gerdes R. Decadal hindcasts initialised using observed surface wind stress: Evaluation and Prediction out to 2024. Geophys Res Lett 42: 6454–6461 2015, doi: 10.1002/2015GL064833.

Thomas MA, Giorgetta M, **Timmreck C**, Graf HF, Stenchikov G. Effects of volcanic eruptions on the quasi-biennial oscillation. Geophysical Research Abstracts 2008, 10, EGU2008-A-08404.

Thomas MA. Simulation of the climate impact of Mt. Pinatubo eruption using ECHAM5. PhD Thesis Universität Hamburg 2008 (also Berichte zur Erdsystemforschung Max Planck Institut für Meteorologie No 52).

Thomas MA, **Timmreck C**, Giorgetta M, Graf HF, Stenchikov G. Simulation of the climate impact of Mt. Pinatubo eruption using ECHAM5. Part-I: Sensitivity to the modes of atmospheric circulation and boundary conditions. Atmos Chem Phys 2009, 9: 757-769, doi: 10.5194/acp-9-757-2009.

Thomas MA, Giorgetta M, **Timmreck C**, Graf HF, Stenchikov G. Simulation of the climate impact of Mt. Pinatubo eruption using ECHAM5. Part-II: Sensitivity to the phase of the QBO. Atmos Chem Phys 2009, 9: 3001-3009, doi: 10.5194/acp-9-3001-2009.

Thomason LW, Poole LR, Deshler T. A global climatology of stratospheric aerosol surface area density deduced from Stratospheric Aerosol and Gas Experiments II measurements: 1984–1994. J Geophys Res 1997, 102: 8967–8976, doi: 10.1029/96JD02962.

Thomason LW, Vernier JP, Bourassa A, Arfeuille F, Bingen C, Peter T, Luo B. Stratospheric Aerosol Data Set (SADS Version 2) Prospectus. In preparation for Geosc. Model Dev 2017.

Thompson DWJ, Wallace JM, Jones PD, Kennedy JJ. Identifying signatures of natural climate variability in time series of global-mean surface temperature: Methodology and Insights. J Climate 2009, 22: 6120–6141, doi: 10.1175/2009JCLI3089.1.

Thordarson T, Self S. Atmospheric and environmental effects of the 1783–1784 Laki eruption: A review and reassessment. J Geophys Res 2003, 108: 4011, doi: 10.1029/2001JD002042.

Tie X, Brasseur GP, Briegleb B, Granier C.Two-dimensional simulation of Pinatubo aerosol and its effect on stratospheric ozone. J Geophys Res 1994, 99: 20545–20562, doi: 10.1029/94JD01488.

Tie X, Brasseur G. The response of the stratospheric ozone to volcanic eruptions: sensitivity to atmospheric chlorine loading. Geophys Res Lett 1995, 22: 3035–3038. doi: 10.1029/95GL03057.

Timmreck, C. (1997), Simulationen zur Bildung und Entwicklung von stratosphärischem Aerosol unter besonderer Berücksichtigung der Pinatuboepisode. Max-Planck-Institut für Meteorologie, Examensarbeit Nr. 46, Hamburg, Germany. ISSN 0938-5177. (Ph.D. Thesis).

Timmreck C, Graf HF, Feichter J. Simulation of Mt. Pinatubo aerosol with the Hamburg climate model ECHAM4. Theor Appl Climatol 1999, 62: 85-108, doi: 10.1007/s007040050076.

Timmreck C, Graf HF, Kirchner I. A one and a half year interactive simulation of Mt. Pinatubo aerosol. J Geophys Res 1999, 104: 9337-9360, doi: 10.1029/1999JD900088.

Timmreck C, Graf HF. A microphysical model to simulate the development of stratospheric aerosol in a GCM. Meteorol Z 2000, 9: 263-282.

Timmreck C, Three-dimensional simulation of stratospheric background aerosol: First results of a multiannual GCM simulation. J Geophys Res 2001, 106: 28313- 28332. doi: 10.1029/2001JD000765.

Timmreck C, Graf H-F, Steil B. Aerosol chemistry interactions after the Mt. Pinatubo eruption. In: Robock A, Oppenheimer C, eds. Volcanism and the Earth's Atmosphere. Washington, DC: AGU; 2003, 213-225, doi: 10.1029/139GM13.

Timmreck C, Graf HF. The initial dispersal and radiative forcing of a Northern Hemisphere mid-latitude super volcano: a model study. Atmos Chem Phys 2006, 6: 35-49, doi: 10.5194/acp-6-35-2006.

Timmreck C, Giorgetta M, Thomas M, Esch M, Haak H, Jungclaus J, Müller W, Roeckner E, Schmidt H, Graf HF, Stenchikov G. Volcanic eruptions and ENSO: Studies with a coupled atmosphere-ocean model, AGU spring meeting 22-25 May, 2007 Acapulco, Mexico (Invited talk).

Timmreck C, Hagemann S, Esch M, Graf HF, Jungclaus J, Landerer F, Schmidt H, Thomas MA. Impact of the 1991 Mt. Pinatubo eruption on the hydrological cycle with implications for geoengineering. SPARC 4th General Assembly, August 31-September 5, 2008 Bologna, Italy.

Timmreck C, Lorenz SJ, Crowley TJ, Kinne S, Raddatz TJ, Thomas MA, Jungclaus JH. Limited temperature response to the very large AD 1258 volcanic eruption. Geophys Res Lett 2009, 36: L21708, doi: 10.1029/2009GL040083.

Timmreck C, Graf HF, Lorenz SJ, Niemeier U, Zanchettin D, Matei D, Jungclaus JH, Crowley TJ. Aerosol size confines climate response to volcanic super-eruptions. Geophys Res Lett 2010, 37: L24705, doi: 10.1029/2010GL045464.

Timmreck C, Graf HF, Zanchettin D, Hagemann S, Kleinen T, Krüger K. Climate response to the Toba eruption: regional changes. Quat Int 2012, 258:30-44, doi: 10.1016/j.quaint.2011.10.008.

Timmreck C. Modeling the climatic effects o large explosive f volcanic eruptions, invited review paper. WIREs Clim Change 2012; 3: 545-564, doi: 10.1002/wcc.192.

Timmreck, C, Pohlmann H, Illing S, Kadow C. The impact of stratospheric volcanic aerosol on decadal scale predictability. Geophys Res Lett 2016, 43: 834-842, doi: 10.1002/2015GL067431.

Timmreck C, Mann GW, Aquila V, Hommel R, Lee LA, Schmidt A, Brühl C, Carn S., Chin M, Dhomse SS, English JM, Diehl T, Mills MJ, Neely R, Sheng JX, Toohey M, Weisenstein D. ISA-MIP: A co-ordinated intercomparison of Interactive Stratospheric Aerosol models: Motivation, experiments and specifications, to be submitted to Geosci Model Dev 2017.

Tjiputra JF, Otterå OH. Role of volcanic forcing on future global carbon cycle. Earth Syst Dynam 2011, 2: 53-67, doi: 10.5194/esd-2-53-2011.

Toohey M, Krüger K, Niemeier U, **Timmreck C**. The influence of eruption season on the global aerosol transport and radiative impact of tropical volcanoes. Atmos Chem Phys 2011, 11:12351-12367, doi:10.5194/acp-11-12351-2011.

Toohey M, Krüger K **Timmreck C**. Volcanic sulfate deposition to Greenland and Antarctica: a modeling sensitivity study. J Geophys Res 2013, 118: 4788–4800, doi: 10.1002/jgrd.50428.

Toohey M, Krüger K, Bittner M, **Timmreck C**, Schmidt H. The role of volcanic aerosol on the Northern Hemisphere stratospheric winter polar vortex: mechanisms and sensitivity to prescribed forcings for the 1991 Pinatubo eruption. Atmos Chem Phys 2014, 14: 13063-13079. doi:10.5194/acp14-13063-2014.

Toohey M, Stevens B, Schmidt H, **Timmreck C.** Easy Volcanic Aerosol (EVA v1.0): An idealized forcing generator for climate simulations. Geosci Model Dev 2016, 9: 4049-4070, doi: 10.5194/gmd-9-4049-2016.

Toohey M., Sigl, M. Ice core-inferred volcanic stratospheric sulfur injection from 500 BCE to 1900 CE. World Data Center for Climate at DKRZ Hamburg 2016, doi: 10.1594/WDCC/eVolv2k_v1 http://cera-www.dkrz.de/WDCC/ui/Compact.jsp?acronym=eVolv2k_v1 .

Toohey M, Krüger K**, Timmreck C,** Schmidt H. Revisiting the potential radiative and climatic impact of extratropical vs. tropical volcanic eruptions. in prep. Atmos Chem Phys 2017.

Trenberth K, Dai A. Effect of Mount Pinatubo volcanic eruption on the hydrological cycle as analog of geoengineering. Geophys Res Lett 2007, 34: L15702, doi: 10.1029/2007GL030524.

Trepte CR, Hitchman MH.Tropical stratospheric circulation deduced from satellite aerosol data. Nature 1992, 355: 626-628, doi: 10.1038/355626a0.

Trepte CR. Veiga RV, McCormick MP. The poleward dispersal of Mount Pinatubo volcanic aerosol. J Geophys Res 1993, 98: 18563–18573, doi: 10.1029/93JD01362..

Vehkamäki H, Kulmala M, Napari I, Lehtinen KEJ**, Timmreck C**, Noppel M, Laaksonen A. An improved parameterization for sulfuric acid-water nucleation rates for tropospheric and stratospheric conditions, J Geophys Res 2002, 107: 4622, doi: 10.1029/2002JD002184.

Vehkamäki H, Kulmala M, Napari I, Lehtinen KEJ, **Timmreck C,** Noppel M, Laaksonen A Correction to “An improved parameterization for sulfuric acid/water nucleation rates for tropospheric and stratospheric conditions”. J Geophys Res Atmos 2013, 118: 9330, doi: 10.1002/jgrd.50603.

Vernier JP, Thomason LW, Pommereau JP, Bourassa A, Pelon J, Garnier A, Hauchecorne A, Blanot L, Trepte C, Degenstein D, Vargas F. Major influence of tropical volcanic eruptions on the stratospheric aerosol layer during the last decade. Geophys Res Lett 2011, 38: L12807, doi: 10.1029/2011GL047563.

Vignati E, Wilson J, Stier P. M7: An efficient size-resolved aerosol microphysics module for large-scale aerosol transport models. J Geophys Res 2004, 109: D22202, doi: 10.1029/2003JD004485.

von Glasow R, Bobrowski N, Kern C. The effects of volcanic eruptions on atmospheric chemistry. Chem Geol 2009, 263:131–142, doi: 10.1016/j.chemgeo.2008.08.020.

Wang PH, Minnis P, Yue GK. Extinction coefficient (1 mm) properties of high-altitude clouds from solar occultation measurements (1985 – 1990): Evidence for volcanic aerosol effect. J Geophys Res 1995, 100: 3181– 3199, doi: 10.1029/94JD02325.

Wang T, Otterå OH, Gao Y, Wang H. The response of the North Pacific Decadal Variability to strong tropical volcanic eruptions. Clim Dyn 2012, 39: 2917–2936, doi 10.1007/s00382-012-1373-5.

Wegmann M, Brönnimann S, Bhend J, Franke J, Folini D, Wild M, Luterbacher J. Volcanic influence on European summer precipitation through monsoons: possible cause for "years without summer". J Climate 2014, 27: 3683–3691, doi: 10.1175/JCLI-D-13-00524.1.

Weil M, Grassl H, Hoshyaripour G, Kloster S, Kominek J, Misios S, Scheffran J, Starr S., Stenchikov G, Sudarchikova N, **Timmreck C,** Zhang D, Kalinowski M. Pathways, impacts, and policies on severe aerosol injections into the atmosphere. Bull Am Meteorol Soc 2012, 93: ES85–ES88, doi: 10.1175/BAMS-D-11-00272.1.

Weisenstein DK, Penner JE, Herzog M, Liu X. Global 2-D intercomparison of sectional and modal aerosol modules. Atmos Chem Phys 2007, 7: 2339-2355, doi: 10.5194/acp-7-2339-2007.

Wigley TML, Ammann CM, Santer BD, Raper SCB. Effect of climate sensitivity on the response to volcanic forcing. J Geophys Res 2005, 110: D09107, doi: 10.1029/2004JD005557.

Williams MAJ, Ambrose SH, van der Kaars S, Chattopadhyaya U, Pal J, Chauhan PR, Ruehlemann C. Environmental impact of the 73 ka Toba super-eruption in South Asia. Palaeo Palaeo Palaeo 2009, 284:295-314, doi: 10.1016/j.palaeo.2009.10.009.

Williams MAJ, Ambrose SH, van der Kaars S, Chattopadhyaya U, Pal J, Chauhan PR, Ruehlemann C Reply to the comment on "Environmental impact of the 73 ka Toba super-eruption in South Asia" by M. A. J. Williams, S. H. Ambrose, S. van der Kaars, C. Ruehlemann, U. Chattopadhyaya, J. Pal, P. R. Chauhan [Palaeo, Palaeo, Palaeo 84 (2009) 295–314] Palaeo Palaeo Palaeo 2010, 296: 204-211, doi: 10.1016/j.palaeo.2010.05.043.

Wilmes SB, Raible CC, Stocker TF. Climate variability of the mid- and high-latitudes of the Southern Hemisphere in ensemble simulations from 1500 to 2000 AD. Clim Past 2012, 8: 373-390, doi: 10.5194/cp-8-373-2012.

Wilson JC, Jonsson HH, Brock CA, Toohey DW, Avallone LM, D. Baumgardner, Dye JE, Poole LR, Woods DC, DeCoursey RJ, Osborn M, Pitts MC, Kelly KK, Chan KR, Ferry GV, Loewenstein M, Podolske JR, Weaver A.In Situ Observations of Aerosol and Chlorine Monoxide After the 1991 Eruption of Mount Pinatubo: Effect of Reactions on Sulfate Aerosol. Science 1993, 261: 1140-1143 doi: 10.1126/science.261.5125.1140.

Winter A, Zanchettin D, Miller T, Kushnir Y, Black D, Lohmann G, Burnett A, Haug G, Estrella-Martínez J, Breitenbach SFM, Beaufort L, Cheng H. Persistent drying in the tropics linked to natural forcing. Nature Communications, 2015, 6: 7627, doi: 10.1038/ncomms8627.

World Meteorological Organization (WMO), Scientific Assessment of Ozone Depletion: 2010, Global Ozone Research and Monitoring Project Report 2011, 50, World Meteorological Organization, Geneva.

Yokohata T, Emori S, Nozawa T, Tsushima Y, Ogura T, Kimoto M. Climate response to volcanic forcing: validation of climate sensitivity of a coupled atmosphere–ocean general circulation model. Geophys Res Lett 2005, 32: L21710, doi: 10.1029/2005GL023542.

Yoshimori M, Stocker TF, Raible CC, Renold M. Externally-forced and internal variability in ensemble climate simulations of the Maunder Minimum. J Climate 2005, 18: 4253-4270, doi: 10.1175/JCLI3537.1.

Young RE, Houben H, Toon OB. Radiatively forced dispersion of the Mt. Pinatubo volcanic cloud and induced temperature perturbations in the stratosphere during the first few months following the eruption. Geophys Res Lett 1994, 21: 369-372, doi: 10.1029/93GL03302

Yue GK, Deepak A. Latitudinal and altitudinal variation of size distribution of stratospheric aerosols inferred from SAGE aerosol extinction coefficient measurements at two wavelengths. Geophys Res Lett 1984, 11: 999-1002, doi: 10.1029/GL011i010p00999.

Zanchettin D, Rubino A, Lorenz SJ, **Timmreck C,** Jungclaus JH. Implications of El Niño-Southern Oscillation on volcanic impacts on Northern Hemisphere winter climates during the Last Millennium. Geophysical Research Abstracts 2010, 12, EGU2010-11749.

Zanchettin D, **Timmreck C**, Graf HF, Rubino A, Lorenz SJ, Lohmann K, Krüger K, Jungclaus JH. Bi-decadal variability excited in the coupled ocean-atmosphere system by strong tropical volcanic eruptions. Clim Dyn 2012a, 39: 419-444, doi: 10.1007/s00382-011-1167-1.

Zanchettin D, Rubino A, Matei D, Bothe O, Jungclaus J. Multidecadal-tocentennial SST variability in the MPI-ESM simulation ensemble for the last millennium. Clim Dyn 2012b, 40: 1301–1318, doi: 10.1007/s00382-012-1361-9.

Zanchettin D, **Timmreck C**, Bothe O, Lorenz S, Hegerl G, Graf HF, Luterbacher J, Jungclaus, J. Delayed winter warming: a decadal dynamical response to strong tropical volcanic eruptions. Geophys Res Lett 2013a, 40: 204–209, doi: 10.1029/2012GL054403.

Zanchettin D, Bothe O, Graf HF, Lorenz S, Luterbacher J, **Timmreck C**, Jungclaus J. Background conditions influence the decadal climate response to strong volcanic eruptions. J Geophys Res Atmos 2013b, 118: 4090–4106, doi: 10.1002/jgrd.50229.

Zanchettin D, Bothe O, **Timmreck C**, Bader J, Beitsch A, Graf HF, Notz N and Jungclaus JH. Inter-hemispheric asymmetry in the sea-ice response to volcanic forcing simulated by MPI-ESM (COSMOS-Mill). Earth Syst Dynam 2014, 5:223–242, doi: 10.5194/esd-5-223-2014

Zanchettin D, **Timmreck C**, Khodri M, Robock A, Rubino A, Schmidt A, Toohey M, A coordinated modeling assessment of the climate response to volcanic forcing, Past Global Changes Magazine 2015, 23: 2, 54-55, doi: 10.22498/pages.23.2.54.

Zanchettin D, Khodri M, **Timmreck C,** Toohey M, Schmidt A, Gerber, E. P., Hegerl, G., Robock, A., Pausata, FS, Ball WT, Bauer SE, Bekki S, Dhomse, SS, LeGrande AN, Mann, GW, Marshall L, Mills, M., Marchand M, Niemeier U, Paulain V, Rubino A, Stenke A, Tsigaridis K, Tummon F: The Model Intercomparison Project on the climatic response to Volcanic forcing (VolMIP): Experimental design and forcing input data, Geosci Model Dev 2016, 9: 2701-2719, doi: 10.5194/gmd-9-2701-2016.

Zhong Y, Miller GH, Otto-Bliesner BL, Holland MM, Bailey DA, Schneider DP, Geirsdottir A. Centennial-scale climate change from decadally-paced explosive volcanism: a coupled sea ice-ocean mechanism. Clim Dyn 2011, 37: 2373–2387, doi: 10.1007/s00382-010-0967-z.

Zielinski GA. Stratospheric loading and optical depth estimates of explosive volcanism over the last 2100 years derived from the Greenland Ice Sheet Project 2 ice cores. J Geophys Res 1995, 100: 20937–20955, doi: 10.1029/95JD01751.

Zielinski GA, Mayewski PA, Meeker LD, Whitlow S, Twickler MS, Taylor K. Potential atmospheric impact of the Toba mega-eruption B71,000 years ago. Geophys Res Lett 1996, 23: 837–840, doi: 10.1029/96GL00706.

Zielinski GA. Use of paleo-records in determining variability within the volcanism-climate system. Quat Sci Rev 2000, 19: 417-438, doi:1 0.1016/S0277-3791(99)00073-6.

List of Abbrevations

AGU	American Geophysical Union
AOD	Aerosol Optical Depth
AMOC	Atlantic Meridional Overturning Circulation
AR4	Fourth Assessment of the IPCC Report
ASAP2006	Assessment of Stratospheric Aerosol properties (WMO, 2006)
AVHRR	Advanced Very High Resolution Radiometer
B1-LR/MR	baseline 1 simulations
B1-NVA	baseline 1 simulations without volcanic aerosol
BDC	Brewer Dobson circulation
CALIPSO	Cloud-Aerosol Lidar and Infrared Pathfinder Satellite Observations
CARMA	Community Aerosol and Radiation Model for Atmospheres
CAVA	Central American Volcanic Arc
CCM2	NCAR's Community Climate Model, version 2
CCM	Chemistry climate model
CCMVal	Chemistry-Climate Model Validation Activity
CCMI	Chemistry-Climate Model Initiative
CCN	Cloud Condensation Nuclei
CCSM3	NCAR's Community Climate System Model Version 3
CDN	Cloud Droplet Number Concentration
CDR	Cloud Droplet Radius
CESM-LME	Community Earth System Model Last Millennium Ensemble
CLM-DGVM	Community Land Model Dynamic Global Vegetation Model
CMIP	Coupled Model Intercomparison Project
CMIP5	Coupled Model Intercomparison Project, phase 5
CMIP6	Coupled Model Intercomparison Project, phase 6
DCPP	Decadal Climate precition Panel
DGVM	Dynamic global vegetation model
DJF	December-January-February
ECHAM	European Center/ HAMburg model, atmospheric GCM
ECS	Equilibrium climate sensitivity
EGU	European Geophysical Union
EMIC	Earth system Model of Intermediate Complexity
ECMWF	European Centre for Medium-Range Weather Forecasting
EESC	Equivalent Effective Stratospheric Chlorine
ENSO	El Niño Southern Oscillation
ERA-Interim	ECMWF Interim Re-Analysis
ERBE	Earth Radiation Budget Experiment
ESM	Earth System Model
ETHZ	Eidgenössische Technische Hochschule Zürich
EVA	Easy Volcanic Aerosol
GCM	General Circulation Model
GHG	GreenHouse Gases

GISP(2)	Greenland Ice Sheet Project (Two)
GPCP	Global Precipitation Climatology Project
HAM	Hamburg Aerosol Model
HadCM3	Hadley Centre Climate model, version 3 (includes TRIFFID DGVM)
HadCRUT3	Dataset of global historical surface temperature anomalies from the Met Office Hadley Centre and the Climatic Research Unit at the University of East Anglia. 3 dnotes version3.
HadGEM	Hadley Centre Global Environmental Model
JSBACH	Jena Scheme for Biosphere-Atmosphere Coupling in Hamburg; land surface model of MPI-ESM
ISA-MIP	Interactive Stratospheric Aerosol Model Intercomparions Project
ICESM	International Conference on Earth System Modelling
IFS	Integrated Forecasting System
IPCC	Intergovernmental Panel on Climate Change
ISCCP	International Satellite Cloud Climatology Project (ISCCP)
ITCZ	Intertropical Convergence Zone
JJA	June-July-August
LAI	Leaf Area Index
LaMEVE	Large Magnitude Explosive Volcanic Eruptions database
LMD-LSCE	Atmospheric GCM developed at LMD (Laboratoire deMÈtÈorologie Dynamique) and LSCE (Laboratoire de Sciences du Climat et de l'Environnement), Paris, France
LMD	Laboratoire de Meteorologie Dynamique
LMDZ	"LMD-Zoom "GCM
LPJ	Lund-Potsdam-Jena DGVM
LSG	The Hamburg Large-Scale Geostrophic Ocean Circulation Model
LW	Longwave
LWP	Liquid Water Path
MAIA	Model of Aerosols and Ions in the Atmosphere
MiKlIP	Mittelfristige Klimaprognosen
MIROC	Model for Interdisciplinary Research on Climate Version 3
MODIS	Moderate Imaging Spectroradiometer
MPI-ESM	Earth System model of Max Planck Institute for Meteorology
MPIOM	The Max Planck Institute ocean model (MPIOM) is the ocean-sea ice component of the MPI-ESM
MPI-SV	Max Planck Institute for Meteorology Super Volcano
MXD	Maximum latewood density parameter
NAO	North Atlantic Oscillation
NCAR	The National Center for Atmospheric Research, Boulder, USA
NH	Northern hemisphere
NPP	Net primary productivity
OCS	Carbonyl sulfide
OPC	Optical Particle Counter
OLR	Outgoing longwave radiation
OMI	Ozone Monitoring Instrument

PNA	Pacific/North American
PCS	Passive cavity aerosol spectrometer
PDF	Probability Density Function
QBO	Quasi-biennial oscillation
RH	Relative Humidity
SAGE	Stratospheric Aerosol and Gas Experiment
SAM	Southern Annular Mode
SAM (2)	Stratospheric Aerosol Model (version 2)
SALSA	Sectional Aerosol module for Large Scale Applications
SCM	Single-Column Model
SH	Southern Hemisphere
SPARC	Stratosphere-troposphere Processes And their Role in Climate
SRES	Special Report on Emissions Scenarios of IPCC
SSiRC	Stratospheric Sulfur and its Role in Climate
SST	Sea Surface Temperature
SW	Shortwave
TCC	Total cloud cover
TCS	Transient Climate Sensitivity
ToA	Top of the Atmosphere
THC	Oceanic thermohaline circulation
VEI	Volcanic Explosivity Index
VolMIP	Model Intercomparison Project on the climate response to Volcanic forcing
WACCM	Whole Atmosphere Community Climate Model
YTT	YoungToba Tuff

List of Chemical Abbreviations

BC	Black carbon
Br	Bromine
CH4	Methane
Cl	Chlorine
ClOx	Chloride oxides
CO_2	Carbon dioxide
CS2	Carbon disulfide
DMS	Dimethyl sulfide
HCl	Hydrogen chloride
H_2O	Water vapor
H_2S	Hydrogen sulfide
H2SO4 (g)	Sulfuric acid (vapor)
I	Iodine
OCS	Carbonyl sulfide
O_3	Ozone
NO_x	Nitrogen oxides
N_2O	Nitrous oxide
SO_2	Sulfur dioxide

Notation list

γ	The global carbon cycle-climate sensitivity γ is defined as change in atmospheric CO_2 per unit change in global mean surface temperature
M	The eruption magnitude M is defined as M = log(m)−7, where m is erupted magma mass in [kg].
r_{eff}	Effective radius
σ	Standard deviation

Appendix

Overview of SSIRC ISA-MIP experiments

Experiment	Focus	Number of specific experiments	Years per experiment	Total years	Knowledge-gap to be addressed
Background Stratospheric Aerosol (BG)	Stratospheric sulfur budget in volcanically quiescent conditions	1 mandatory + 2 recommended	20	60	20 year climatology to understand sources and sinks of stratospheric background aerosol, assessment of sulfate aerosol load under volcanically quiescent conditions
Transient Stratospheric Aerosol (TAR)	Transient stratospheric aerosol properties over the period 1998 to 2012 using different volcanic emission datasets	4 mandatory +3 optional experiments recommended are 5	15	60 (105)	Evaluate models over the period 1998-2012 with different volcanic emission data sets Understand drivers and mechanisms for observed stratospheric aerosol changes since 1998
Historic Eruption SO_2 Emission Assessment (HErSEA)	Perturbation to stratospheric aerosol from SO_2 emission appropriate for 1991 Pinatubo, 1982 El Chichon,1963 Agung	for each (x3) eruption (Control, median and 4 (2x2) of high /low emission scenario deep/shallow injection height	4 recom. 6	180 (270)	Assess how injected SO_2 propagates through to radiative effects for different historical major tropical eruptions in the different interactive stratospheric aerosol models Use stratospheric aerosol measurements to constrain uncertainties in emissions and gain new observationally-constrained volcanic forcing and surface area density datasets Explore the relationship between volcanic emission uncertainties and volcanic forcing uncertainties
Pinatubo Emulation in Multiple Models (PoEMS)	Perturbed parameter ensemble (PPE) of runs to quantify uncertainty in each model's predictions	Each model to vary 7, 5 or 3 of 8 parameters (7 per parameter = 49, 35 or 21)	5 per parameter	245, 175 or 105 (7, 5 or 3)	Intercompare Pinatubo perturbation to strat. aerosol properties with full uncertainty analysis over PPE run by each model. Quantify sensitivity of predicted Pinatubo perturbation stratospheric aerosol properties and radiative effects to uncertainties in injection settings and model processes Quantify and intercompare sources of uncertainty in simulated Pinatubo effective radiaitive forcing for the different complexity models.

Table A.1 Overview of the SSiRC ISA-MIP experiments. The "Background" (BG) experiment will concentrate on microphysics and transport processes under volcanically quiescent conditions, where the stratospheric aerosol is modulated by seasonal changes and interannual variability. The "Transient Aerosol Record" (TAR) experiment will explore the role of small- to moderate-magnitude volcanic eruptions and transport processes between 1998-2012 and its possible role for the warm hiatus period. Two experiments will investigate the stratospheric sulfate aerosol size distribution under the influence of large volcanic eruptions. The "Historical Eruptions SO2 Emission Assessment" (HErSEA) experiment will focus on the uncertainty in the initial emission of recent large volcanic eruptions, while the "Pinatubo Emulation in Multiple models" (PoEMS) experimen will provide a full uncertainty analysis of the radiative forcing of the Mt. Pinatubo eruption. All simulations will be carried out with global stratospheric aerosol models, prescribed SST and well defined emission scenario. From *Timmreck et al. to be submitted to Geosc. Mod Dev. 2017.*

Overview of VolMIP volc-pinatubo experiments

Name	Description	Ens. Size	Years per simulation	Gaps of knowledge being addressed with this experiment
volc-pinatubo-full	1991 Pinatubo forcing as used in the CMIP6 historical simulations. Requires special diagnostics of parameterized and resolved wave forcings, radiative and latent heating rates.	25	3	Uncertainty in the climate response to strong volcanic eruptions with focus on short-term response. Robustness of volcanic impacts on Northern Hemisphere's winter climate and of associated dynamics.
volc-pinatubo-surf	As volc-pinatubo-full, but with prescribed perturbation to the shortwave flux to mimic the attenuation of solar radiation by volcanic aerosols	25	3	Mechanism(s) underlying the dynamical atmospheric response to large volcanic eruptions, in particular in Northern Hemisphere's winters. The experiment considers only the effect of volcanically induced surface cooling. Complimentary experiment to volc-pinatubo-strat.
volc-pinatubo-strat	As volc-pinatubo-full, but with prescribed perturbation to the total (LW+SW) radiative heating rates	25	3	Mechanism(s) underlying the dynamical atmospheric response to large volcanic eruptions, in particular in Northern Hemisphere's winter. The experiment considers only the effect of volcanically-induced stratospheric heating. Complimentary experiment to volc-pinatubo-surf.
volc-pinatubo-slab	As volc-pinatubo-full, but with a slab ocean	25	3	Effects of volcanic eruptions on ENSO dynamics.
volc-pinatubo-ini/ DCPP C3.4	As volc-pinatubo-full, but as decadal prediction experiment initialized 1.11. 2015;joint experiment with the Decadal Climate Predicton Panel (DCPP, Boer et al., 2016). Forcing input and implementation of the forcing fully comply with the VolMIP protocol.	10(5)	5	Influence of large volcanic eruptions on future climate. Influence of large volcanic eruptions on seasonal and decadal climate predictability

Table A.2 Overview of VolMIP short-term experiments of the 1991 Mt Pinatubo eruption (volc-pinatubo). *A* key aim of the "volc-pinatubo" experiments is the question about the physical mechanism which drives NH post-volcanic winter variability; therefore a large number of ensemble members is required to address internal atmospheric variability. The volcanic forcing is derived from radiation or source parameters of documented eruptions but the experiments (except volc-pinatubo-ini) generally do not include information about the actual climate conditions when these events occurred. The experiments are designed as ensemble simulations, with sets of initial climate states sampled from the CMIP6-DECK "piControl" (i.e., preindustrial control) simulation describing unperturbed preindustrial climate conditions (Eyring et al., 2016) unless specified otherwise. Adapted from *Zanchettin et al. (2016)*

Overview of VolMIP volc-long and volc-cluster experiments

Name	Description	Ens. Size	Years per simulation	Gaps of knowledge being addressed with this experiment
volc-long-eq	Idealized equatorial eruption corresponding to an initial emission of 56.2 Tg SO_2. The eruption magnitude corresponds to recent estimates for the 1815 Tambora eruption (Sigl et al., 2015), the largest tropical eruption of the last five centuries, which was linked to the "year without a summer" in 1816.	9	20	Uncertainty in the climate response to strong volcanic eruptions, with focus on coupled ocean-atmosphere feedbacks and interannual to decadal global as well as regional responses. Mismatch between reconstructed and simulated climate responses to historical strong volcanic eruptions, with focus on the role of simulated background internal climate variability.
volc-long-hlN	Idealized Northern Hemisphere high-latitude eruption emitting 28.1 Tg SO_2.	9	20	Uncertainty in climate response to strong NH high-latitude volcanic eruptions (focus on coupled ocean-atmosphere). Outstanding questions about the magnitude of the climatic impact of a NH high-latitude eruptions.
volc-long-hlS	Idealized Southern Hemisphere high-latitude eruption emitting 28.1 Tg SO_2.	9	20	Uncertainty in climate response to strong SH high-latitude volcanic eruptions (focus on coupled ocean-atmosphere). Outstanding questions about the magnitude of the climatic impact of SH high-latitude eruptions.
volc-cluster-ctrl	Early 19th century cluster of strong tropical volcanic eruptions, including the 1809 event of unknown location, and the 1815 Tambora and 1835 Cosigüina eruptions.	3	50	Uncertainty in the multi-decadal climate response to strong volcanic eruptions (focus on long-term climatic implications). Contribution of volcanic forcing to the climate of the early 19th century, the coldest period in the past 500 years. Discrepancies between simulated and reconstructed climates of the early 19th century.
volc-cluster-mill	Parallel experiment to volc-cluster-ctrl, but with initial conditions taken from last millennium simulation *(Jungclaus et al., 2016)* to account for the effects of a more realistic history of past natural forcing	3(1)	69	Contribution of volcanic forcing to the climate of the early 19th century, the coldest period in the past 500 years. Discrepancies between simulated and reconstructed climates of the early 19th century. Effect of history of volcanic forcing on the response to volcanic eruptions.
volc-cluster-21C	Parallel experiment to volc-cluster-ctrl, using restart files from the end of the historical simulation instead from piControl, and boundary conditions from the 21st century SSP2-4.5 scenario experiment of ScenarioMIP (O'Neill et al., 2016).	3(1)	85	Contribution of volcanic forcing uncertainty to uncertainty in future climate projections Long-term climate response to volcanic eruptions under warm background climate conditions

Table A.3 Overview of VolMIP volc-long and volc-cluster experiments. The central focus of the VolMIP volc-long and vol-cluster experiments is placed on a better understanding of the role of volcanoes in the climate system on decadal time scales which is essential to understand future and past climate variability. The experiments are designed as ensemble simulations, with sets of initial climate states sampled from the CMIP6-DECK "piControl" (i.e., preindustrial control) simulation describing unperturbed preindustrial climate conditions (Eyring et al., 2016) unless specified otherwise. Adapted from Zanchettin et al. (2016).